Contribution of the Pannexin-1 Channel to Amyloid-β Induced Synaptic Dysfunction

By

Albert Yeung

A Thesis submitted to the Faculty of Graduate Studies of

The University of Manitoba

in partial fulfillment of the requirements of the degree of

MASTER OF SCIENCE

Department of Pharmacology and Therapeutics

University of Manitoba

Winnipeg, Canada

ABSTRACT

Alzheimer's disease is a progressive neurodegenerative disease associated with the buildup of amyloid-β protein. Toxic amyloid-β oligomers (AβOs) are known to impair the function of excitatory synapses of the hippocampus, leading to deficits in synaptic plasticity, loss of synaptic structure, and eventual neuronal death. Pannexin-1 (Panx1) is a membrane channel which has an emerging role in central nervous system physiology and pathophysiology. My thesis investigates the contribution of Panx1 to these AβO induced degenerative events by using fluorescence imaging, immunoblotting, and electrophysiology techniques on in vitro primary neuronal cultures and acute hippocampal slices. Here I demonstrate that the activity of Panx1 channels is facilitated by AβO treatment following the stimulation of NMDA receptors. However, KO of Panx1 failed to ameliorate AβO induced synaptic degeneration or deficits in long-term potentiation.

ACKNOWLEDGMENTS

I would like to start by acknowledging my supervisor, Dr. Michael Jackson, who provided me with the opportunity to join his lab and conduct the work contained in this thesis. His expertise and mentorship were invaluable to my growth as a researcher, and in more than one occasion helped guide me through the inevitable challenges of scientific inquiry. I would also like to acknowledge my advisory committee members Dr. Tiina Kauppinen and Dr. Tabrez Siddiqui, not only for their guidance in this project, but also for the collaborative opportunities that they have offered me over these past two years. They have opened my eyes to many amazing aspects of neuroscience research.

Thank you to Natalie Lavine, Ying Wang, and Chetan Patil, who provided technical support in this project, including the preparation and maintenance of primary neuronal cultures. I would also like to thank Dr. Satchin Katyal for accommodating my use of the Cytation 5, and to Asha Sinha, Marina Mostafizar, and Haynes Yuan in helping me set up these experiments. I am grateful for the help provided by Benjamin Karimi and Shreya Dhume in performing the mouse behavioural tests. It was truly the combined efforts of everyone mentioned that made this thesis possible.

I was lucky to have wonderful lab mates, who made lunch time, coffee break and bench-side (or rig-side) chats something to look forward to. First and foremost, I extend my gratitude to my good friends Shubham Tanwar and Harish Gangadharappa, who made me feel truly welcome when I first joined the lab two years ago. Thank you to Chetan and Prajwal Raghunatha, who have helped me out on numerous occasions in and out of the lab, even to this day. And of course, I would like to thank Natalie, who's advice on all things biochemistry was only trumped by her infectious laugh.

It is also important for me to acknowledge some of the people behind the scenes. Karen Donald was immensely helpful in navigating departmental requirements, answering my questions and fulfilling any requests I had. I am thankful for the opportunity to undertake this project through the MD/MSc program which was run by Dr. Kent Hayglass and Kim Ormiston and now Dr. Mark Nachtigal and Allison Birch. Funding through the MD/MSc program was provided by the CIHR.

Lastly, I am privileged to have a great supporting cast of family and friends. Behind this accomplishment is the unconditional support that my parents have given me over the years. I am also deeply grateful for my partner Linda Lam, who has been one of my greatest role models in this journey and an unwavering source of love and strength.

TABLE OF CONTENTS

LIST OF TABLES

LIST OF FIGURES

LIST OF ABBREVIATIONS

µM	Micromolar
4-AP	4-aminopyridine
A1R	Adenosine A1 receptor
AC	Associational/commissural pathway
aCSF	Artificial cerebrospinal fluid
AD	Alzheimer's Disease
AM	Acetoxymethyl ester
AMPA	α-amino-3-hydroxy-5-methyl-4-isoxazolepropionic acid
ANOVA	Analysis of variance
AP-1	Activating protein-1
APOE	Apolipoprotein E
APOE-ε4	Apolipoprotein E epsilon 4 isoform
APP	Amyloid precursor protein
APV	2-amino-5-phosphonovalerate
ATP	Adenosine triphosphate
$A\beta_{1-40}$	Amyloid-β protein fragment 1-42
$A\beta_{1-42}$	Amyloid-β protein fragment 1-40
$A\beta_{25-35}$	Amyloid-β protein fragment 25-35
AβO	Amyloid-β oligomers
Bic	Bicuculline
BLA	Basolateral amygdala
BNST	Bed nucleus of the stria terminals
CA1	Cornu Ammonis 1
CA3	Cornu Ammonis 3
CamK	Calcium/calmodulin dependent protein kinases
CamKII	Calcium/calmodulin dependent protein kinase II
cAMP	Cyclic adenosine monophosphate
CHO	Chinese hamster ovarian cell line
ChR	Channelrhodopsin
CICR	Calcium-induced calcium release
CNS	Central nervous system
CREB	Cyclic AMP response element binding protein
CSF	Cerebrospinal fluid
Cx26	Connexin-26
Cx43	Connexin-43
DG	Dentate gyrus
DHPG	Dihydroxyphenylglycine
DMEM	Dulbecco's Modified Eagle Media
ECF	Extracellular fluid

ELISA	Enzyme-linked immunosorbent assay
EPSP	Excitatory post-synaptic potential
ER	Endoplasmic reticulum
EthD-1	Ethidium homodimer-1
F-actin	Filamentous actin
FTD	Frontotemporal dementia
GFP	Green fluorescent protein
GPCR	G-protein coupled receptor
HEK293T	Human embryonic kidney cells 293T
HEPES	4-(2-hydroxyethyl)-1-piperazineethanesulfonic acid
HFS	High-frequency stimulation
HRP	Horseradish peroxidase
ICF	Intracellular fluid
IEG	Immediate early genes
Il-1β	Interleukin-1β
INX-6	Innexin-6
IP3	Inositol triphosphate
IP3R	Inositol triphosphate receptor
I-V	Current-voltage
La^{3+}	Lanthenum ion
LDH	Lactate dehydrogenase
LTD	Long-term depression
LTP	Long-term potentiation
MAPK	Mitogen activated protein kinases
MCAO	Middle cerebral artery occlusion
mEPSC	Miniature excitatory post-synaptic current
MF	Mossy fiber
mGluR	Metabotropic glutamate receptor
mM	Millimolar
mPFC	Medial prefrontal cortex
NFT	Neurofibrillary tangles
NF-κB	Nuclear factor κ-B
nM	Nanomolar
NMDA	N-methyl-D-aspartate
NMDG	N-methyl-D-glucamine
NPC	Neuroprogenitor cell
NR2A	NMDA receptor subtype 2A
NR2B	NMDA receptor subtype 2B
OAT	Organic anion transporter
OGD	Oxygen glucose deprivation
P2X7	P2X purinoreceptor 7

P2Y1	P2Y purinorecepor 1
Panx1	Pannexin-1
Panx2	Pannexin-2
Panx3	Pannexin-3
PARP	Poly ADP ribose polymerase
PKM-zeta	N-terminal truncated form of protein kinase C zeta
PrPc	Cellular prion protein
pS	Picosiemens
PSD	Post-synaptic density
PSD-95	Post-synaptic density protein 95
PSEN	Presenilin
RMS	Root mean squared
ROS	Reactive oxygen species
RyR	Ryanodine receptors
SC	Schaffer col
SDS	Sodium dodecyl sulfate
SERCA	Sarco/endoplasmic reticulum Ca^{2+}-ATPase
SFK	Src Family Kinase
SH3	SRC homology 3 (domain)
shRNA	Short hairpin ribonucleic acid
siRNA	Small interfering ribonucleic acid
STIM	Stromal interacting molecule
TBS-T	Tris-buffered saline with Tween 20
TCE	2,2,2-trichloroethanol
TRPM	Transient receptor potential melastatin
TRPM2	Transient receptor potential melastatin 2
TRPV	Transient receptor potential, vanilloid
TTX	Tetrodotoxin
VGCC	Voltage-gated calcium channel

CHAPTER 1: INTRODUCTION

1.1 Introduction to Alzheimer's Disease

Alzheimer's disease (AD) is the leading cause of dementia affecting the elderly, significantly contributing to morbidity and mortality in this population. Dementia is characterized by the deterioration of cognitive functions such as memory which manifest with progressive neurodegeneration of the brain. AD and other forms of dementia lead to the loss of functional independence, eventually resulting in the reliance on caregivers such as family, friends and formal health care providers. In addition, the deterioration in the ability to form and retrieve memories represents a significant emotional burden to both the patient and their caregivers.

The worldwide prevalence of dementia in 2010 was estimated to be 35.6 million people (Prince et al., 2013). In Canada, the prevalence of dementia is approximately 564,000 people and is estimated to cost the health care system $8.3 billion dollars, with an additional $2.1 billion coming out of pocket from caregivers. The number of people living with dementia increases with age, representing roughly a third of Canadians over the age of 85. With the aging population, the prevalence of dementia, along with the costs and burden of caring for those with dementia, is projected to double by 2030 and triple by 2050 (Alzheimer Society of Canada, 2016). These realities have prompted governments, funding agencies, advocacy groups, and public health agencies to recognize AD and other dementias as a major societal challenge which requires urgent action (World Health Organization, 2012). This includes the diversion of resources towards the research and development of therapeutics.

Current drug treatments for AD are limited and only provide modest improvements to cognition and memory. As a result, research efforts have been devoted to understanding the

pathogenesis of AD to identify key molecular targets, with the hope of developing therapies which may reverse or significantly delay disease progression. One key area of focus is on how neurodegeneration occurs in the hippocampus, an area of the brain which is integral for the encoding and retrieval of memories. It is now recognized that early pathological changes in AD impact the function of glutamate synapses, the primary drivers of excitatory transmission which mediate the communication between neurons. This is significant as the dynamic changes in synapses known as synaptic plasticity are regarded as the basic substrate for learning and memory. Impairments in these synaptic processes are thought to promote AD pathogenesis. This next section will elaborate on the mechanisms underlying synaptic plasticity in the hippocampus, and how they come together to contribute to memory and learning.

1.2 Hippocampal dependent plasticity, learning, and memory

The Canadian psychologist Donald Hebb famously postulated in 1949 that during memory and learning, the synaptic connections between neurons become strengthened, a process now known as synaptic plasticity. Concrete evidence supporting this hypothesis would come decades later, when it was discovered that a long-lasting increase in the efficacy of synaptic transmission called long-term potentiation (LTP) could be induced by certain patterns of electrical stimulation. However, studies uncovering the molecular mechanisms behind the expression of LTP would only emerge after a deeper understanding of glutamate signalling at the excitatory synapse (Nicoll, 2017).

1.2.1 Excitatory synapses and glutamate signalling

The electrical activity between neurons is communicated through the activity of billions of connections called excitatory synapses. The excitatory synapse is composed of a pre-synaptic terminal which comes into close apposition with a dendritic spine, a highly specialized post-synaptic structure present on the dendrites of neurons. Synaptic transmission starts when glutamate, the primary excitatory neurotransmitter in the nervous system, is released from the pre-synaptic terminal. After spanning the synaptic cleft, glutamate binds to glutamate receptors expressed on the post-synaptic density, an area on the distal membrane of the dendritic spine which is enriched with synaptic receptors and scaffolding proteins (Figure 1.1) (Luscher & Malenka, 2012). The binding of glutamate induces a transient depolarization of the membrane called an excitatory post-synaptic potential (EPSP). This fast electrical transmission is primarily mediated by the α-amino-3-hydroxy-5-methyl-4-isoxazolepropionic acid (AMPA) receptor. AMPA receptors assemble as hetero tetrameric channels generally composed of GluA1/A2 or GluA2/A3 subunits which form a cation selective pore permeable to sodium but not calcium (although GluA2 lacking AMPA receptors are permeable to calcium, they are more rarely expressed) (Man, 2011). The opening of these receptors by glutamate binding allows the entry of sodium and leads to depolarization of the membrane, forming the basis for the EPSP.

The N-methyl-D-aspartate (NMDA) receptor is another type of ionotropic (ie. signalling through ion flux) glutamate receptor which is also enriched at the post-synaptic density. NMDA receptors are obligate hetero-tetrameric channels, consisting of two NR1 subunits and two NR2 or NR3 subunits. However, there are several unique features of NMDA receptors. In addition to the binding of glutamate to the NR2 or NR3 subunits, the activation of NMDA receptors requires the binding of the co-agonist glycine or serine to the NR1 subunits. Interestingly, NMDA

receptors contribute very little to the EPSPs following the release of glutamate, despite a high affinity for glutamate and sufficient basal levels of glycine/serine at the synaptic cleft. This is due to a voltage dependent block of the NMDA receptor pore by Mg^{2+}, which binds at resting membrane potentials and is relieved at depolarized potentials. Ion flux through NMDA receptors only occurs after sufficient depolarization of the post-synaptic membrane, often following the summation of AMPA receptor mediated EPSPs. Lastly, unlike AMPA receptors which primarily mediate the flux of sodium, NMDA receptors are permeable to both sodium and calcium. NMDA receptors therefore have a distinct function as they also play a role in intracellular calcium signalling (Iacobucci & Popescu, 2017). These features of the NMDA receptor would later hint at its importance in mechanisms of synaptic plasticity in the hippocampus.

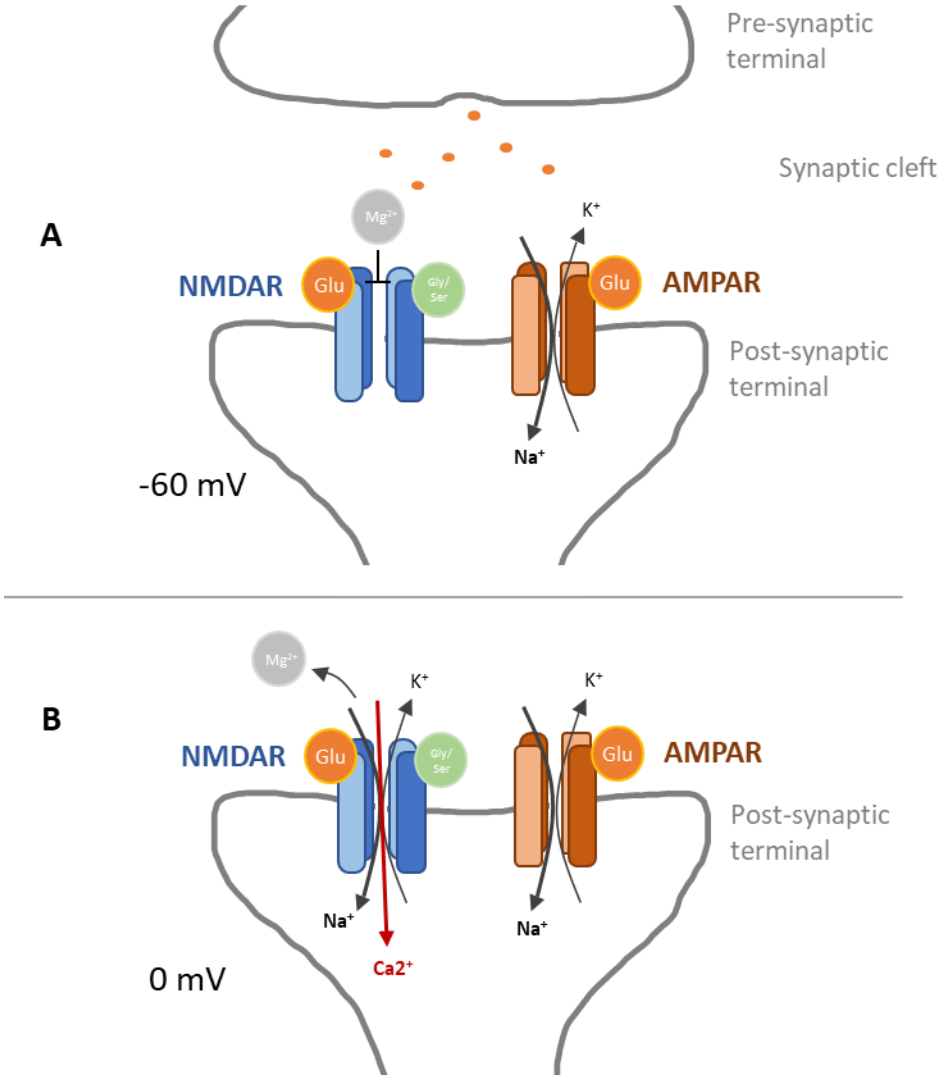

Figure 1.1: Excitatory synaptic transmission is driven by release and binding of glutamate to ionotropic glutamate receptors. Synaptic transmission begins with the release of glutamate from the pre-synaptic terminal. Glutamate diffuses across the synaptic cleft and binds to NMDA and AMPA receptors on the post-synaptic membrane. Glutamate binding to AMPA receptors opens the channel pore, allowing for the influx of Na^+ and efflux of K^+. The influx of Na^+ causes transient depolarization of the membrane potential (ie. EPSPs). **(A)** When the post-synaptic membrane is close to resting membrane potentials (ie. -60 mV), glutamate binding to NMDARs is insufficient to cause ion flux due to the block of the channel pore by Mg^{2+} ions. **(B)** At depolarized membrane potentials (ie. 0 mV), the Mg2+ block of NMDARs is expelled, allowing for ionic flux following glutamate binding. NMDA receptors are permeable to Ca^{2+} in addition to Na^+ and K^+.

1.2.2 NMDA receptors and LTP in the hippocampus

LTP and synaptic plasticity mechanisms have been best studied in the hippocampus, a pair of highly-organized brain structures tucked within the medial temporal lobes of the brain. The predominant excitatory pathway in the hippocampus is composed of a tri-synaptic circuit: Afferent information from the entorhinal cortex is transmitted through the perforant path to the granule cells of the dentate gyrus (DG), which project mossy fibres onto the proximal dendrites of CA3 neurons; CA3 neurons then send this signal through the Schaffer collateral pathway to CA1 pyramidal neurons that project back into the entorhinal cortex (Figure 1.2). CA3 neurons also have a high density of recurrent projections to other CA3 neurons in the ipsilateral and contralateral hippocampus through the associational/commissural (AC) pathway (Neves, Cooke, & Bliss, 2008).

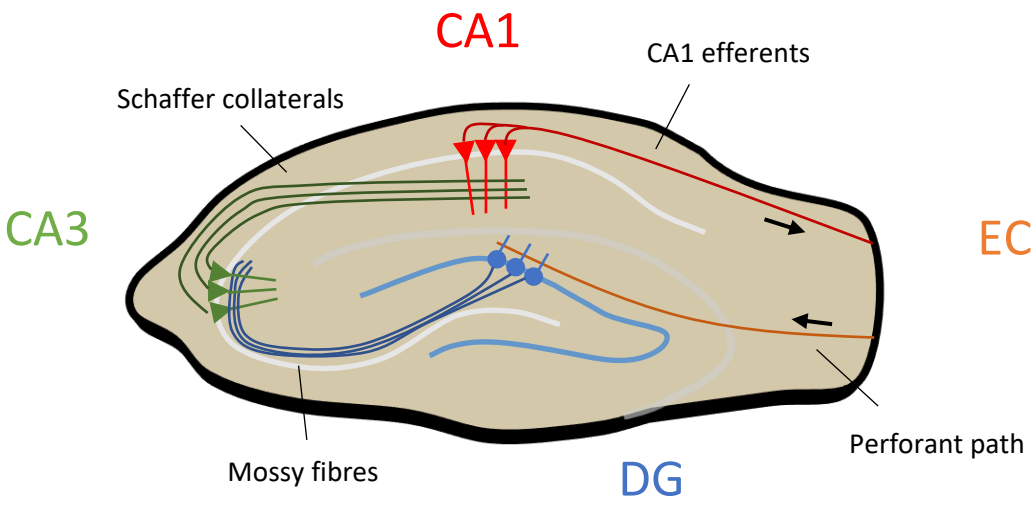

Figure 1.2: The tri-synaptic circuit of the hippocampus. Simplified cross-sectional diagram depicting the main excitatory circuit in the hippocampus. Afferent fibres from layer II neurons of the enthorhinal cortex (EC) travel through the perforant path and synapse with the granule cells of the dentrate gyrus (DG). Mossy fibres from the DG then project toward the CA3 region of the hippocampus and synapse at the proximal dendrites of the pyramidal neurons. CA3 pyramidal neurons synapse with CA1 pyramidal neurons through the schaffer collateral pathway which runs through the CA1 dendritic layer. CA1 efferents then project back into the entorhinal cortex.

LTP was first defined at the CA3-CA1 synapse, where it was revealed that the repetitive high frequency stimulation (HFS) at the Schaffer collateral pathway leads to the long-lasting enhancement of synaptic transmission at CA1 neurons. This quickly led to efforts in elucidating the molecular events behind the expression of LTP. Historically, two candidate mechanisms were proposed. In the pre-synaptic hypothesis, LTP occurs due to the long-term increase in glutamate release from the pre-synaptic terminal. This was thought to either occur intrinsically (ie. independent of post-synaptic involvement) or through retrograde signalling from molecules released by the post-synaptic terminal. Others hypothesized that LTP was intrinsic to the post-synaptic membrane, where there is a long-lasting increase in the response to glutamate at the

post-synaptic membrane. The first clues came from early experiments looking at the functions of the NMDA receptor at CA3-CA1 synapses. It was found that while the block of NMDA receptors with the glutamate binding antagonist APV alone did not cause a change in synaptic transmission, administration of APV during HFS completely blocked the induction of LTP (Collingridge, Kehl, & McLennan, 1983). This demonstrated that NMDA receptors are activated during HFS and play a vital role in the expression of LTP, giving weight to the hypothesis that the mechanism of LTP induction at the CA3-CA1 synapse at least requires post-synaptic involvement. During HFS, the sustained depolarization of the post-synaptic membrane due to the summation of AMPA receptor-mediated EPSPs leads to relief of Mg^{2+} block on the NMDA receptor, allowing for channel activation. The next breakthrough came when it became apparent that LTP involved the increase in the post-synaptic activity of AMPA receptors (Kauer, Malenka, & Nicoll, 1988) which is now known to be mediated by the trafficking of additional AMPA receptors to the PSD (Hayashi et al., 2000). Together, these post-synaptic mechanisms readily explained the sustained increase in synaptic strength following LTP induction. It is however important to note that there is still merit to the pre-synaptic hypothesis of LTP. A number of NMDA receptor independent mechanisms of LTP have been described (Bayazitov, Richardson, Fricke, & Zakharenko, 2007; Nicoll & Schmitz, 2005), and it is now understood that the mechanisms of LTP expression can vary across different types synapses and may change depending on the pattern of stimulation used.

1.2.3 Calcium signalling, protein phosphorylation, and bidirectional plasticity

How does NMDA receptors activity lead to the increased trafficking of AMPA receptors to the post-synaptic membrane following LTP induction? When NMDA receptors become

activated during HFS, there is an influx of calcium into the dendritic spine. This leads to the activation of calcium dependent protein kinases such as calcium/calmodulin dependent kinase II (CamKII). One of the targets for CamKII are AMPA receptors – phosphorylation of AMPA receptors by CamKII leads to both an increase in its trafficking to the post-synaptic membrane as well as an increase in channel conductance (Nicoll, 2017).

Interestingly, low-frequency stimulation (LFS) applied at the Schaffer collateral pathway induces a stable decrease in synaptic transmission at the CA3-CA1 synapse, a process called long-term depression (LTD). Like LTP, it has been demonstrated that LTD is dependent on NMDA receptor activity. Whereas HFS activates protein kinases, LFS leads to the activation of calcium dependent protein phosphatases such as calcineurin (also known as PP2B) and STEP (Luscher & Malenka, 2012). How do NMDA receptors mediate this bidirectional plasticity? It has been proposed that the frequency dependent pattern of Ca^{2+} influx through NMDA receptors differentially favours LTP or LTD by modulating the balance between protein kinase and phosphatase activity (Castellani, Quinlan, Bersani, Cooper, & Shouval, 2005). However, more recent evidence suggests that calcium flux through NMDA receptors is not required for LTD (Nabavi et al., 2013). Evidence for this assertion was provided by experiments demonstrating that LTD could be blocked by APV, but not MK-801. APV acts as a competitive antagonist of the glutamate binding site of the NMDA receptor, which inhibits channel opening by preventing the agonist induced conformational change of the channel. On the other hand, MK801 is an open pore blocker which only prevents ion flux through the channel following its activation (ie. uncompetitive antagonist). Therefore, it is the signalling functions of the NMDA receptor independent of ion flux through its pore which mediate LTD. More and more studies are

supporting this non-canonical “metabotropic” function of NMDA receptors (Dore, Aow, & Malinow, 2016).

1.2.4 Maintenance of LTP requires gene transcription and translation

While the early phase of plasticity is mediated by post-translational modifications such as phosphorylation, these effects are ultimately unstable. More permanent changes at the synapse require gene transcription and translation. LTP induced kinase activity causes the downstream activation of key transcription factors. The cAMP response element binding protein (CREB) is activated by its calcium dependent phosphorylation via the CaMK family of kinases and through the Ras/MAPK pathway (Kornhauser et al., 2002). Other transcription factors include NF-κB, as well as activating protein-1 (AP-1) which is composed of Jun, Fos and ATF homo- or heterodimers. Activation of these transcription factors in turn regulate the expression of early immediate genes necessary for the long-term strengthening of the synapse (Alberini, 2009). On the other hand, LTD is associated with the expression of the IEGs such as Arc which weaken the synapse. The persistent activity of Arc at the synapse is thought to mediate a sustained increase in AMPA receptor endocytosis after LTD induction (Jang & Chung, 2016; Josselyn, Köhler, & Frankland, 2015).

1.2.5 Synaptic plasticity is associated with dynamic structural changes

Changes in synaptic transmission after the induction of LTP and LTD are reinforced by structural changes at the level of the dendritic spine. The morphology of the spine reflects the strength and maturity of the synapse; stubby and thin spines represent weaker synapses, while mushroom spines which have large spine heads are stable synapses (Rochefort & Konnerth,

2012). Dendritic spine structure is highly dynamic; its shape and size is controlled by the constant polymerization and depolymerization of an F-actin meshwork within the spine head (Bosch & Hayashi, 2012). Two-photon imaging experiments have allowed for the in vitro and in vivo observation of spine dynamics during synaptic plasticity. After LTP induction, the formation of new immature spines called filopodia have been observed. Pre-existing dendritic spines rapidly enlarge through the stabilization of F-actin and the resulting expansion of the actin meshwork (Bosch et al., 2014; Sala & Segal, 2014). On the flipside, LTD causes the shrinkage and removal of spines. Changes in actin dynamics are accompanied by a change in the surface area of the PSD (Bosch et al., 2014). Scaffolding proteins such as Homer, Shank and PSD-95 are important in the regulation of post-synaptic receptor trafficking and mediate downstream signalling cascades through the formation of signalling complexes with glutamate receptors. Together, structural plasticity contributes to the functional strengthening or weakening of the synapse by altering dendritic spine structure.

1.2.6 The synaptic plasticity and memory hypothesis

It was first discovered that the hippocampus is functionally important for memory and learning in the 1953 report on the case of H.M, a patient who developed amnesia following the surgical removal of both hippocampi as a treatment for intractable seizures. Ablation experiments in animal models further delineated the role of the hippocampus in the encoding and retrieval of episodic and spatial memory (Neves et al., 2008). Memory is now thought to reside in associated synaptic networks called engrams which are distributed throughout the brain. The role of the hippocampus then is to act as the central hub which facilitates the encoding and retrieval of these engrams (Josselyn et al., 2015).

When LTP in the hippocampus began to be characterized in 1971, a concrete link between synaptic plasticity and memory, as proposed earlier by Hebb, started to take shape. This synaptic plasticity and memory (SPM) hypothesis is now convincingly supported by multiple lines of evidence (Neves et al., 2008; Takeuchi, Duszkiewicz, & Morris, 2013):

i) Hippocampal memory formation is correlated with an increase in synaptic efficiency associated with LTP. Matsuo et al. showed that AMPAR expression and recruitment to CA1 mushroom spines is increased and maintained for 24 hours after contextual fear conditioning (Matsuo, Reijmers, & Mayford, 2008).

ii) The ablation of key molecular targets in synaptic plasticity can cause an alteration in anterograde memory formation. This is best shown in pharmacological block and KO studies of NMDA receptors. For example, treatment of rodents with APV during in vivo extracellular recording at the CA1 region has been shown to inhibit LTP and concomitantly cause deficits in spatial memory tasks (Davis, Butcher, & Morris, 1992; Morris, Anderson, Lynch, & Baudry, 1986).

iii) Hippocampal synaptic plasticity is also important in memory storage, as alterations of plasticity mechanisms after learning can cause retrograde amnesia. In a pivotal study focusing on the role of PKM-zeta, a key kinase in LTP maintenance, it was shown that inhibition of PKM-zeta with the inhibitory peptide ZIP causes retrograde amnesia of active place avoidance memory (Pastalkova et al., 2006). Subsequent studies have shown that PKMzeta is necessary for the maintenance of object location memory (Hardt, Migues, Hastings, Wong, & Nader, 2009; Virginia Migues et al., 2010).

iv) LTP induction causes the activation of transcription factors such as CREB and NF-kB which mediate the expression of immediate-early genes. The activity of these transcription factors has been shown to be necessary for late-phase LTP maintenance as well as memory consolidation and reconsolidation (Alberini, 2009).

v) Learning-dependent cell labelling techniques have allowed researchers to more directly link the encoding of an engram to formation of the memory. The Tonegawa lab linked channelrhodopsin (ChR) to the promotor of the IEG c-Fos. During fear memory tasks, this caused expression of ChR in a specific assembly of hippocampal neurons associated with that fear memory. Optogenetic re-activation of these neurons then caused re-expression of the fear response (T. J. Ryan, Roy, Pignatelli, Arons, & Tonegawa, 2015).

1.2.7 Synaptic plasticity and memory in other regions of the hippocampus

Synaptic plasticity has also been studied at other excitatory synapses in the hippocampus. Like the CA3-CA1 synapse, the perforant path inputs onto dentate granule cells and CA3-CA3 pyramidal cell recurrent synapses exhibit a post-synaptic NMDA receptor dependent LTP as described above. Interestingly, KO studies of the NMDAR NR1 subunit in the dentate gyrus and CA3 regions have uncovered subtle memory functions independent of gross spatial memory impairments (McHugh et al., 2007; Nakazawa et al., 2002, 2003). Granule cells and their mossy fibre projections onto CA3 neurons play a role in pattern separation, or the ability to pick out and remember small details which distinguish an object within a spatial context (Leutgeb, Leutgeb, Moser, & Moser, 2007). On the other hand, the high density of recurrent synapses from associational/commissural fibres in the CA3 region is important for the process of pattern completion, that is the ability to recall a memory when only given an incomplete subset of

contextual clues (Rebola, Carta, & Mulle, 2017). Therefore, it is important to keep in mind that regional deficits in plasticity mechanisms may lead to subtle memory deficits which are not detected with standard memory tasks.

The DG-CA3 synapse is unique as it expresses a pre-synaptic, NMDA receptor independent form of LTP. Here, giant mossy fibre terminals called mossy fiber boutons synapse with multiple thorny excrescences on the proximal dendrite of CA3 neurons. MF synapses exhibit low tonic release probability, but are highly amenable to short-term facilitation by repetitive stimulation (Nicoll & Schmitz, 2005). Unlike at other synapses of the hippocampus, HFS at MF synapses cause a large and prolonged increase in neurotransmitter release mediated by pre-synaptic calcium (Y. Kawamura et al., 2004; Nicoll & Schmitz, 2005). MF LTD induced by LFS (eg. 1 Hz for 15 min) is also expressed pre-synaptically and is thought to act through the action of pre-synaptic mGluR2 (Kobayashi, Manabe, & Takahashi, 1996; Tzounopoulos, Janz, Südhof, Nicoll, & Malenka, 1998).

In conclusion, the elements of synaptic strengthening and weakening known as synaptic plasticity act as the substrates for memory formation in the hippocampus. The next section will discuss how the dysfunction and degeneration of excitatory synapses is a major pathological feature which underlies cognitive decline and memory loss in AD.

1.3 Alzheimer's disease pathogenesis

1.3.1 AD as a proteinopathy: amyloid-β and hyperphosphorylated tau

In 1907, the German psychiatrist and neuropathologist Dr. Alois Alzheimer described the pathological hallmark of senile plaques and neurofibrillary tangles in post-mortem brain samples of dementia patients with AD. Subsequent research isolated the protein from the senile plaques

which were found to be composed of aggregates of amyloid-β; later it was found that neurofibrillary tangles (NFT) contained aggregates of hyperphosphorylated tau. The characterization of these proteins served as the first clue towards a causative agent for the disease. Today, AD is described as a disease of proteinopathy, where the accumulation of amyloid-β and tau are implicated in AD progression.

Amyloid-β is a small ~4.5 kDa peptide which is produced by cleavage of the membrane bound amyloid precursor protein (APP). APP cleavage is catalyzed by the pair of enzymes β-secretase and the γ-secretase. Due to variation in the C-term cleavage location by γ-secretase, amyloid-β peptides exist with different lengths, the most common being 40 residues (ie. $A\beta_{1-40}$) and 42 residues (ie. $A\beta_{1-42}$). N-term truncated amyloid-β peptides are also present, and are likely formed by post cleavage degradation (Kummer & Heneka, 2014). When released into the extracellular space, amyloid-β peptides do not only merely exist as monomeric peptides; instead, amyloid-β is in equilibrium between a pool of soluble monomers, soluble oligomers, and insoluble fibrils which aggregate to form amyloid plaques. The relative quantity of different lengths of amyloid-β peptides has been proposed to shift this equilibrium. For example, the $A\beta_{1-42}$ species is known to be more prone to oligomerization than $A\beta_{1-40}$, and a larger ratio of $A\beta_{1-42}$ to $A\beta_{1-40}$ has been used as a predictor of disease (Mucke & Selkoe, 2012). Changes in the clearance of amyloid-β by putative degradation enzymes such as insulin degradation enzyme (IDE) and matrix metalloproteinases (MME) and its phagocytosis by immune cells (ie. microglia and peripheral monocytes) can also affect levels of amyloid-β (Baranello et al., 2015; Lai & McLaurin, 2012). Therefore, a global increase in amyloid-β production, a decrease in its clearance, and an imbalance in the equilibrium of amyloid-β aggregation are all key factors which contribute to the buildup of amyloid-β in AD (Figure 1.3).

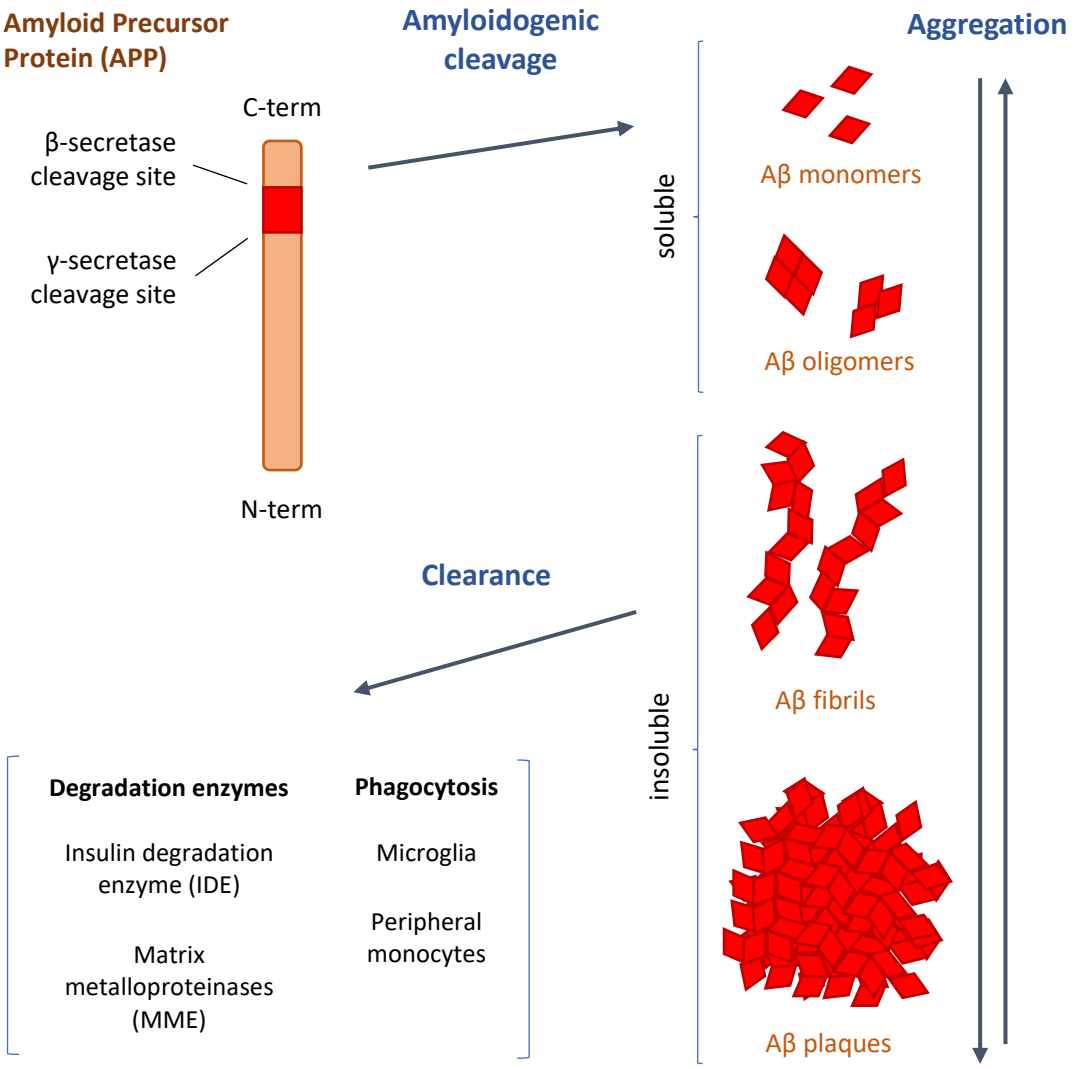

Figure 1.3: Amyloid-β production, aggregation and clearance. Cleavage of APP by γ- and β-secretases produces soluble amyloid-β monomers. Amyloid-β monomers can aggregate to form soluble amyloid-β oligomers and insoluble fibrils which eventually form plaques. The clearance of the various forms of amyloid-β is managed by enzymatic degradation by IDE and MMEs as well as phagocytosis by immune cells.

Tau is a microtubule associated protein (MAP) which binds tubulin and help stabilize microtubules in mature neurons. Six isoforms of tau exist ranging in lengths of between 352 and

441 amino acids. Tau is a phosphoprotein, requiring the 3-4 phosphorylation groups to serve its function. In the normal physiological setting, tau is almost completely bound to tubulin in the neuron. However, in pathological contexts such as AD and other tau related diseases such as frontotemporal dementia (FTD), tau can become hyperphosphorylated; these forms of tau do not bind tubulin, but aggregate in the cytosol as soluble oligomers and insoluble neurofibrillary tangles. Soluble hyperphosphorylated tau has been shown to disrupt microtubules by sequestering normal tau and other MAPs. In addition, hyperphosphorylated tau is more resistant to proteolysis than regular tau, leading to its buildup in the AD brain. Tau function was classically thought to be restricted to the axon; however evidence now points to important roles of tau in dendritic and post-synaptic compartments as well (Spires-Jones & Hyman, 2014).

1.3.2 Amyloid-β cascade hypothesis

It is thought that the early accumulation of amyloid-β is the primary insult which triggers AD disease progression. Multiple arguments support this amyloid-β cascade hypothesis (Selkoe & Hardy, 2016):

i) The accumulation of amyloid-β can precede clinical manifestation of AD by up to 20 years. Biomarker studies of AD patients have demonstrated that a rise in the levels of amyloid-β are seen before the accumulation of tau, neuroimaging derived structural changes and memory deficits (Jack et al., 2013).

ii) The two common familial forms of AD involve autosomal dominant mutations in APP and presenilin (PSEN), the catalytic subunit of the gamma secretase complex. Mutations in these genes lead to early onset AD and have been shown to alter amyloid-

β processing, increasing total amyloid-β levels and an increased proportion of the oligomerized and fibrillary forms (N. S. Ryan & Rossor, 2010).

iii) In sporadic AD, disease risk can be predicted by genetic variants of the APOE gene, where the APOE-ε4 variant is known to greatly increase risk of developing AD. The APOE protein is also implicated in modulating the clearance of amyloid-β (Verghese et al., 2013).

iv) While neurofibrillary tangles are a hallmark of AD pathology, they are not exclusive to AD. NFT accumulation is linked to frontotemporal dementia and several other forms of neurodegenerative diseases which progress independently of amyloid-β levels (Iqbal, Liu, Gong, & Grundke-Iqbal, 2010).

v) The accumulation of amyloid-β has been shown to be sufficient in inducing AD-like memory deficits in animal models. Genetic mouse models of AD have been generated to study the effects of amyloid-β accumulation. Several APP/PS1 mouse models have been produced which express human APP and PS1 mutations. These mice exhibit an age dependent increase in amyloid plaque deposition which lead to deficits in hippocampal dependent memory tasks such as spatial working memory (Ittner et al., 2010).

These arguments do not preclude the importance of tau in AD. Indeed, the accumulation tau has been shown to better correlate with the start of cognitive decline in AD patients (Jack et al., 2013). This observation lead to the analogy of amyloid-β acting as a trigger and tau acting as the bullet of the gun – several studies support a model where tau synergistically acts with amyloid-β to cause progressive neurodegeneration (Bloom, 2014). While efforts to link the

pathological mechanisms of these two proteins continue to be important, it is equally essential to tease out their independent actions. The remainder of this thesis will focus on the toxic effects of amyloid-β on synaptic function in the hippocampus.

1.3.3 AD mouse models and hippocampal synapse dysfunction

Much research has focused on elucidating the mechanism by which amyloid-β leads to memory dysfunction. The prevailing hypothesis is that amyloid-β directly exerts its toxic effects by initiating dysfunction of glutamate synapses (Mucke & Selkoe, 2012; Selkoe & Hardy, 2016). Much of the evidence supporting this hypothesis started in studies of transgenic AD mouse models. Electrophysiological recordings have showed that AD mice exhibit deficits in synaptic plasticity which correlate or even precede impairments in cognitive behavioural tests (Selkoe, 2008). When compared to age matched controls, AD mice have a reduction in the expression of NMDA receptor dependent LTP along with a potentiation of LTD in the CA1 and dentate gyrus. It is thought that by favouring LTD and inhibiting LTP, amyloid-β directly effects the plasticity mechanisms required for memory formation. This shift towards LTD mechanisms is thought to destabilize dendritic spines (Henriques, Oliveira, Carvalho, & da Cruz e Silva, 2015), leading to the long-term reduction in the number of synapses. Indeed, AD mice exhibit an age-dependent reduction in glutamatergic synapses in the hippocampus (Shankar et al., 2007; Shankar & Walsh, 2009). Markers for both pre-synaptic terminals such as synaptophysin, as well as markers for mature spines such as PSD-95 and drebrin are reduced in AD mouse models and in post-mortem brain tissue of AD patients. It is important to note that frank neuronal loss in AD manifests long after the first appearance cognitive symptoms; degeneration begins at the synapses, which spread

back into the neurites and finally the soma. Therefore, amyloid-β initiates memory deficits by impairing excitatory synapse function in the hippocampus.

1.3.4 Synaptotoxicity is driven by soluble amyloid-β oligomers

Early hypotheses tried to link the buildup of insoluble fibrillary amyloid-β and the formation of senile plaques to AD pathogenesis. However, pathological studies of post-mortem brain samples have concluded that plaque burden does not necessarily correlate with manifestation of disease; instead, it is the concentration of amyloid-β oligomers (AβO) which are better correlated (Esparza et al., 2013).

There is now a large body of evidence implicating AβOs as a neurotoxic agent which contributes to disease progression in AD (Kayed & Lasagna-Reeves, 2013; Lesne, 2014; Selkoe & Hardy, 2016). The acute treatment of healthy rodents with AβOs has been shown to be sufficient for the induction of synaptic deficits similar to those seen in AD mouse models. In one convincing study by Shankar et al, AβOs isolated from AD patient brains were injected into the hippocampus of mice. AβO treatment led to deficits in hippocampal synaptic plasticity, changes in synapse structure, and behavioural deficits in cognitive and memory tasks. In contrast, these effects were not seen after treatment with monomeric isolates of amyloid-β (Shankar et al., 2008). Numerous studies also demonstrate the synaptotoxic effect of synthetic and cell line derived amyloid-β oligomers on in vivo and in vitro models (Calabrese et al., 2007).

1.3.5 Amyloid-targeted therapies

Evidence supporting the amyloid cascade hypothesis of AD has driven tremendous effort in developing amyloid-targeted therapies. The aim of these drugs is lower the levels of amyloid-β in the brain, either by increasing its clearance (eg. passive and active antibodies) or reducing its

production (eg. β-secretase and γ-secretase inhibitors and modulators). By removing the primary driver of disease pathogenesis, it is thought that clinical improvements would follow. But despite promising results in pre-clinical trials and a proven ability to lower brain amyloid-β levels, these drugs have been unsuccessful in Phase III trials, showing no improvement in the progression of cognitive impairments in AD patients (Mehta, Jackson, Paul, Shi, & Sabbagh, 2017).

While the failure of amyloid-targeting trials has been used as evidence against the notion that amyloid-β is the primary driver behind the pathogenesis of AD, several other factors better account for the shortcoming of these trials. Failure in improving clinical outcomes in some of these trials are due to inherent failures in the strategy used to lower amyloid-β. In a phase III study of the γ-secretase inhibitor semagacestat, cognitive decline was actually shown to worsen in the treatment group (R. S. Doody et al., 2013). This has been attributed to the broad physiological function of gamma secretase, which is known to also cleave important signalling molecules such as Notch (Selkoe & Hardy, 2016). In the case of antibody targeting of amyloid-β, the types of species or aggregates which are targeted may have an important bearing on clinical effectiveness and tolerability of the drugs. Promising Phase I clinical data on the anti-amyloid antibody aducanumab has been attributed to its ability to bind oligomers and plaques but not monomers, possibly allowing for a better therapeutic index compared to bapineuzumab (Sevigny et al., 2016).

It has also been proposed amyloid-lowering therapies haven't been effective due to the advanced stages of AD patients enrolled in these studies. Given that accumulation of amyloid-β occurs years before clinical manifestation of the disease, it is hypothesized that amyloid-β causes a pathological cascade of changes which may not be sensitive to the reduction of amyloid-β after clinically apparent disease. Indeed, post-hoc analysis in some of the anti-amyloid antibody trials

have showed improvements in cognitive outcomes in patients with mild AD (R. S. Doody et al., 2014; Salloway et al., 2014). Current trials are now also targeting patients with prodromal AD – patients who fall under the criteria of mild cognitive impairment and also exhibit a high amyloid-β burden as determined by brain amyloid imaging protocols (Sevigny et al., 2016). Other trials are aimed at the prevention or delay in the development of cognitive impairment in cohorts of patients with familial forms of AD (Bateman et al., 2017).

It has been argued that the amount of time and resources that was allocated to these amyloid-targeted clinical trials may have been premature – we simply do not know enough about the pathogenic role of AβOs and its interactions with other disease mechanisms in AD. By better understanding the molecular mechanisms of AβO toxicity, we may discover novel therapeutic targets for the treatment of AD. A wide range of mechanisms of toxicity have been reported for AβOs, including its effects on glial cells and the induction of neuroinflammatory pathways. However, the focus of this thesis is on the overarching hypothesis that toxic AβOs can directly act at the level of glutamatergic synapses to mediate neurotoxicity.

1.4 Chronic glutamate excitotoxicity model of AD

The action of glutamate on excitatory synapses is the driver for communication between the pyramidal neurons of the hippocampus as well as other excitatory neurons of the CNS. However, excessive glutamate signalling is detrimental to excitatory synapse function and can eventually lead to neurodegeneration and cell death. This process is called glutamate excitotoxicity and is primarily driven by the overactivation of NMDA receptors and the loss of calcium homeostasis in the cell. Glutamate excitotoxicity is known to be the primary driver of pathology in stroke; following metabolic compromise, there is an uncontrolled release of

glutamate which leads to the acute and sub-acute degeneration of these neurons. However, there is also evidence that prolonged dysregulations in glutamate signalling can lead to slower pathological changes in neurodegenerative diseases such as AD. This chronic glutamate excitotoxicity hypothesis and its link to the synaptic actions of AβOs will be the topic of discussion in this section, including mechanisms behind the binding of AβOs to the synapse and their downstream effects on glutamate reuptake and glutamate receptors function. The impact of AβOs on calcium homeostasis will then be discussed.

1.4.1 Effects on glutamate release and reuptake

AβOs contributes to excitotoxicity by inducing an increase in extracellular levels of glutamate through the impairment of glutamate re-uptake. Li et al. showed that scavenging of extracellular glutamate reduces AβO induced facilitation of LTD in mouse hippocampal slice. Conversely, the block of glutamate reuptake produces a similar facilitation of LTD as AβO treatment (S. Li et al., 2009). Given that extracellular glutamate is heavily regulated by astrocytes, some studies have also looked at the effects of AβOs on astrocytes function. AβOs have been shown to downregulate astrocytic glutamate re-uptake by reducing the expression of glutamate transporters (Matos et al., 2012). Astrocytes can also become hyperactive with AβO treatment, leading to increased glutamate release through connexin hemichannels (Delekate et al., 2014; Orellana, Froger, et al., 2011). In addition, AβOs may directly alter synaptic release of glutamate at the pre-synaptic terminals of neurons. AβOs can induce an increase in the number of primed synaptic vesicles through the disruption of vesicular release machinery following its internalization into pre-synaptic terminals (Russell et al., 2012). Pre-synaptic glutamate release may also be altered by the extracellular binding of AβOs to pre-synaptic scaffolding proteins

such as neurexin (Naito, Tanabe, Lee, Hamel, & Takahashi, 2017). It is important to note that if extracellular glutamate is not tightly regulated, it can spill over from the synaptic cleft and accumulate in extra-synaptic compartments. Excess glutamate therefore contributes to excitotoxicity in AD through the over-stimulation of both synaptic and extra synaptic glutamate receptors (Hardingham, Fukunaga, & Bading, 2002; S. Li et al., 2011).

1.4.2 Post-synaptic binding of amyloid-β oligomers

AβOs are also thought to directly disrupt signalling at the post-synaptic membrane. AβOs have been described as "sticky" proteins which directly bind to the post-synaptic density at excitatory synapses (Lacor, 2004; Lacor et al., 2007; Renner et al., 2010; Sinnen, Bowen, Gibson, & Kennedy, 2016). This interaction is thought to directly impact the function of glutamate receptors. AβOs have been shown to complex with PrPc, a GPI-anchored extracellular scaffolding protein enriched at the post-synaptic density. PrPc is necessary for AβO induced deficits in plasticity which can be rescued by using a targeted antibody to block the binding domain of AβOs to PrPc (J. W. Um et al., 2012). PrPc is known to associate with several synaptic receptors, including glutamate receptors (Wulf, Senatore, & Aguzzi, 2017). Um et al. proved that LTD deficits caused by AβO binding to PrPc are mediated through the dysregulated activation of the metabotropic glutamate receptor 5 (mGluR5) and downstream Fyn kinase signalling (J. Um et al., 2013). In the hippocampus, mGluR5 is expressed in a peri-synaptic zone which surrounds the post-synaptic density. This receptor closely interacts with NMDA receptors, and is known to modulate the expression of LTP and LTD by regulating their function (Sarantis, Tsiamaki, Kouvaros, Papatheodoropoulos, & Angelatou, 2015). The pharmacological block of mGluR5 has been shown to ameliorate the AβO induced deficit in LTP and facillitation of LTD

in hippocampal slice (Rammes, Hasenjäger, Sroka-Saidi, Deussing, & Parsons, 2011; Shankar et al., 2008; J. Um et al., 2013) and even in vivo (Neng-Wei Hu et al., 2014). This was correlated with a reduction in amyloid-β oligomer induced spine loss and improvements in spatial learning tasks (J. Um et al., 2013). Later, groups have showed that the AβO-PrPc complex may also directly interact with NMDA receptors. PrPc acts as a negative regulator of NMDA receptor activity - the binding of AβOs to PrPc disrupts this association, leading to NMDA receptor hyperactivity (Black, Stys, Zamponi, & Tsutsui, 2014; You et al., 2012).

1.4.3 Amyloid-β Oligomers and NMDA receptors

NMDA receptors play a central role in the dysregulation of synaptic function seen in AD. As discussed earlier, NMDA receptors are integral to the expression of bidirectional plasticity at hippocampal synapses, and AβOs have been shown to induce a deficit in LTP and facilitation of LTD at the CA3-CA1 and the perforant path to DG synapses. Interestingly, it has been shown that there is a subunit specific effect of AβOs on NMDA receptor signalling. In the CA1 region of the hippocampus, NR2B subunit containing NMDA receptors are thought to predominantly mediate LTD whereas the NR2A subunit containing NMDA receptors mediate LTP (L. D. Liu et al., 2004). It is also known that NMDA receptors expressed outside of the synapse (ie. extrasynaptic NMDA receptors) are primarily composed of NR2B subunits. Evidence points to a greater contribution of NR2B containing NMDA receptor activation to the synaptotoxic effects of AβOs. The selective pharmacological block of the NR2B but not NR2A are sufficient to rescue deficits in synaptic plasticity, prevent amyloid induced synapse loss, and ameliorate memory deficits in rodent models (N.-W. Hu, Klyubin, Anwyl, & Rowan, 2009; S. Li et al., 2011; Rönicke et al., 2011). Intriguingly, emerging literature has also suggested that the

synaptotoxic effects of AβOs can act through metabotropic NMDA receptor signalling (Birnbaum, Bali, Rajendran, Nitsch, & Tackenberg, 2015; Tamburri, Dudilot, Licea, Bourgeois, & Boehm, 2013). That is synaptic depression induced by AβOs does not necessarily require ionic flux, and is instead contingent on the non-canonical signalling of NR2B containing NMDA receptors (Kessels, Nabavi, & Malinow, 2013). Regardless, the excitotoxic activation of NMDA receptors is thought to lead to calcium dyshomeostasis in the neuron, resulting in synaptic dysfunction and neurodegeneration (Agostini & Fasolato, 2016; Magi et al., 2016; Supnet & Bezprozvanny, 2010).

1.4.4 Calcium dyshomeostasis in synaptic dysfunction and neurodegeneration

Calcium overload is one of the common pathological mechanism in neurodegenerative diseases. AβO induced glutamate excitotoxicity contributes to the dyshomeostasis of intracellular calcium; indeed, evidence supports the notion that amyloid-β accumulation leads to an elevation in neuronal calcium in mouse models of AD (Arbel-Ornath et al., 2017; Chakroborty et al., 2012; Kuchibhotla et al., 2008). Increased intracellular calcium is hypothesized to partially mediate the early deficits in synaptic plasticity in AD. Calcium signalling depends on the maintenance of a large calcium gradient (10,000 fold difference) between the intracellular and extracellular compartments. The magnitude of calcium transients, as well as their spatial and temporal patterns, have differential effects on the variety of calcium dependent proteins in the neuron. At the synapse, it is thought that CAMKII is induced by large calcium transients through NMDA receptors, leading to LTP. On the other hand, calcineurin is induced by a more sustained lower level calcium influx, causing LTD. When intracellular calcium is increased in AD, then this calcium gradient becomes smaller, effectively decreasing the signal to noise ratio of calcium.

This impairs the ability of CAMKII to resolve large transients, while favouring the activation of calcineurin by more slow and sustained increases in calcium (Parsons, Stöffler, & Danysz, 2007).

The prolonged dysregulation of neuronal calcium eventually causes synaptic degeneration and cell death. This is mediated by a number of calcium dependent processes. The long-term activation of calcineurin leads to the pathological reduction in synapse numbers. Calcium can also activate calpains, a calcium dependent protease which has been shown to degrade pro-survival proteins. The activity of both of these enzymes have been shown to be upregulated in AD neurons (Trinchese et al., 2008; Yu, Chang, & Tan, 2009). Elevated calcium levels disrupt the function of mitochondria, leading to the accumulation of reactive oxygen species (ROS) and the induction of apoptotic pathways (Yu et al., 2009). Similarly, the loss of calcium homeostasis can involve the depletion of ER calcium stores, causing ER stress. Prolonged ER stress can also trigger cell death (Matus, Glimcher, & Hetz, 2011).

1.5 Therapeutic development in AD

Research into amyloid-lowering therapies has dominated the field over that past few decades and future efforts in area realm may still prove to be fruitful. However, AD is a complex disease with many different factors which contribute to pathology. For the successful pharmacological management of AD, multiple drug targets will likely be needed. In addition, it is important to keep in mind that the effectiveness of different strategies may change according to the stage of the disease – while amyloid-targeting therapies may prove to be an effective strategy for prevention, a different set of therapies may need to be instituted as cognitive function deteriorates.

Currently approved drugs for the treatment of AD work by rectifying imbalances in neurotransmitter signalling. Therapeutic progress may be gained from better understanding how these systems are affected in the disease and funnelling resources into discovering improved drug targets within these signalling pathways. Acetylcholinesterase inhibitors such as donepezil were the first drugs approved for the treatment of AD and are thought to improve cognition by helping to restore cholinergic tone innervating hippocampal neurons. Unfortunately, these drugs only provide modest improvements in cognitive performance, do not respond in all patients, and often become ineffective as the disease progresses.

1.5.1 NMDA receptor blockade in AD

Given the apparent pathological role of the NMDA receptor in excitotoxity in a range of CNS diseases, the development of NMDA receptor antagonists as a therapeutic strategy was thoroughly pursued. The problem with this approach is that NMDA receptors are ubiquitously expressed throughout the nervous system and have important physiological roles. In clinical trials for stroke and traumatic brain injury, competitive antagonists for the glutamate and glycine site of the NMDA receptor as well as open pore blockers were tested with hopes of reducing excitotoxic cell death. However, these trials proved to be unsuccessful. The administration of therapeutic doses of many of the drugs were limited by unacceptable adverse events, including psychiatric side effects. In hindsight these results were unsurprising. It is already known that NMDA receptors are required for learning and memory. Also, basal levels of NMDA receptor activity are needed to maintain synapses and the complete block of NMDA receptors is known to induce neuronal apoptosis (Hardingham & Bading, 2010).

On the other hand, the NMDA receptor pore blocker memantine has emerged as an effective drug in the treatment of mild to moderate AD, showing improvements in cognitive performance, behavioural disturbances and activities of daily living in clinical trials (Cummings, Schneider, Tariot, & Graham, 2006; R. Doody, Wirth, Schmitt, & Möbius, 2004; Gauthier, Wirth, & Möbius, 2005), although benefits have not been seen in mild AD patients (Schneider, 2011). The success of memantine has been attributed to the pharmacokinetics of the drug, which exhibits fast on/off kinetics and a voltage-dependent response when compared to other pore blockers such as MK-801 (Parsons et al., 2007). These properties are thought to allow memantine to inhibit the low-level pathological activity of the NMDA receptor while still allowing for its physiological activation during transient depolarizations of the post-synaptic membrane. The relative success of memantine shows us that the careful targeting of NMDA receptors has therapeutic potential in the treatment of AD; further research into ways of targeting NMDA receptors, and more importantly their downstream signalling pathways, may be promising.

1.5.2 NMDA receptor secondary currents: a possible contributing mechanism to AD?

Excitotoxic activation of NMDA receptors is known to lead to the recruitment of secondary cation currents. In the stroke field, these NMDA receptor secondary currents have been of interest as they mediate the prolonged depolarization and the elevation of intracellular calcium in neurons, contributing to delayed cell death following reperfusion. Therefore, the identification and targeting of channels contributing to these currents has been proposed as a therapeutic strategy to increase neuronal survival. However, less information is known about the extent to which NMDA receptor secondary currents may contribute to chronic excitotoxicity and

calcium dysregulation in AD. Various non-selective cation channels have been proposed to contribute to secondary currents evoked by NMDA receptor stimulation, including members of the transient receptor potential (TRP) family of receptors. Neuronal TRPM2 channels are activated secondary to calcium influx and oxidative stress signalling following excitotoxic NMDA receptor stimulation. In APP/PS1 mice, the knockout of the TRPM2 channel has been shown to reduce synapse loss and ameliorate cognitive deficits (Ostapchenko et al., 2015), providing some precedence for the role of secondary currents in AD pathogenesis.

The large-pore channel Pannexin-1 (Panx1) is also strongly implicated in mediating secondary currents following excitotoxic NMDA receptor exposure. While the role of Panx1 channels have been studied in various diseases of the CNS, less is known about their contribution to AD pathogenesis. The unique structure and function of these channels, and their possible relevance to CNS disease are the topic of the next sections of this chapter.

1.6 Introduction to Pannexin-1: Structure and function

Pannexins were first described in the early 2000s as a membrane channel with sequence homology with the invertebrate gap junction protein innexin (Panchina et al., 2000). Since then, there has been a keen interest in elucidating the structure and function of pannexins, particularly in mammalian systems. Three isomers of the pannexins have been identified (Panx1, Panx2 and Panx3) which generally form homomeric channels. Panx1 is the best characterized of the three isomers and is broadly expressed throughout the body, whereas Panx2 and Panx3 expression is largely restricted to the CNS and bone marrow respectively (Penuela & Laird, 2012). Panx1 is the best characterized of the three isomers, and will be the primary subject of study in this thesis. The next sections will discuss what is known about Panx1 structure and function. This will be

followed by a brief summary of mechanisms which regulate the channel. Finally, the relevance of the Panx1 channel to CNS physiology and pathophysiology, including AD, will be explored.

1.6.1 Panx1 Structure

Studies of Panx1 structure are crucial in understanding how they may function. Pannexins share a membrane topology to innexins and connexins, consisting of four transmembrane domains with two extracellular loops and intracellular C-term and N-term tails. Six subunits come together to form a hexameric channel with a large central pore estimated to be up ~50 angstroms from EM studies (Wang et al., 2014) (Figure 1.4). Higher resolution models for pannexins have not been produced so far. However, some features of their structure may be gleaned from X-ray crystallography experiments on the gap junction channels connexin-26 (Cx26) and innexin-6 (INX-6). Despite low sequence homology, the three-dimensional structure of Cx26 and INX-6 are very similar. In both channels, the first transmembrane domain and first extracellular loop form the pore. On the intracellular side, a funnel structure is formed in the channel pore by the N-terminal helices of each Cx26 subunit. Likewise, the crystal structure of INX-6 shows close interactions of both the N-term and C-term tails in the channel pore (Oshima, Tani, & Fujiyoshi, 2016) implicating their role in regulating channel function. To specifically compare the similarities and differences in the pore structure of Panx1 channels to connexin channels, the Dahl lab used the substituted cysteine accessibility method for determining amino acids which line or interact with the channel pore (Wang & Dahl, 2010). They found that the outer portion of the Panx1 channel pore is composed of its first TM segment and first extracellular loop, consistent with the crystal structure of Cx26. More interestingly, cysteine substitution of the intracellular N-term tail residues abolished channel activity after thiol

modification, whereas substitution of the distal C-term amino acids caused a reduction in channel function. Together, these findings suggest a role of the N-term in pore permeability, and the C-term in gating the channel. Indeed, functional studies of Panx1 have shown that cleavage of the C-term tail causes constitutive channel activation (Chiu et al., 2017; Dourado, Wong, Hackos, Wang, & Goldin, 2014; Sandilos, Chiu, et al., 2012).

There are several important distinctions to be made between the structure of connexins and Panx1. Early studies focused on the possible function of Panx1 in gap junctions due to its structural similarities to connexins. However, several seminal papers proved that Panx1 channels do not form gap junctions in physiological systems (Dahl, Qiu, & Wang, 2013; Huang, Grinspan, Abrams, & Scherer, 2007), instead existing as unopposed channels which span the plasma membrane. The glycosylation of asparagine 254 on the second extracellular loop is thought to prevent pannexins from forming gap junctions, and may additionally play a role in regulating trafficking of the channels to the plasma membrane (Boassa et al., 2007; Penuela et al., 2007). Another important characteristic of Panx1 structure is the lack of canonical voltage sensor motifs within the transmembrane domains. Indeed, Panx1 activation is voltage independent, in contrast to connexin-43 (Cx43) hemi-channels, which require membrane depolarization for their activation (Maeda et al., 2009; Nomura et al., 2017).

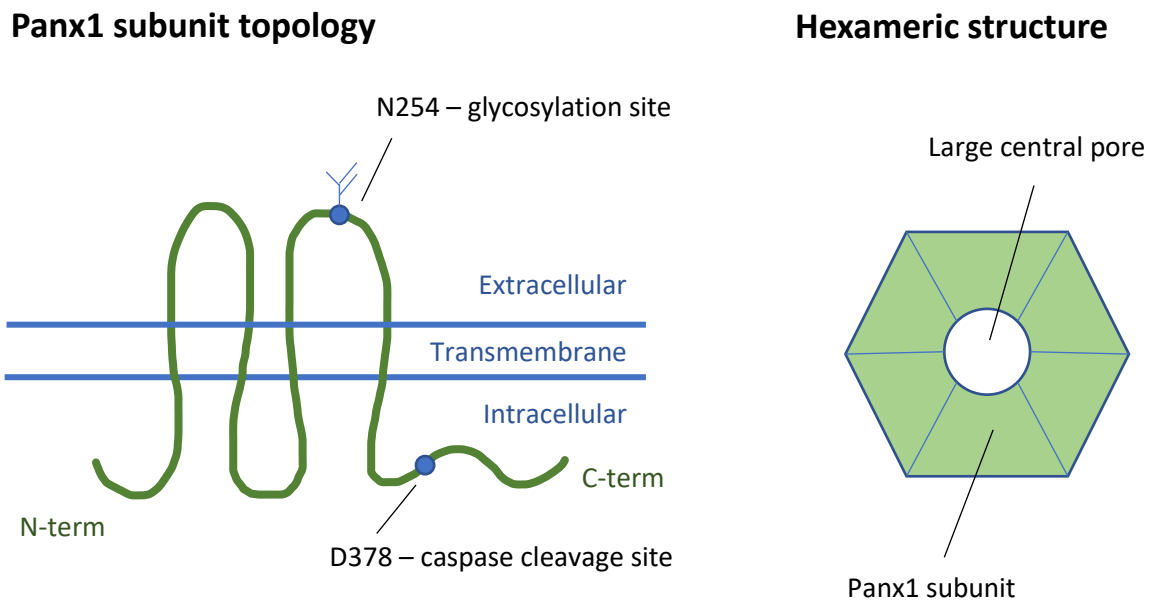

Figure 1.4: Panx1 channel topology and structure. The membrane topology of Panx1 consists of four transmembrane domains, two extracellular loops, one intracellular loop, and intracellular N- and C-term tails. Notable amino-acids labelled included the glycosylation site at amino acid 254 on the extracellular loop and the caspase-cleavage site at amino acid 378 on the C-term tail. Six Panx1 subunits come together to form a hexameric channel with a large central pore.

1.6.2 Panx1 permeability and conformational states

The defining property of the Panx1 channel is its ability to mediate the flux of metabolites up to 1kDa across the plasma membrane. A large body of literature supports Panx1's role in mediating autocrine and paracrine function, most notably as an ATP release channel. The ability for Panx1 to readily release ATP into the extracellular space has implicated it in a variety of physiological processes throughout the body, including airway defense (Ransford et al., 2009), red blood cell and platelet function (S. Locovei, Bao, & Dahl, 2006), control of vascular tone (Billaud et al., 2011; Gaynullina, Shestopalov, Panchin, & Tarasova, 2015; Good et al., 2015a),

and immune function (Glass, Elizabeth Snyder, & Steven Taffet, 1966; Maslieieva & Thompson, 2014; Velasquez, Malik, Lutz, Scemes, & Eugenin, 2016).

The release of other small metabolites from Panx1 channels has been studied much less. Panx1 channels are thought to also mediate glutamate release as Cx43 hemichannels are known to be permeable to glutamate (Contreras, Saez, Bukauskas, & Bennett, 2003). Evidence for glutamate release through Panx1 has been demonstrated in cerebrocortical synaptosomes (Mannelli et al., 2015). Panx1 channels also allow the passage of certain molecular dyes, including ethidium bromide, propidium iodide, YoPro-1, lucifer yellow and calcein. These are widely used as a method for measuring Panx1 channel activity by quantifying fluorescence uptake or loss (Dahl et al., 2013; Sandilos, Bayliss, & Sandilos, 2012).

What constitutes the activated state of the Panx1 channel which allows the flux of ATP and molecular dyes? Panx1 channels basally reside in a "small pore" conformation, which behave as low conductance voltage-dependent chloride permeable channel. On the other hand, various stimuli can convert Panx1 into a "large pore" conformation – these channels are capable of mediating large non-selective ion currents. In Panx1 transfected oocyte recordings, a maximum single channel conductance of ~500pS was measured in the large pore conformation, though channels typically resided in sub-conductance states ranging from 5%, 25%, 30% and 90% of this maximal conductance (Wang et al., 2014). It is best understood that this large pore conformation represents the state of the Panx1 channel which mediates the flux of ATP and molecular dyes (Figure 1.5).

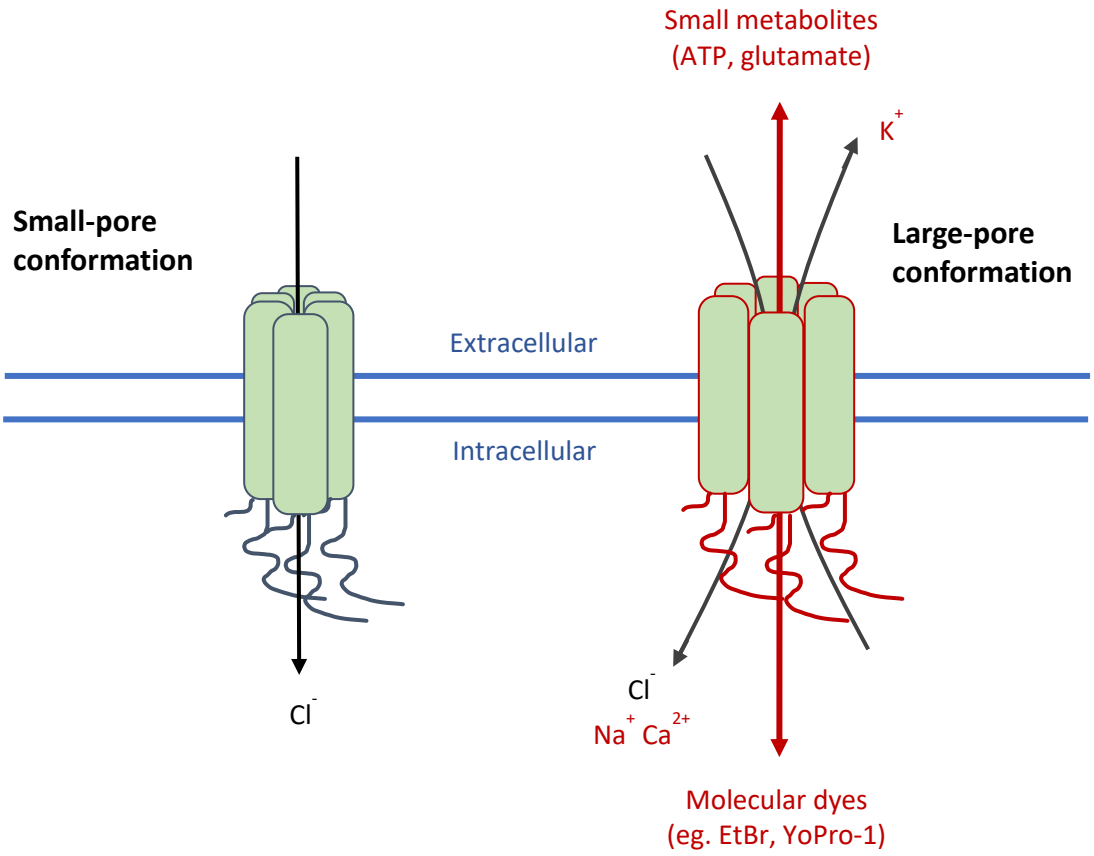

Figure 1.5: Panx1 channels reside in two conformational states. Panx1 channels constitutively reside in a small-pore state that is permeable to chloride ions. The activation of Panx1 by a variety of stimuli can induce the conformational change of Panx1 to a large-pore state, acting as a non-selective ion channel which also allows the flux of small molecules up to 1 kDa in size. These include ATP and glutamate as well as molecular dyes such as Ethidium bromide (EtBr) and YoPro-1.

There is however some disagreement on whether this large-pore conformation is necessary for the release of metabolites. The Bayliss group asserts that the C-term tail of Panx1 is responsible for blocking the channel pore, and the expulsion of the C-term tails from the pore leads to activation of the channel. The cleavage of at least 2 C-term tails was shown to facilitate

permeability to ATP and ToPro-3 dye. However, channels remained in their small pore state with a maximum conductance of 100 pS (Chiu et al., 2017). On the other hand, the Dahl group recently showed that cleavage of the Panx1 C-term tails alone is insufficient for ATP permeability, only leading to an increase in open probability and a larger total chloride selective current. They argue that the large pore conformation is truly necessary for the flux of ATP and molecular dyes (Wang & Dahl, 2018). The variation in the behaviour of activated Panx1 channels is commonly attributed to differences in recording or assay conditions, expression systems and the type of activation mechanisms studied. However, these findings also suggest that in previous studies working with C-term cleaved Panx1 channels, other parallel mechanisms may have also been recruited which culminated in the release of ATP. But how various primary and modulating mechanisms for Panx1 activation come together needs to be clarified, especially under more physiological contexts.

1.6.3 Panx1 pharmacology

In order to categorically identify Panx1 mediated currents, ATP release, or dye flux within physiological systems, pharmacological blockers of Panx1 must be used. However, many of the blockers are non-specific for Panx1, acting at other targets such as connexin hemi-channels (Dahl et al., 2013). For example, lanthanum (La^{3+}) and other trivalent cations are used as a pore blocking agent for both connexin hemi-channels and pannexin channels. Carbenoxolone acts as a connexin blocker at high μM concentrations but has been shown to be more selective for Panx1 at low μM concentrations. Probenecid, better known as an organic anion transporter (OAT) blocker, is also capable of inhibiting Panx1 currents. Though exact mechanisms for carbenoxolone and probenecid mediated Panx1 block have not been elucidated,

they appear to act at the first extracellular loop of Panx1 (Michalski & Kawate, 2016). Other drugs which can inhibit Panx1 include the anti-malarial agent mefloquine (Rodolfo Iglesias, Spray, & Scemes, 2010) and the quinolone antibiotic trovafloxacin (Poon et al., 2014).

Given the non-specific nature of these various compounds, researchers have turned to developing specific peptide blockers for Panx1. $Panx^{10}$ is a mimetic peptide comprising of residues of the first extracellular loop. It was originally modelled after connexin mimetic peptides which were designed to bind and prevent gap junction formation between connexin hemichannels. However, it was found that both $Panx^{10}$ and connexin mimetic peptides can inhibit Panx1 activation, and $Panx^{10}$ can inhibit Cx43 hemi-channels (Wang, Ma, Locovei, Keane, & Dahl, 2007). It has been suggested that these mimetic peptides act through steric interference of the pore, calling into question their specificity (Dahl et al., 2013). To date, a truly specific Panx1 blocker has yet to be found, though groups are starting to use peptide inhibitors to target intracellular regulatory domains of Panx1 (Weilinger et al., 2016; Weilinger, Tang, & Thompson, 2012). In addition, specific agonists or positive modulators of Panx1 are lacking, though optogenetic tools are beginning to be developed that allow for regulation of channel opening by light (Zhang et al., 2017).

1.7 Panx1 channel regulation and activation mechanisms

A myriad of mechanisms have been described for the regulation of Panx1 channels which exert differential effects on its ion permeability (ie. small vs. large pore) and its ability to mediate the flux of ATP and dyes. These mechanisms have been studied in cell line models overexpressing Panx1 and in various cell types expressing endogenous levels of the channel (summarized in Table 1.1). It is worth noting that the goal of this section is not to provide a

comprehensive list of regulatory mechanisms in various cell models which have been described for the channel; instead it aims to outline some major activation mechanisms that may be relevant in CNS physiology and disease. Broadly speaking, mechanisms of Panx1 regulation can be divided into (1) direct regulation by chemical or physical stimuli and (2) mechanisms which involve interactions with other membrane receptors and their secondary signalling mediators.

Table 1.1: Mechanisms of Panx1 activation

Activation Stimulus	Small or large pore (ion permeability)	ATP/Dye flux	Cell type	References
None	Small pore	None	Transfected Hek293/N2A	(W. Ma, Hui, Pelegrin, & Surprenant, 2009; Weihong Ma et al., 2012; Nomura et al., 2017)
C-term caspase cleavage	Small pore	ATP Dye flux	Transfected Hek293/Jurkat	(Chekeni et al., 2010; Chiu et al., 2017; Sandilos et al., 2012)
Reduced extracellular glucose	Small pore	ATP Dye not tested	CA3 pyramidal neurons (in slice)	(Kawamura, Ruskin, & Masino, 2010)
High extracellular potassium	Large pore	ATP Dye flux	Transfected oocyte	(Bao, Locovei, & Dahl, 2004; Wang et al., 2014; Silverman et al, 2009)
Hypo-osmotic stress	Small pore	ATP not tested Dye not tested	Transfected Hek 293	Jackson lab (unpublished)
Mechanical sitmulation	Large pore	ATP release Dye flux	Erythrocytes, retinal ganglion cells	Locovei, Bao, Dahl, 2006; Xia et al,. 2012; Dviorantchokova et al., 2018)
NMDA	Large pore	ATP not tested Dye flux	Hippocampal neurons	(Thompson et al., 2008; Weilinger, Tang, & Thompson, 2012)
P2X7 agonist	Large pore	ATP Dye flux	Transfected oocytes, Macrophage, Adult mouse NPC	(Messemer et al., 2013; Pelegrin et al., 2006)
ER Ca^{2+} depletion	Large pore	Not yet tested	Transfected Hek293	Jackson lab (unpublished)

1.7.1 Direct activation

In Panx1 overexpressing oocyte models, high extracellular potassium has been reliably used to convert channels into the their large-pore conformation, facilitating dye flux and ATP release (Bao, Locovei, & Dahl, 2004; Wang et al., 2014). This effect has been reproduced in experiments with neuronal and astrocyte cultures (Silverman et al., 2009). While the high millimolar concentrations of extracellular potassium used in these experiments are generally out of the physiological range, localized increases could occur in certain contexts such as seizure and anoxia.

As mentioned previously, the role of the C-term tail of the Panx1 in gating the channel has been extensively studied. Much of the impetus for these studies are due to the presence of a caspase cleavage site at amino acid 378 in the C-term tail. Studies have confirmed that treatment of cells with caspases leads to the cleavage of the C-term tail, resulting in an increased open probability of the channel. In this way, it has been suggested that Panx1 channels facilitate the release of ATP during apoptosis (Chekeni et al., 2010; Chiu et al., 2017; Dourado et al., 2014; Sandilos, Chiu, et al., 2012).

Panx1 function has also been linked to mechanical stimulation. Hypo-osmotic stress, membrane stretch, or shear force in a various cell types and tissues such as erythrocytes (Silviu Locovei, Bao, & Dahl, 2006), endothelial cells (Good et al., 2015b), and retinal ganglion neurons (Dvoriantchikova et al., 2018) were all shown to induce Panx1 mediated ATP release. The mechanosensitive properties of Panx1 are thought to be facilitated through its confirmed interaction with the actin cytoskeleton.

1.7.2 Receptor-mediated activation

The recruitment of Panx1 channel activity has been linked to its interaction with other membrane receptors. Panx1 channels can be activated by NMDA receptor stimulation. Exposure of neurons with 100 μM NMDA for several minutes leads to the secondary induction of a non-selective cation current mediated by large-pore activated Panx1 channels. This was confirmed with various pharmacological inhibitors of Panx1 as well as knock-down of Panx1 expression with shRNA (Roger J Thompson et al., 2008; Weilinger et al., 2012). Immunoprecipitation experiments demonstrate a co-localization of Panx1 with NMDA receptors, suggesting a close signalling relationship (Weilinger et al., 2016).

Panx1 activity is also to be associated with the ionotropic ATP receptor P2X7. The stimulation of P2X7 receptors with the persistent application of ATP is known to facilitate the formation of large pores which mediate ATP release and the flux of dyes. While this was first attributed to the induction of P2X7 pore dilation, evidence points to a P2X7 dependent activation of Panx1 channels. Panx1 coimmunoprecipitates with P2X7, and ATP induced large pore currents and dye flux could be abolished with Panx1 blockers and Panx1 siRNA knockdown (Wei, Caseley, Li, & Jiang, 2016). Together, the interaction of the Panx1 channel with NMDA and P2X7 receptors link its activity to extracellular signalling cascades involving glutamate and ATP.

1.7.3 Src Family Kinases

What are the downstream signalling events which regulate Panx1 channels downstream of NMDA and P2X7 receptors? Evidence points to tyrosine phosphorylation of Panx1 by Src Family Kinases (SFK) as an important mechanism. Peptide block of the P2X7 SH3 binding

domain for Src as well as inhibition of Src activity with the SFK blocker PP2 reduced Panx1 currents (R Iglesias et al., 2008; Suadicani, Iglesias, Spray, & Scemes, 2009). Similarly, NMDA receptors can recruit SFKs, and NMDA receptor initiated Panx1 currents in neurons are reduced by treatment with PP2. Weilinger et al. identified tyrosine 308 (T308) of Panx1 as a Src interaction site. The administration of an interfering peptide for this site reduced the Panx1 current (Weilinger et al., 2012). It is worth noting that in general, tyrosine phosphorylation acts as a gating modifier in the regulation of channel activity. In the case of Panx1, tyrosine phosphorylation of the C-term tails may modify its interaction with the channel pore, leading to an increase in the open probability of the channel. However, a mechanism downstream of NMDAR stimulation which more directly leads to the conversion of Panx1 channels to their large-pore conformation remains to be identified.

1.7.4 Calcium signalling

Given that NMDA and P2X7 receptors are both permeable to calcium, the activation of Panx1 could also be dependent on calcium signalling. Indeed evidence points to intracellular calcium as an important regulator of Panx1 channels. In oocytes over-expressing Panx1, the intracellular loading of calcium or the stimulation of intracellular calcium signalling through the G-protein coupled purine receptor P2Y1 both lead to the induction of Panx1 currents and the release of ATP (Silviu Locovei, Wang, & Dahl, 2006). Intracellular calcium appeared to have a direct effect on Panx1 as single channel inside-out patch recordings superfused with micromolar calcium led to increased channel conductance. Alternatively, elevations in intracellular calcium can lead to calcium-induced calcium release from the ER and the subsequent depletion of ER calcium stores. Our lab has demonstrated that depletion of ER calcium with the SERCA pump

inhibitor thapsigargin is sufficient to cause large-pore Panx1 opening in HEK293 overexpression model and in neuronal cultures. We have shown that there is an interaction of Panx1 with stromal interacting molecule (STIM), an ER calcium sensing protein which mediates store-operated calcium entry; this interaction is hypothesized to mediate large-pore activation of the Panx1 channel (unpublished). Together, this points to calcium signalling as an important regulator of Panx1 channels which may contribute to its activation downstream of NMDA and P2X7 receptors.

1.8 Panx1 in CNS physiology and pathophysiology

1.8.1 Panx1 expression in the CNS

Functions of Panx1 channels have been described in various cell types and organ systems in the body. This includes the CNS, where Panx1 is present on both neuronal and glial cells (Huang et al., 2007). Panx1 expression is highest at early developmental stages and gradually decreases until adulthood where it is particularly enriched in the cortex and hippocampus (Vogt, Hormuzdi, & Monyer, 2005). This suggests an important role for Panx1 in CNS development, where it Panx1 has been shown to promote NPC proliferation and migration, and regulate neurite outgrowth (Swayne & Bennett, 2016). In 2016, the first case of a human autosomal recessive Panx1 missense gene variant was reported; the proband exhibited intellectual disability and severe hearing loss, along with deficits in other organ systems (Shao et al., 2016). This gene variant resulted in an arginine to histidine substitution at position 217 (p.Arg217His) which was shown to reduce channel currents, dye flux, and ATP release while preserving surface expression. It is unclear how much of this phenotype is due to a developmental dysfunction of Panx1 versus its loss of function in the adult brain.

Panx1 has been shown to be expressed at the PSD in the cortex and hippocampus of adult mice (Zoidl et al., 2007), implicating this channel in synaptic function in the developed CNS. However, the majority of studies of Panx1 in CNS have been in the context of disease. A pathological role of Panx1 has been linked to stroke (Cisneros-Mejorado et al., 2015; Freitas-Andrade et al., 2017; Weilinger et al., 2016), seizure (Santiago et al., 2011), migraine headache (S.-P. Chen et al., 2017; Karatas et al., 2013), neuropathic pain (Bravo et al., 2014; Mannelli et al., 2015), and neurodegenerative disease (Olivier et al., 2016; Orellana, Shoji, et al., 2011). Information on how Panx1 functions at the synapse can be gleaned from its activity in these pathologies.

1.8.2 Activity dependent recruitment of Panx1 channels in seizure models

Large pore channels have been shown to contribute to ATP and adenosine accumulation during heightened neuronal activity, including over-active states such as seizures. Several studies have implicated the role of Panx1 in seizure formation. Kainate induced status epilepticus was shown to cause Panx1 mediated dye influx and ATP release, and pharmacological block or KO of Panx1 improved seizure outcomes (Santiago et al., 2011). Lopatar et al. showed that bursting induced by mGluR5 agonist DHPG causes ATP release in the hippocampal CA3 region which is mediated by Panx1, but not P2X7. They also observed that ATP release in the CA1 region was limited with this seizure model (Lopatář, Dale, & Frenguelli, 2015). This may point to a regional difference in Panx1 expression and function. ATP release was found to exacerbate mGluR5 induced bursting through P2Y receptors. While Panx1 activation is implicated in the pathogenesis of seizures, particularly in the seizure prone CA3 region, Panx1 has also been proposed to be involved in the reduction of seizure risk with glucose restriction. Kawamura et al.

showed that reducing extracellular glucose caused activation of Panx1 on CA3 pyramidal neurons, leading to ATP release, adenosine accumulation and subsequent reduction in neuronal excitability through A1R signalling (M. Kawamura, Ruskin, & Masino, 2010). These findings support both a physiological and pathophysiological role of Panx1 in the control of excitability in the CA3 region of the hippocampus.

1.8.3 Panx1 link to NMDA channels and excitotoxicity

How is Panx1 activated in the context of heightened neuronal activity? During cortical spreading depression, anoxia, and seizure events, levels of extracellular potassium can locally increase in the CNS and may be sufficient to directly activate Panx1. Another model of activity dependent Panx1 activation is through the upstream activity of NMDA receptors. Activation of NMDA receptors by removal of Mg^{2+} triggers epileptiform activity in acute hippocampal slices, and block of Panx1 in this context reduced spike amplitude and prolonged inter-burst intervals (Roger J Thompson et al., 2008). Heinrich et al. showed that high potassium induced depolarization causes a rise in both ATP and adenosine to micromolar levels in the CA1 region of the hippocampus. This purine release required NMDA receptor activation and was blocked by the P2X7 and Panx1 antagonists (Heinrich, Andõ, Túri, Rõzsa, & Sperlágh, 2012).

The link between NMDA receptors and Panx1 channels has been best demonstrated in models of oxygen glucose deprivation (OGD) and stroke. During OGD, excitotoxic NMDA receptor activation leads to delayed anoxic depolarization. The major contributor to this secondary current was found to be large-pore activated Panx1 channels (R. J. Thompson, Zhou, & MacVicar, 2006). Several groups have subsequently showed that genetic knockout or pharmacological block of Panx1 can attenuate ischemic damage in stroke models (Cisneros-

Mejorado et al., 2015; Dvoriantchikova et al., 2012; Freitas-Andrade et al., 2017; Weilinger et al., 2016).

1.8.4 Panx1 role in synaptic plasticity and memory

Given that NMDA receptor signalling can recruit Panx1 channel activity, it is possible that Panx1 may contribute to NMDA receptor dependent plasticity mechanisms. Some evidence supports a modulatory role of Panx1 in synaptic plasticity. It has been reported that acute hippocampal slices from CNS restricted conditional Panx1 KO mice exhibited an increase in NMDA dependent LTP following high frequency stimulation at the CA3-CA1 synapse. These findings were paired with behavioural studies which showed memory impairments in the Panx1 KO mice (Prochnow et al., 2012). Ardiles et al. showed that Panx1 KO mice also have an attenuation of LTD, and that there is ultimately a decrease in the threshold for the induction of LTP (Ardiles et al., 2014). These effects could be partially recapitulated by pharmacological block with probenecid. These results imply that Panx1 activation during NMDA dependent plasticity may limit LTP and favour LTD. Normal expression of LTD is important in various memory tasks, including behavioural flexibility in spatial learning. Behavioural studies revealed that Panx1 KO mice exhibit deficits in the reversal of spatial learning as tested by Morris Water Maze (Gajardo et al., 2018).

So far, the mechanism by which Panx1 mediates this change in plasticity have not been fully elucidated. Given that activity-dependent Panx1 activation can cause the release of purines at the synapse, Panx1 contribution to purine modulation of plasticity is an attractive hypothesis. In both studies, it was shown that there was an increase in excitability and pre-synaptic glutamate release compared to control, which may hint at the contribution of Panx1 to purine mediated pre-

synaptic inhibition during LTP induction. Gajardo et al. also demonstrated that there was a change in NR2 subunit composition and contribution to LTP and LTD in Panx1 KO mice, possibly due to developmental changes in the KO model. However, given that acute treatment with probenecid was sufficient for partially inducing Panx1 KO plasticity phenotype, it is unlikely that the expression of NR2 subunits alone could account for Panx1's effect on plasticity.

1.8.5 Panx1 in Alzheimer's Disease

Few studies have directly looked at the role of Panx1 in AD. Orellana et al. showed that Panx1 contributes to amyloid-β induced neuronal death (Orellana, Shoji, et al., 2011). In their study, $A\beta_{25\text{-}35}$ was associated with raised extracellular glutamate and ATP levels which were attributed to increased Panx1 channel activity in neuronal and microglial cultures, and increased Cx43 hemi-channel activity in astrocytes cultures. Treatment of neuronal cultures with the conditioned media of amyloid-β treated microglia and astrocytes both induced neuronal cell death which could be blocked by NMDA and P2X receptor antagonists. These antagonists also caused a reduction in cell death in $A\beta_{25\text{-}35}$ treated hippocampal slices. Likewise, the block of Panx1 channels in these experiments resulted in a modest reduction in cell death.

Several questions regarding the role of Panx1 in AD remain to be answered. As discussed in Section 1.3, the toxic effects of AβOs first involve dysfunction at the level of the synapse. Given that there is evidence for Panx1 role in plasticity, they may contribute to AβO induced deficits in LTP and facilitation of LTD. While Panx1 is shown to mediate neuronal cell death, the contribution of this channel to the more relevant mechanism of synaptic degeneration in AD has not been studied.

1.9 Experimental aims and hypothesis

Therapeutics for AD are currently limited, and research into the pathogenesis of this complex disease may uncover novel therapeutics. The primary aim of this study was to determine whether Panx1 channels expressed on hippocampal neurons may contribute to AD pathology. More specifically, we hypothesize that: (1) AβOs sensitize the signalling between NMDA receptors and Panx1 channels; (2) Large-pore activity of Panx1, which result in the influx of calcium and the release of signalling molecules such as ATP and glutamate, is a downstream consequence of AβO interactions at the PSD; (3) The pathological activity of Panx1 channels contributes to AβO induced synaptic dysfunction, which may include acute deficits of synaptic plasticity and synaptic degeneration (Figure 1.6). By using mice with a global genetic knockdown of Panx1, we would expect an amelioration or reversal of amyloid-β mediated synaptotoxicity.

Another aim of this study is to learn more about the physiological role of Panx1 in the adult brain. A better understanding Panx1 function in the CNS may give clues about how it may contribute to AD pathogenesis. Furthermore, in the development of therapeutics which target Panx1 channels, it is important to know of possible side effects related to its inhibition. Therefore, we wish to study the physiological function of Panx1 in hippocampus by comparing synaptic plasticity mechanisms, and hippocampal dependent behaviours in Panx1 WT and KO mice.

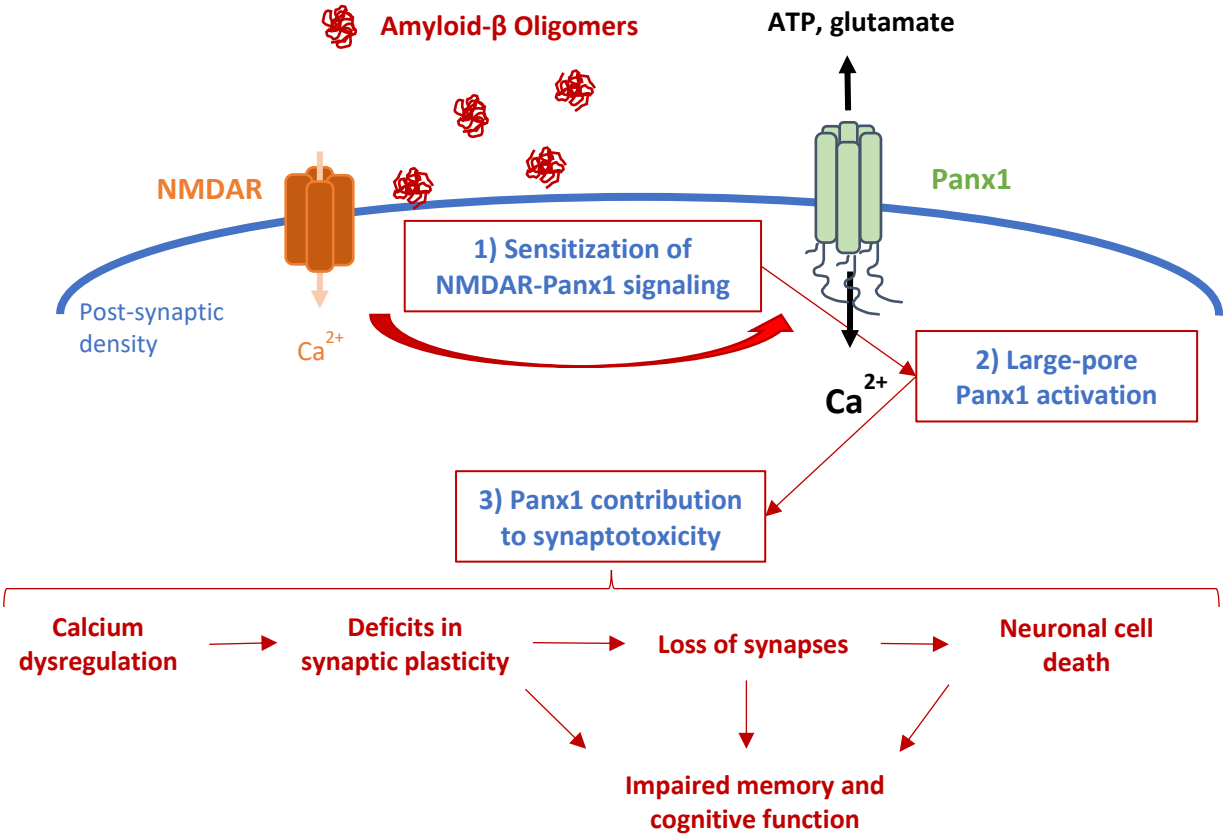

Figure 1.6: Hypothesized mechanism for the pathological contribution of Panx1 channels to AβO induced synaptic dysfunction

CHAPTER 2: MATERIALS AND METHODS

2.1 Production of secreted amyloid-β oligomers

Secreted AβOs were produced from the 7PA2 CHO cell line following established protocols. Briefly, control CHO cells and 7PA2 CHO cells were grown and expanded onto 150mm culture dishes. When cultures were at 90% confluency, cells were washed twice with serum free Dulbecco's Modified Eagle Media (DMEM) and returned to the incubator. After 18 hours, the conditioned media was collected into 50 mL tubes and centrifuged for 10 minutes at 200xg at 4^{o}C to remove cell debris. The supernatant was then collected and concentrated using Centripep YM-3 concentrators: first concentrators were sterilized by running ethanol through and letting sit for 5 minutes. The concentrators were then washed twice by adding 10 mL phosphate buffered saline (PBS) and centrifuging at maximum speed (3200 rpm) for 5 minutes. Finally, the control CHO conditioned media (CHO-CM) and 7PA2 CHO conditioned media (7PA2-CM) was concentrated. Conditioned media was added to the concentrators and centrifuged at maximum speed for 15 minutes. The inner filtrate (ie. < 3 kDa) was discarded while the outer filtrate (ie. > 3 kDA) was collected. This step was repeated until the conditioned media was concentrated to 1/30 of the original volume (eg. 900 mL to 30 mL). Aliquots of the 30 times concentrated CHO-CM and 7PA2-CM were then frozen and stored at -80^{o}C.

2.2 Validation of amyloid-β oligomers in 7PA2-CM

The concentration of $A\beta_{1-42}$ and total amyloid-β in 7PA2-CM and CHO-CM was measured by enzyme-linked immunosorbent assay (ELISA) using the Amyloid-β 42 human ELISA kit, Ultrasensitive (Life tech) and Human Amyloid beta (1-x) Assay Kit (IBL)

respectively. Procedures provided with the kits were followed, and three dilutions of concentrated 7PA2-CM were tested per kit.

To confirm the presence of AβOs in 7PA2-CM, Western blots were performed using 16.5% Tris-Tricine gels (Bio-Rad). Equal parts of concentrated 7PA2-CM and 2X Trix-Tricine loading buffer were prepared and loaded onto the gel. Following standard SDS-PAGE procedures, protein was then transferred onto nitrocellulose membrane in transfer buffer containing 25mM Tris, 192 mM glycine, 0.02% SDS and 20% methanol. Membranes were washed with TBS-T,and boiled in PBS for 10 minutes. Blots were then blocked in 5% milk/TBS-T for 1 hour in RT before incubating at 4^{o}C overnight with gentle mixing in 1:2000 anti-Amyloid (6E10) mouse IgG1. The next day, blots were washed and incubated with anti-mouse secondary antibody conjugated to horse-radish peroxidase (HRP). Blots were then visualized using SuperSignal West Pico enhanced chemiluminescent substrate (Thermo scientific) and Imager Gel Doc imaging system (Bio-Rad Laboratories, Inc.).

2.3 Experimental animals

Wild-type CD1 mouse colony were primarily used for cell culture experiments. The Panx1 KO mouse line (Panx1$^{tm1a(KOMP)Wtsi}$) generated in the C57BL/6 background was used in studies comparing Panx1 WT to KO genotypes. Animals were housed and maintained at the animal care facilities of the University of Manitoba. Experimental protocols were conducted with approval by the Animal Welfare Committee at the University of Manitoba.

2.4 Neuronal cell culture and treatments

The hippocampus was dissected from embryonic day 17-18 CD1 mice pups under sterile conditions. Dissected hippocampal tissue were placed in cold phosphate buffered saline (PBS) before mechanical dissociation by trituration. Cells were then plated on to poly-D-lysine coated 12 well plates and 35 mm culture dishes. The neuron cultures were maintained in neural basal media supplemented with GS21 and glucose. The cultures were incubated at 37 ˚C with 5% CO2 and media was replenished every 3-4 days.

Treatments began in at DIV 18-23 and were directly added to wells containing conditioned media. For 3 to 5 day AβO treatments, concentrated 7PA2-CM was diluted to a final $A\beta_{1\text{-}42}$ treatment concentration of 13.6-26.1 pM and total amyloid-β concentration 1.1-4.6 ng/mL as determined by ELISA assay. For synaptic NMDA receptors stimulation, 50 µM bicuculline methiodide and 2.5 mM 4-aminopyridine with or without co-treatment with 10 µM MK-801, 50 µM APV, or 1 µM Ro 25-6981 were used. NMDA treatments were applied with solution lacking Mg^{2+} and containing D-serine consisting of (in mmol/L) 52 NaCl, 5.3 KCl, 1.8 $CaCl_2$, 26.2 $NaCO_3$, 10.9 HEPES, 25 D-glucose; pH adjusted to 7.4 with NaOH; osmolarity adjusted to 270 mOsM/liter.

2.5 LDH assay

LDH assays were performed using the Cytotoxicity LDH assay kit-WST (Dojindo Molecular Technologies). Media from treated neuronal cultures was collected and transferred in duplicate to a 96 well plate (100 µL per well). Supernatant of lysed cells following addition of “Lysis buffer” diluted in PBS (equal volume to conditioned media) was also transferred in duplicate. “Dye solution” (100 µL per well) was added and the plate was incubated at 37ºC for

30 minutes; the reaction was then terminated by adding 50 µL of "Stop solution". Absorbance was read on a microplate reader (Synergy HT, Biotek) under a 490 nm filter. Technical duplicate values were averaged; absorbance values of treatment media and lysates were then subtracted from absorbance of media or PBS blanks respectively. Percent total LDH release was calculated from "(absorbance of treatment media/absorbance of corresponding lysate)*100%".

2.6 Dye uptake experiments

For qualitative neurotoxicity experiments, neurons were incubated at 37ºC for 30 minutes in dye solution containing 2 µM Calcein-AM (Invitrogen) and 2 µM Ethidium homodimer-1 (Invitrogen) diluted in extracellular fluid (ECF) containing (in mmol/L) 140 NaCl, 5.6 KCl, 1 MgCl2, 2 CaCl2, 33 D-glucose, 25 HEPES; pH adjusted to 7.4 with NaOH; osmolarity adjusted to 300-310 mOsM/liter. Cells were washed once with ECF, then imaged on a EVOS fluorescence imaging system (Thermo Scientific) at 10X and 20X magnification with GFP and Texas Red filters. Exposure levels in each filter setting were kept constant between treatment groups.

For YoPro-1 uptake experiments, neurons were incubated at 37ºC for 30 minutes in dye solution containing 2uM YoPro-1 (Invitrogen), 2uM Calcein Red-orange AM (Invitrogen), and Hoechst 33342 (NucBlue Ready probes, Invitrogen) diluted in ECF. After washing with ECF, images were acquired on an automated Cytation 5 Cell Imaging Multi-mode Reader (Biotek) using DAPI, Texas Red and GFP filter sets. Before each experiment, auto-exposure was applied to DAPI and Texas Red channels, while exposure settings were kept constant for the GFP channel across all experiments. Images were analyzed with Gen 5 data analysis software (Biotek, ver. 3.03). Automated cell counts were performed by counting nuclei co-localized with either

Calcein Red-Orange or YoPro-1 fluorescence above a manually set threshold. Performance of automated cell counting was visually checked for each experiment.

2.7 Whole-cell patch clamp in cultured neurons

Tight-seal whole-cell recordings of neuronally enriched hippocampal cultures were conducted at room temperature using an Axon MultiClamp 700A patch clamp amplifier and Digidata 1322A data acquisition system (Molecular Devices). Culture media was replaced with ECF (as above) with the addition of 10 μM tetrodotoxin to block action potential firing. Patch pipettes were pulled from borosilicate glass (World Precision Instruments, Inc., Sarasota, FL) and had a resistance of 4–5 MΩ when filled with intracellular pipette solution (ICF) containing (in mmol/L) 150 cesium gluconate, 2mM MgCl2 and 10mM HEPES adjusted to pH 7.2 with CsOH; osmolarity adjusted to 290 and 300 mOsM/liter.

Pyramidal neurons were selected to be patched if they had a phase bright cell body with 2-3 large primary neurites. Neurons exhibiting YoPro-1 fluorescence were selected to be patched if a bright condensed nuclear fluorescence was absent. Neurons were voltage clamped at -60mV and miniature excitatory post-synaptic currents (mEPSCs) were recorded. Current-voltage relationships were measured by applying voltage-ramps (-100 to 100mV) over 500ms. Signals filtered at 2 kHz and sampled at 10 kHz were collected and analyzed using Clampex 9.2 and Clampfit 10.7 software (Molecular Devices). The amplitude and frequency of mEPSCs were analyzed though the template event detection analysis function in the Clampfit software. Events below a threshold amplitude were not included in the analysis as determined by the average RMS noise across all recordings

2.8 Western blotting

2.8.1 Sample preparation and protein estimation

Cells were washed 3x with ECF and lysed directly with loading buffer containing (3.5 mL 1M Tris-Cl pH 6.8, 4.5 mL glycerol, 1 g SDS, 1 mL 0.5% Bromophenol Blue, 1 mL dH_2O, 70 µl 2-β-mercaptoethanol). Lysates were transferred to -80^oC for storage. Protein concentrations were not estimated for samples directly lysed in loading buffer.

For samples probed for Panx1 protein, cells were scraped in ECF and transferred to microtubes which were centrifuged at 4^oC for 5 minutes at 1000xg to form a cell pellet. Cells were then reconstituted in lysis buffer containing (1% Triton-X-100, 0.1% SDS, 0.5% Sodium deoxycholate, 150 mM NaCl, 50 mM Tris, 10 mM EDTA) supplemented with protease inhibitor (Mini Complete Tablets, Roche Applied Science) and Halt phosphatase inhibitor (Thermo Scientific) added just before use and allowed to lyse on a shaker for 30 minutes at 4^oC. Cell debris was centrifuged down at max rpm and the supernatant was collected and stored at -80^oC.

To estimate protein concentrations, the Pierce BCA protein assay kit (Thermo Scientific) was used; absorbance values samples were measured using a spectrophotometer and compared to a standardized curve to determine protein concentrations. Aliquots of samples were mixed with loading buffer and distilled water to the desired loading concentrations.

2.8.2 SDS-PAGE and immunoblotting

On the day of the Western Blot, samples were thawed and heated at 94^oC for 5 minutes. Whole-cell lysates were loaded onto 10% SDS gel and run at 120 mV. As a control for protein loading, the SDS gel contained 0.5% 2,2,2-trichloroethanol (TCE). After protein samples were resolved, gels were exposed to UV light for 60 seconds to activate TCE and imaged under UV

light to assess total protein loading. The resolved samples were then transferred onto nitrocellulose membranes at 10-12V at room temperature for 75-90 minutes. Total transferred protein as represented by TCE staining of the blots was imaged. Blots were blocked for 1 hour with either 5% BSA in 0.5% TBST or 5% Skim milk in 0.5% TBST. Blots were then incubated in primary antibody overnight at 4^{o}C on a rocker. Following overnight incubation, blots were washed 3X with TBST, 10 minutes per wash, and incubated with HRP-conjugated secondary antibody for 1 hour. Following another washing step, blots were treated with either SuperSignal West Pico enhanced chemiluminescent substrate or SuperSignal West Femto Maximum chemiluminescent substrate (Thermo Scientific). Protein signals were visualized using Molecular Imager Gel Doc imaging system (Bio-Rad Laboratories, Inc.).

Anti-bodies used were Panx1 CT-395 rabbit monoclonal (1:1000, Laird lab), PSD-95 rabbit monoclonal (1:2000, Sigma) and synaptophysin mouse monoclonal (1:2500, Sigma).

2.9 Brain slice electrophysiology

2.9.1 Acute hippocampal slice preparation

Hippocampal slices were prepared from male Panx1 WT and KO mice with ages ranging from 5-14 weeks. Following isoflurane anesthesia and decapitation, brains were extracted and quickly submerged into ice-cold oxygenated (5% CO_2, 95% O_2) standard artificial CSF (in mmol/L: 124 NaCl, 3 KCl, 1.3 MgCl2, 2.6 CaCl2, 1.25 NaH2PO4, 26 NaHCO3, and 10 D-glucose; osmolarity adjusted to 300-310 mOsM). Hippocami were then dissected and transverse sections (350 µm) were prepared using a vibratome.

In some experiments (MF-CA3 field recordings), NMDG cutting aCSF (in mmol/L: 93 NMDG, 3 KCl, 5 MgCl2, 0.5 CaCl2, 1.25 NAH2P04, 30 NaHCO3, 20 HEPES, 25 Glucose, 5

Na ascorbate, 3 Na pyruvate; pH adjusted to 7.4 with HCl, osmolarity adjusted to 300-310 mOsM) was used in place of standard aCSF to better preserve slice viability. Hippocampal slices were left in NMDG cutting solution at 30ºC for 5 minutes before being transferred to HEPES recovery aCSF (in mmol/L: 95 NaCl, 3 KCl, 1.3 MgCl2, 2.6 CaCl2, 1.25 NAH2P04, 30 NaHCO3, 20 HEPES, 25 Glucose, 5 Na ascorbate, 3 Na pyruvate; pH adjusted to 7.4 with NaOH, osmolarity adjusted to 300-310 mOsM).

Slices were allowed to recover at room temperature for 1.5 hours in a submersion holding chamber with well-oxygenated aCSF before recording. For amyloid-β pre-treatment, slices were transferred to a mini submersion holding chamber containing 7PA2-CM diluted in well-oxygenated aCSF ($A\beta_{1-42}$: 11-27 pM; total amyloid-β: 1.4-2.6 ng/ml) for 2-3.5 hours.

2.10.1 Field EPSP recordings

Field recordings were performed in a submersion recording chamber continuously super-perfused with oxygenated aCSF at a flow rate of 3 ml/min and maintained at 30-32ºC. Field EPSPs were evoked by giving stimuli (100 μs duration) with a concentric bipolar stimulating electrode positioned at the Schaffer collateral pathway and recorded with a glass pipette filled with aCSF (pipette resistance between 2-5mOhms) positioned in the CA1 stratum radiatum (Figure 2.1A). Responses were evoked at either 0.05 or 0.033 Hz. To determine the input-output relationship, stimulus intensity was increased gradually starting at a level evoking a minimal field response until either a maximal field response was reached or a population spike was elicited. Stimulus intensity was then set to a level which elicted 30-40% of the maximum response for subsequent tests. Paired-pulse facilitation (PPF) was measured by giving paired stimuli at intervals of 10, 20, 40, 100, 200, 500, and 1000 ms. PPF was expressed as the ratio of

the peak amplitude of the second response (P1) and the first response (P2). For long-term potentiation experiments (LTP), baseline fEPSPs were recorded over 20 minutes before induction by high-frequency stimulation (HFS) consisting of two consecutive 100Hz stimulation trains lasting 1 second, with an inter-train interval of 20 seconds. Responses were then recorded for 60 minutes. Slopes of fEPSPs were analyzed and normalized to baseline.

Field EPSP recordings at the MF-CA3 synapse were performed as above, except with the stimulating electrode positioned on the cell layer of the dentate gyrus, and recording electrode positioned at the stratum lucidum of the CA3 area (Figure 2.1B). Frequency facilitation was assessed by recording baseline response for 2 minutes at 0.05 Hz, switching to 1Hz stimulation for 40 seconds, and then switching back to 0.05 Hz stimulation. To confirm that the fEPSPs were predominantly contributed by MF-CA3 synapses, the metabotropic glutamate receptor mGluR2 agonist DCG-IV (1 μM) was applied at the end of recordings – an 80% reduction in fEPSPs amplitude was regarded as a reliable recording.

The field potentials were amplified 100 using Molecular Devices 200B amplifier and digitized with Digidata 1322A. The data were sampled at 10 kHz and filtered at 2 kHz. Traces were obtained by pClamp 9.2 and analyzed using Clampfit 10.7.

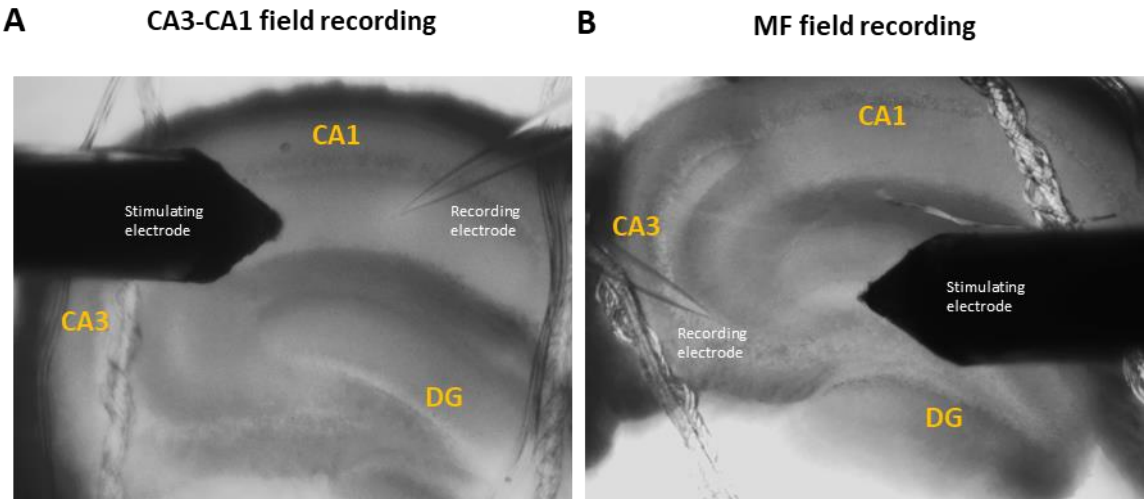

Figure 2.1: Field EPSP recordings in acute hippocampal slice. (A) For CA3-CA1 field recordings, the stimulating electrode was positioned at the junction between the CA3 and CA1 regions of the hippocampus to stimulate the Schaffer collateral pathway. The recording electrode was positioned 350 µm away in the stratum radiatum layer of the CA1 region. **(B)** For MF field recordings, the stimulating electrode was positioned on the cell layer of the dentate gyrus to stimulate mossy fibers. The recording electrode was placed at the stratum lucidum layer of the CA3 region.

2.11 Behavioural studies

Behavioural studies were conducted on male Panx1 WT and Panx1 KO mice between the ages of 6-11 months. The experimenter was blinded to the genotype of the mice during the administration of the studies. A Quatricide cleaning solution was used to wipe down the apparatus and objects between trials. Videos were taken by webcam mounted above the apparatus. Automated video analysis was performed using ANY-maze behavioural tracking software.

2.11.1 Elevated Plus maze

The elevated plus maze apparatus consisted of a raised platform (61 cm) with four arms of equal length and width (36 cm x 5 cm) forming the shape of a plus sign. Two arms positioned across from each other are enclosed by high walls (20 cm) while the other two arms have very short walls (1cm) that prevent the mice from easily falling. For the test, mice were placed into the maze facing the open arms and allowed to freely explore for 5 minutes. For data analysis, each pair of open arms and closed arms was defined as a single open zone and closed zone respectively. Entries into open arms and closed arms were counted when the animal left one zone and entered the other zone. Time spent in a zone was also timed until the animal entered the other zone.

2.11.2 Novel-object recognition

Mice were allowed to habituate to a square open field box (50 cm x 50 cm x 40 cm) for 10 minutes on two consecutive days. Familiarization and test sessions were performed on the third day; the objects used were screw caps from glass media bottles and T-25 flasks filled with an orange liquid. Familiar and novel objects were pseudo-randomly assigned to each mouse before the start of the test. For the familiarization session, two duplicate objects were positioned at two defined locations at one end of the box, and each mouse was allowed to explore the objects for 5 minutes. The test session was then administered after a 4 hour inter-session interval; for another 5 minutes, mice were presented the familiar object and a novel object which were randomly positioned in the box. For data analysis, a zone bordering each of the objects was drawn and exploration of the object was timed when the head of the mouse was within each object zone.

2.11.3 Contextual Fear Memory

Mice were first allowed to habituate to the shocking chamber (30cm × 25cm × 33 cm) for 10 minutes. The following day, mice underwent contextual fear conditioning; mice were left in the chamber for 2 minutes before application of three electric shock (1 mA shocks lasting 2 seconds) separated by 30 seconds. After 24 hours, mice were tested for contextual fear memory. Mice were returned to the chamber and recorded for 5 minutes. After another 72 hours, mice were again returned in the chamber for 5 minutes. Freezing responses were timed using the freeze detection analysis in AnyMaze and defined by a minimum freeze duration of 2 seconds.

2.12 Statistical Analysis

Statistical analyses were performed using Graphpad Prism 6 (Graphapd software, CA). Student t-tests were used for comparisons between two groups, with data presented as mean ± standard deviation. For multiple comparisons with two independent variables, two-way ANOVA with Sidak's post-hoc test for multiple group comparisons was performed; F-statistics were reported for comparisons across all groups, while individual comparisons between groups were reported as means or mean differences with a significance qualifier. A p-value of less than 0.05 was considered significant.

CHAPTER 3: RESULTS

3.1 7PA2-CM contains amyloid-β oligomers

Several sources of AβOs have been used to study their neurotoxic effects. The most commonly used are synthetically produced $A\beta_{1-42}$ or $A\beta_{1-40}$ peptides. These preparations need to be dissolved in non-physiological solvents and are administered at high nanomolar to micromolar ranges to facilitate their oligomerization. Despite their ubiquitous usage, it has been questioned whether synthetic AβOs represents a good model for studying the AβO toxicity (Selkoe, 2008). Amyloid-β in the extracellular fluids of humans exist at sub-low nanomolar range, contain a heterogeneous mix of amyloid-β species of varying lengths and post-translational modifications. As a result, numerous groups have moved towards the use of "naturally secreted" Aβ from cell lines which more closely mimic the human complement. The most common is the 7PA2 CHO cell line, which expresses the human APP variant V717F and secretes a heterogeneous mix of amyloid-β that oligomerize in the culture media (Shankar, Welzel, McDonald, Selkoe, & Walsh, 2011).

In our lab, media from control CHO cells (CHO-CM) and 7PA2 CHO cells (7PA2-CM) is collected and concentrated down to 1/30 of the original volume (ie. 30X). The concentrated media is stored as frozen aliquots. To confirm the presence of amyloid-β in 7PA2-CM, total amyloid-β levels were measured using ELISA which targeted amyloid-β species with a variable C-term (ie. amyloid-β 1-x). In addition, ELISA for the $A\beta_{1-42}$ species was conducted as this is the species known to promote aggregation of amyloid-β into oligomers. The concentration of total amyloid-β and $A\beta_{1-42}$ in 7PA2-CM diluted to a working concentration of 1X was found to be in the picomolar range, which mimics the physiological range found in the human brain (Figure 3.1A). As expected, amyloid-β was not detected in control CHO-CM. Therefore 7PA2-CM

added to culture media or solutions for experimental treatments was diluted to this range of concentrations. Given that soluble AβOs are the toxic species in AD, we also confirmed that amyloid-β in 7PA2-CM forms oligomers by immunoblot. 7PA2-CM contained a full range of monomers, low-n oligomers, and higher order oligomers (Figure 3.1B).

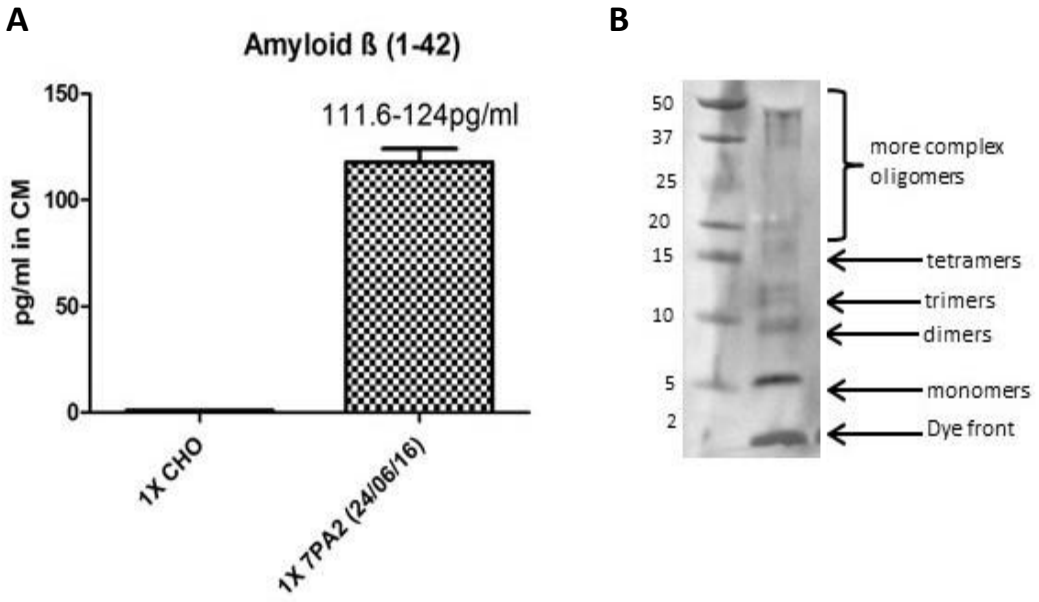

Figure 3.1: Conditioned media from 7PA2 CHO cells contain amyloid-β oligomers. **(A)** Representative ELISA measuring $A\beta_{1-42}$ levels in conditioned media from control CHO cells (CHO-CM) and 7PA2 CHO cells (7PA2-CM). Conditioned media was diluted from concentrated aliquots by a factor of 30. **(B)** Representative immunoblot of ABOs in concentrated 7PA2-CM. Monomers, low-n oligomers, and higher order oligomers could be detected.

3.2 Characterization of neurotoxicity in 7PA2-CM treated cultured hippocampal neurons by morphology

When treating cultured neurons with AβOs, previous studies have shown variable neurotoxic effects depending on the source of AβOs, their concentration, and the time of

treatment. To start, we wanted to establish the neurotoxicity of 7PA2-CM preparations on neuronally enriched primary cultures from mouse hippocampus.

DIV 18-23 cultures were treated with 7PA2-CM for 5 days and observed under a phase contrast bright field microscope. Healthy control neurons exhibit long and continuous neurites originating from phase bright cell bodies. In cultures treated with 7PA2-CM, neuronal morphology remained unchanged for up to 3 days of treatment. However, by 5 days of treatment, the degeneration of neurons was apparent; there was a shortening and fragmentation of dendrites along with the loss of well delineated phase bright cell bodies (Figure 3.2A).

To better visualize neurite morphology, cultures were loaded with calcein-AM, a cell permeable green fluorescent dye. Fluorescent calcein remains trapped within live intact cells following the cleavage of its AM group. We see that calcein evenly fills the neurites of neurons treated for 5 days with conditioned media from control CHO cells. On the other hand, 5 days of 7PA2-CM treatment caused fragmentation of neurites (Figure 3.2B). Cultures were also co-stained with ethidium homodimer-1 (EthD1), a large DNA intercalating dye which stains the nuclei of cells which have lost their membrane integrity. This typically represents cells undergoing the end stages of cell death. We see that with 5 day 7PA2-CM treatment, some of the neurons with degenerating neurites also showed EthD-1 uptake. However, quantification of cell death was not reliable due to a large number of condensed nuclei stained by EthD-1 present in both CHO-CM and 7PA2-CM treated cultures; these are likely the remnants of DNA from cells which had long undergone cell death during the culturing process. We therefore sought alternative methods of quantifying the loss of membrane integrity in these neurons.

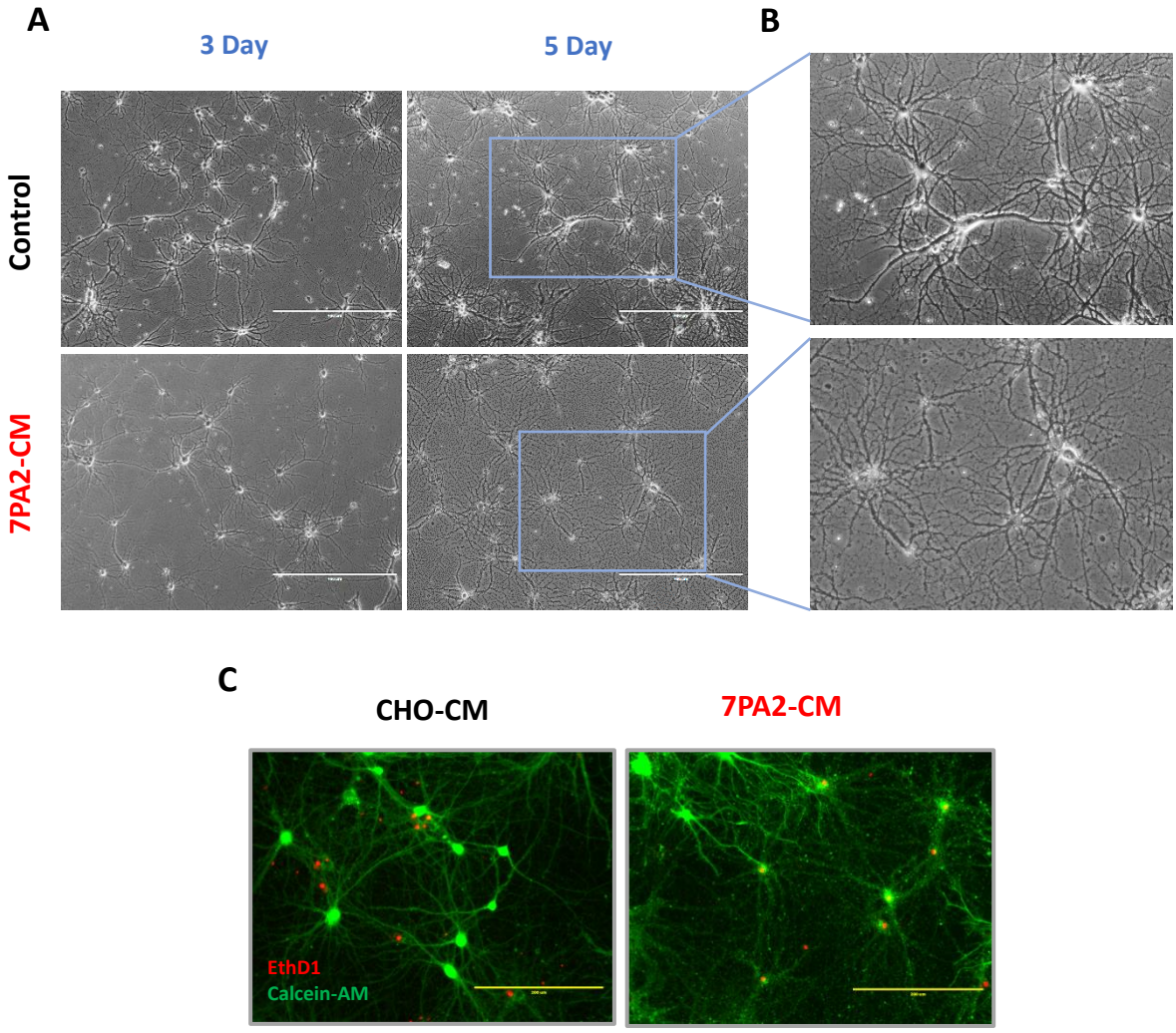

Figure 3.2: Treatment of primary cultured hippocampal neurons with 7PA2-CM leads to neurite degeneration by 5 days. (A) Representative brightfield images (10X magnification) of control and 7PA2-CM treated neurons at 3 days and 5 days. **(B)** Zoomed in image (20X magnification) of neuronal culture depicting degeneration of neurites after 5 day treatment with 7PA2-CM. **(C)** Neurons treated for 5 days with CHO-CM and 7PA2-CM live stained with Calcein-AM and ethidium homodimer-1 (EthD-1) and imaged at 20X magnification

3.3 Quantification of cell death in 7PA2-CM treated neuronal cultures

As an alternative measure of membrane integrity we used a colorimetric lactate dehydrogenase (LDH) assay. LDH is an intracellular enzyme which is released by dying cells and remains stable in the culturing media. For the assay, the media harvested from cells with impaired membrane integrity can be mixed with a substrate which is converted to a formazan dye through dehydrogenation by LDH, where the amount of dye formed is proportional to the concentration of enzyme. Absorbance is then measured by a spectrophotometer and normalized to absorbance values of total LDH released from corresponding cell lysates. Figure 3.3 shows that LDH levels in control and 3 day treated 7PA2-CM cultures were both low at 1% of total LDH (control vs. 7PA2-CM, 0.9850 ± 0.1175 N=6 vs. 0.9056 ± 0.0260 N=6, $p > 0.05$ student t-test). In cultured neurons treated for 5 days with 7PA2-CM, LDH release increased to 7% of total LDH compared to 2% of total LDH in control cultures (control vs. 7PA2-CM; 2.111 ± 0.3302 N=6 vs. 6.984 ± 0.8579 N=6, $p < 0.001$ student t-test). Treatment with 1 mM NMDA for 24 hours was used as a positive control, as prolonged stimulation of NMDA receptors is known to lead to excitotoxic cell death. This data supports our observation that neurodegeneration occurs after 5 days of 7PA2-CM treatment; however, the proportion of LDH released is still relatively small when compared prolonged NMDA application. This is consistent with the notion that AβOs first induce the degeneration of neuritic processes which slowly results in neuronal cell death. Together, these results have demonstrated that secreted AβOs mediate a robust neurodegenerative effect on our neuronal cultures

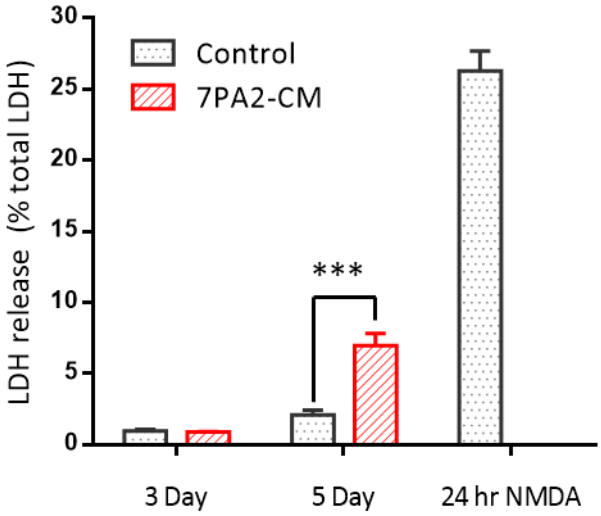

Figure 3.3: Treatment of primary cultured hippocampal neurons with 7PA2-CM leads to increased LDH release after 5 days of treatment. LDH released into the media following 3 day and 5 day treatment with 7PA2-CM (N=3 biological replicates) as a percentage of total LDH in cell lysates. Excitotoxic NMDA treatment (1 mM, 24 hours) was used as a positive control *** $p < 0.001$, students t-test

3.4 Evaluation of the effect of 7PA2-CM on Panx1 activity by YoPro-1 uptake

We next wanted to assess whether Panx1 activity is increased prior to AβO induced neurodegeneration. Large-pore activated Panx1 channels allow the flux of particles up to 1kDa in size, including the influx of small molecular dyes. YoPro-1 (free ion molecular weight of 375.5 kDa) readily passes through large-pore activated Panx1 channels and has been widely used to study the activity of Panx1 channels. It is important to note that the increase in membrane permeability to YoPro-1 facilitated by Panx1 channels is distinct from a total loss of membrane integrity or cell death. Indeed, YoPro-1 is more generally used as an early marker of apoptosis. We therefore wanted to look at YoPro-1 dye flux in cultures treated with 7PA2-CM at a time point preceding overt neurodegeneration to see if large-pore Panx1 channel activity could be

observed. YoPro-1 uptake was monitored in cultured neurons after 3 day treatment with 7PA2-CM. However, very little YoPro-1 dye uptake was observed in both control neuronal cultures and cultures treated with 7PA2-CM (% total of total cells, control vs. 7PA2-CM, 1.941 vs. 1.162, $p > 0.05$) (Figure 3.5).

3.4.1 Panx1 mediated YoPro-1 uptake is induced by activating NMDA receptors

Given the link between NMDA receptors and Panx1 channels, we reasoned that robust Panx1 recruitment would require NMDA receptor activity. Our lab and other groups have validated the use of acute treatment with NMDA to induce large-pore Panx1 currents recorded by whole-cell patch clamp (Roger J Thompson et al., 2008). Likewise, treatment of cultured neurons for 5 minutes with 50 μM NMDA in the absence of Mg^{2+} lead to the uptake of YoPro-1 which can be attenuated by co-treatment with the Panx1 channel blocker probenecid (2.5 mM) (Figure 3.4).

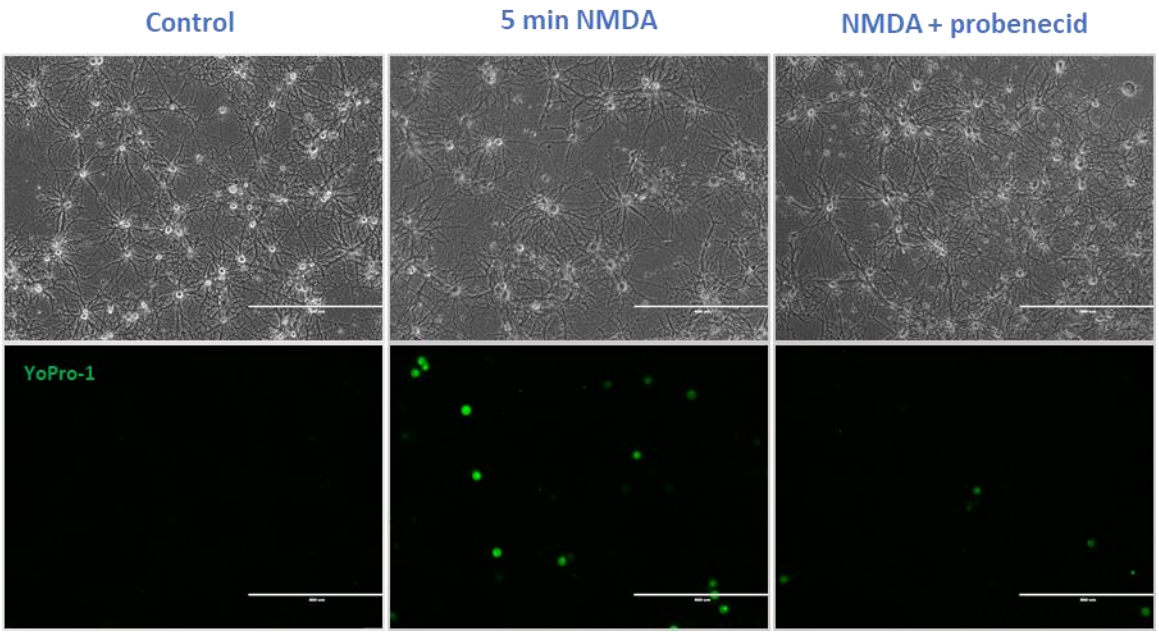

Figure 3.4: Representative images of YoPro-1 uptake following acute NMDA treatment in neuronal cultures. Representative fluorescence images of YoPro-1 uptake under GFP filter and corresponding brightfield images (10X magnification). Treatment with NMDA (50 uM) for 5 minutes causes robust dye uptake in a number of neurons. Co-treatment with the Panx1 blocker probenecid (2.5 mM) during NMDA application and dye incubation attenuated the uptake of YoPro-1.

However, for our experiments we wanted to use a less excitotoxic method of stimulating NMDA receptors to determine whether YoPro-1 flux could be induced with and without 7PA2-CM treatment.

3.4.2 Increased YoPro-1 uptake is observed in 7PA2-CM treated neurons following synaptic NMDA receptor stimulation

Treatment of neuronal cultures with bicuculline (Bic) and 4-aminopyridine (4-AP) has been used previously as a method for stimulating synaptic NMDA receptors (Hardingham et al.,

2002; Karpova et al., 2013; Tauskela et al., 2008). Bicuculline is a $GABA_A$ antagonist which reduces inhibitory tone in the cultures, while 4-AP is a potassium channel blocker which leads to neuronal depolarization. Together this causes a sustained increase in synaptic firing in neuronal cultures. As seen in Figure 3.5, the stimulation of neuronal cultures for 16 hours with Bic/4-AP led to the uptake of YoPro-1 in ~10% of neurons (unstimulated vs. stimulated, 1.941 vs. 8.452, $p < 0.05$). To confirm the role of NMDA receptors in inducing YoPro-1 uptake, cultures where stimulated with Bic/4-AP in the presence of the NMDA receptor blocker MK-801 or NMDA receptor antagonist APV. Both MK801 and APV reduced YoPro-1 uptake to unstimulated levels (unstimulated vs. stimulated + MK-801, 1.941 vs. 0.934, $p > 0.05$; unstimulated vs. stimulated + APV, 1.941 vs. 0.390, $p > 0.05$).

To determine whether AβOs can sensitize NMDA receptor dependent Panx1 large pore activation, cultured hippocampal neurons were treated with 7PA2-CM for 3 days and stimulated for 16 hours with Bic/4-AP prior to measuring YoPro-1 uptake. The proportion of neurons exhibiting YoPro-1 uptake was increased over two-fold compared to control stimulated neurons (control vs. 7PA2-CM, 8.452 vs. 18.91, $p < 0.001$). As with control stimulated neurons, block of NMDA receptors with MK-801 and APV during stimulation abolished dye uptake (unstimulated vs. stimulated + MK-801, 1.162 vs. 2.103, $p > 0.05$; unstimulated vs. stimulated + APV, 1.162 vs. 0.818, $p > 0.05$). This data suggests that AβOs cause an increase in the proportion of neurons exhibiting YoPro-1 dye uptake which is dependent on NMDA receptor stimulation.

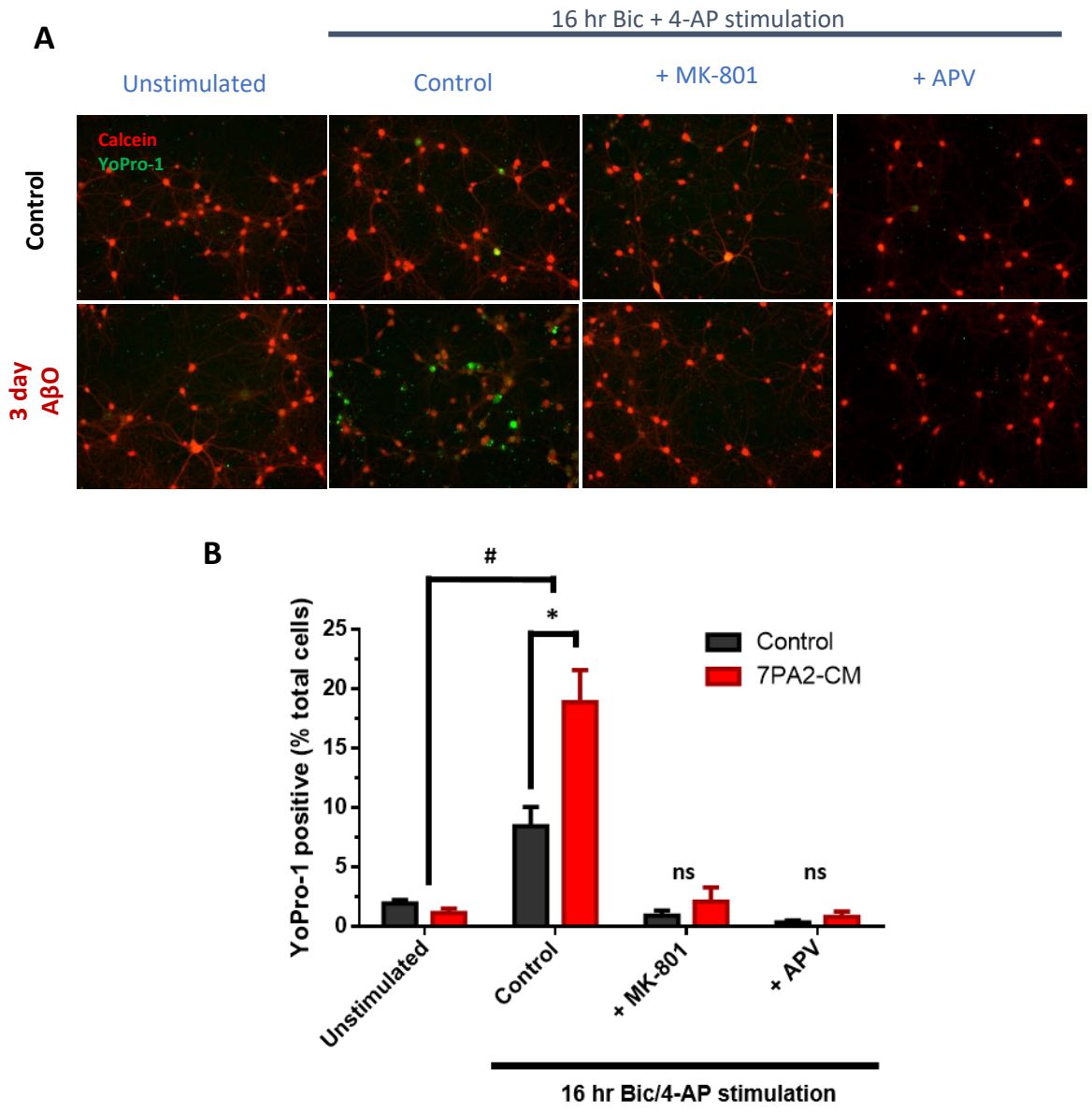

Figure 3.5: YoPro-1 uptake in cultured hippocampal neurons stimulated with Bic/4-AP. **(A)** Representative images of neuronally enriched hippocampal cultures live-stained with calcein-AM red/orange (red) and YoPro-1 (green). Control cultures and 3-day 7PA2-CM treated cultures were stimulated for 16 hours with Bic and 4-AP in the presence or absence of NMDA receptor antagonists MK-801 and APV. **(B)** Quantification of the number of cells with YoPro-1 uptake expressed as a percentage of total cells. *$p < 0.05$, Control vs. 7PA2-CM; #$p < 0.05$, unstimulated vs. stimulated, two-way ANOVA with multiple comparisons.

3.4.2 Increased YoPro-1 dye uptake in stimulated neurons treated with 7PA2-CM is not observed in Panx1 KO neurons

We next wanted to confirm the role of Panx1 channels in mediating YoPro-1 uptake following synaptic NMDA receptor stimulation by repeating these experiments in Panx1 KO neurons (Figure 3.6). We found that while Bic/4-AP stimulation of 7PA2-CM treated Panx1 WT cultures induces an increase in the number of YoPro-1 positive cells, this is not observed in Panx1 KO neurons (control vs. 7PA2-CM, 6.072 vs. 3.689, ns). This supports our hypothesis that AβOs sensitize signalling between NMDA receptors and Panx1 channels, and induces the large-pore activation of these channels. In the control group, Panx1 WT and KO neurons stimulated with Bic/4-AP had similar proportion of neurons with dye uptake (WT vs. KO, 8.452 vs. 6.072, ns) which was elevated from unstimulated levels. This suggests that a baseline population of neurons undergo cell death independent of Panx1 channel activity through this synaptic NMDA receptor stimulation protocol.

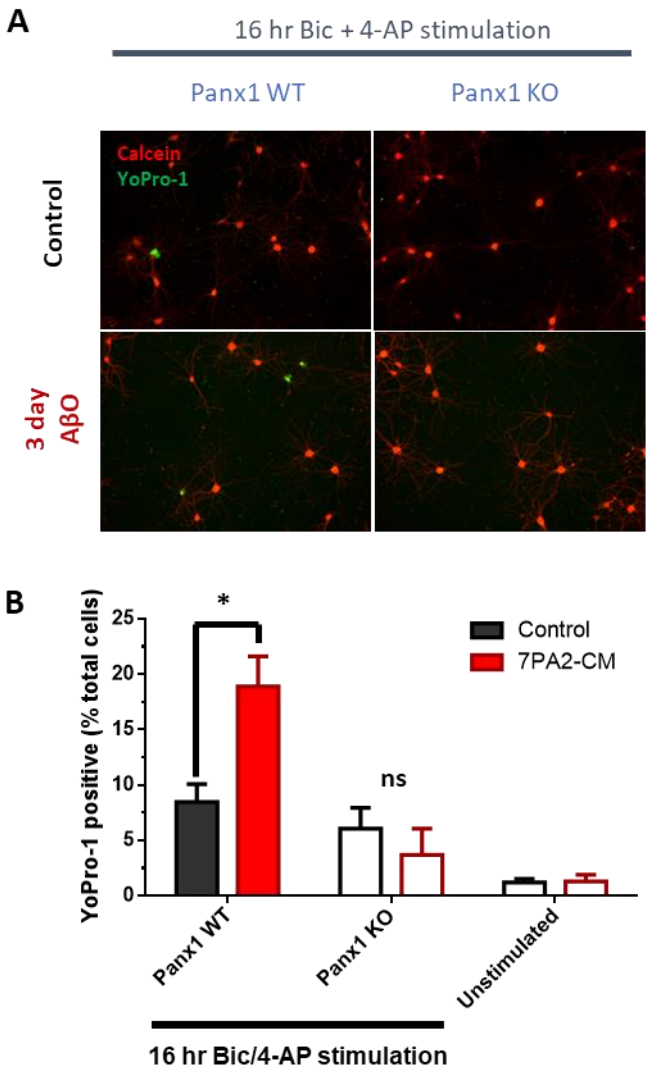

Figure 3.6: YoPro-1 uptake in Panx1 WT and KO hippocampal neurons following stimulation of synaptic NMDA receptors with Bic/4-AP. (A) Representative images of neuronally enriched hippocampal cultures from Panx1 WT and Panx1 KO mice live-stained with Calcein-AM Red/orange (red) and YoPro-1 (green). Control cultures and 3-day 7PA2-CM treated cultures were stimulated for 16 hours with Bic and 4-AP. **(B)** Quantification of the number of cells with YoPro-1 uptake expressed as a percentage of total cells. Panx1 WT data was pooled with CD1 data (Fig. 3.5) to increase statistical power. *$p < 0.05$, Control vs. 7PA2-CM

3.5 Assessing membrane permeability and synaptic function of stimulated neurons exhibiting YoPro-1 uptake by whole-cell patch clamp

We next wanted to characterize the electrophysiological behaviour of neurons which exhibited YoPro-1 uptake using the whole-cell patch clamp technique. Effectively this protocol would allow us to specifically identify neurons in which Panx1 channels were activated to their large-pore state and thereby determine the consequence of such Panx1 channel activity on synaptic function. We recorded whole-cell currents in control and 3 day 7PA2-CM treated neurons following Bic/4-AP stimulation. In these experiments, a 2-hour stimulation time (compared to 16 hours) was chosen with the rationale that this would reveal the earlier consequences of Panx1 activation on synaptic activity versus neurodegeneration at later time points. Cultures were then loaded with YoPro-1 dye to visualize and patch neurons with active Panx1 channels. Neurons were recorded in presence of TTX to prevent action potential firing. The number of recordings in each treatment group is summarized below (Table 3.1).

Table 3.1: Number of recordings across treatment groups in Bic/4-AP stimulated hippocampal neurons

	Control	7PA2-CM
Unstimulated	6	8
Stimulated (2hr Bic + 4-AP)		
YoPro-1 (-) neuron	6	7
YoPro-1 (+) neuron		
Normal permeability	9	8
High permeability	3	5

3.5.1 A proportion of Bic/4-AP stimulated YoPro-1 positive neurons exhibit an increase in membrane permeability

To start, membrane currents were measured with cells voltage-clamped at a holding potential of -60. This informs us of the total ion conductance across the membrane of neurons at resting membrane potentials. From Figure 3.7A we see that the average holding current did not differ between Bic/4-AP stimulated neurons and unstimulated neurons without YoPro-1 uptake (YoPro-1 negative) (-206.8 pA vs. -242.5 pA, ns). However, amongst Bic/4-AP stimulated neurons exhibiting YoPro-1 uptake (YoPro-1 positive), two sub-populations were observed; while some neurons had similar holding currents to unstimulated neurons, others had large holding currents. Therefore, the YoPro-1 positive group was segregated for analysis, as defined by a holding current of either above -500 pA (low conductance) or below -500 pA (high conductance). The low conductance group represented 58% (15/26) of YoPro-1 positive neurons patched and had similar holding currents to the unstimulated group (-242.5 pA vs. -293.6 pA, ns). On the other hand, the high conductance group, which represented 42% (11/26) of YoPro-1 positive neurons, exhibited holding currents which were much larger than the unstimulated group (Control: -232.7 pA vs. -1367 pA, $p < 0.001$).

Unsurprisingly, voltage ramps (-100 mV to +100 mV) applied to neurons in each of these groups revealed distinct voltage-current (I-V) relationships (Figure 3.7B). An important measure from these I-V curves is the reversal potential, or the membrane potential where there is zero net current measured across the membrane. The reversal potential gives us some information about changes in the membrane permeability to various ions. Most notably, a rightward shift in the reversal potential suggests an increased permeability to Na^+ and Ca^{2+}. Neurons in the normal permeability group exhibited an averaged I-V curve which was similar to unstimulated neurons,

with outward rectification at positive potentials and a reversal potential at -45 mV (Ctrl: -45.26 mV, 95% CI [-45.50, -45.02]; 7PA2-CM: -45.56 mV, 95% CI [-45.85, -45.28]). In the high permeability group, the averaged I-V curve was linear with a reversal potential close to 0 mV (Ctrl: -5.86 mV, 95% CI [-6.12, -5.59]; 7PA2-CM: -7.20, 95% CI [-7.356, -7.041]); this "ohmic" relationship is characteristic of non-selective cation permeability. This likely represents the recording of a neuron with large-pore activated Panx1 currents.

Treatment for 3 days with 7PA2-CM did not yield a difference in average holding currents compared to control across all treatment groups ($F_{(1, 44)} = 0.5084$, $p = 0.48$). This means that AβOs do not directly modulate the membrane characteristics of YoPro-1 negative and YoPro-1 positive neurons. Instead, 7PA2-CM simply leads to a greater proportion of neurons which exhibit YoPro-1 uptake as suggested by our quantitative data described above.

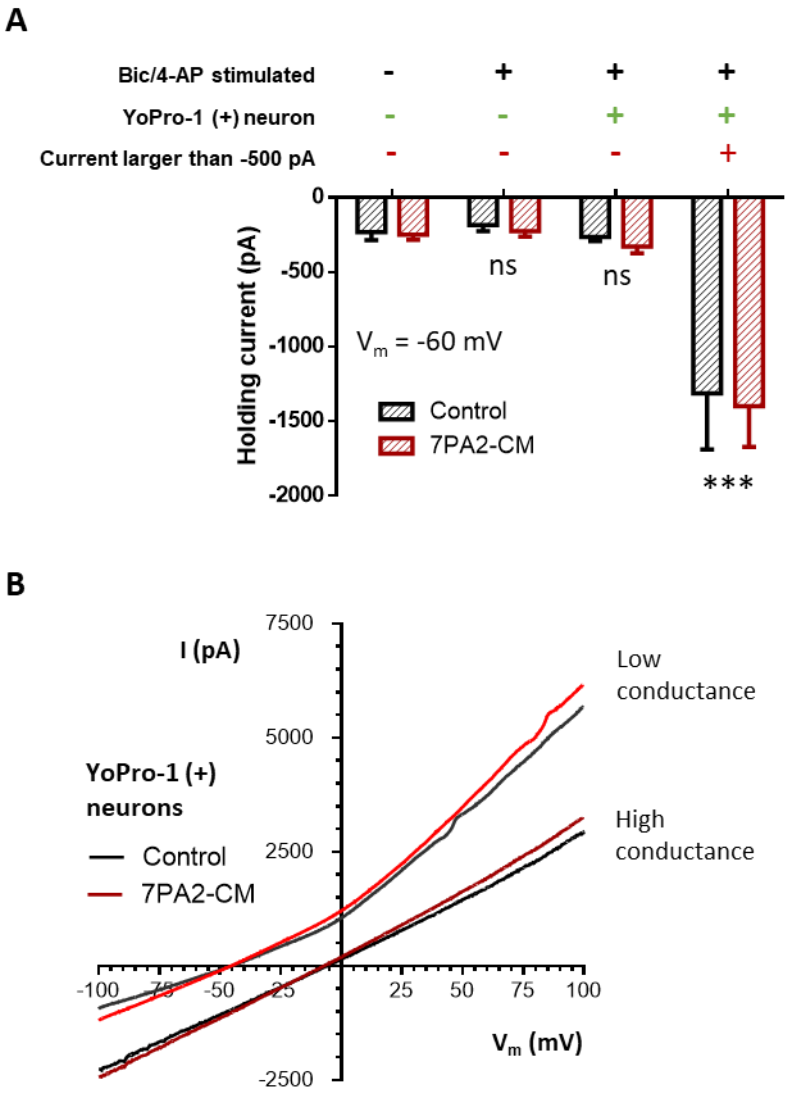

Figure 3.7: Bicuculline and 4-AP stimulated YoPro-1 positive neurons exhibit either a high membrane permeability or a low membrane permeability. (A) Holding currents measured at -60 mV across treatment groups. YoPro-1 positive neurons were grouped into those with holding currents above (low permeability) or below -500 pA (high permeability). **(B)** Voltage ramps (-100 to +100 mV) were applied to patch-clamped neurons. Averaged I-V relationships in YoPro-1 positive neurons. The high membrane permeability group exhibited a linear I-V relationship with a shift of the reversal potential to 0 mV. Two way ANOVA with multiple comparisons, *** $p < 0.001$.

3.5.2 Bic/4-AP stimulated YoPro-1 positive neurons have a higher mEPSC frequency

After Bic/4-AP stimulation, half of YoPro-1 positive neurons patched remained in a low conductance state similar to YoPro-1 negative and unstimulated neurons. We hypothesized that this group represents neurons which expresses transient Panx1 activity that facilitated dye uptake. We next wanted to assess whether this Panx1 activity causes a change in the synaptic function of these neurons.

The synaptic activity is commonly assessed by the recording of miniature excitatory post-synaptic currents (mEPSCs). These are events which occur due to the random quantal release (ie. single vesicular release) of excitatory neurotransmitters at the synapse independent of action potentials (blocked by inclusion of the Na+ blocker TTX in recording solutions). The amplitude and frequency of mEPSCs can give us information about synaptic function. The amplitude of events is dependent on the amount of glutamate released in each quanta, the number of post-synaptic AMPA receptors, and the single channel conductance of these receptors (which may be modified by post-translational modifications). The frequency of events is influenced by the pre-synaptic release probability and the number of synapses. We hypothesized that if Panx1 channels contribute to impaired synaptic function and loss of synapses, we may see a reduction in mEPSC amplitude and/or frequency.

In recordings of stimulated YoPro-1 positive neurons with high membrane conductance, mEPSCs were absent, suggesting that these cells have lost their synaptic function. In the remaining treatment groups, including YoPro-1 positive neurons with low conductance, mEPSCs could be observed and were analyzed in 87% of the recordings (38/44) (Figure 3.8). The mean amplitude of events across all treatment groups was not significantly different ($F_{(2, 32)} = 0.6914$, $p = 0.5082$) (Figure 3.8B). Interestingly, while there was also no difference in mean event

frequency between unstimulated and stimulated YoPro-1 negative neurons (4.407 vs. 5.337, ns), stimulated YoPro-1 positive neurons had an increase in the frequency of mEPSCs when compared to YoPro-1 negative neurons. (4.407 vs. 9.957, $p < 0.01$) (Figure 3.8C). This suggests that neurons permeable to YoPro-1 either had a higher number of synapses or an elevated pre-synaptic release probability. There was no difference in mEPSC frequency between the control and 7PA2-CM groups across all treatments ($F_{(1, 32)} = 0.1435$, $p = 0.7073$).

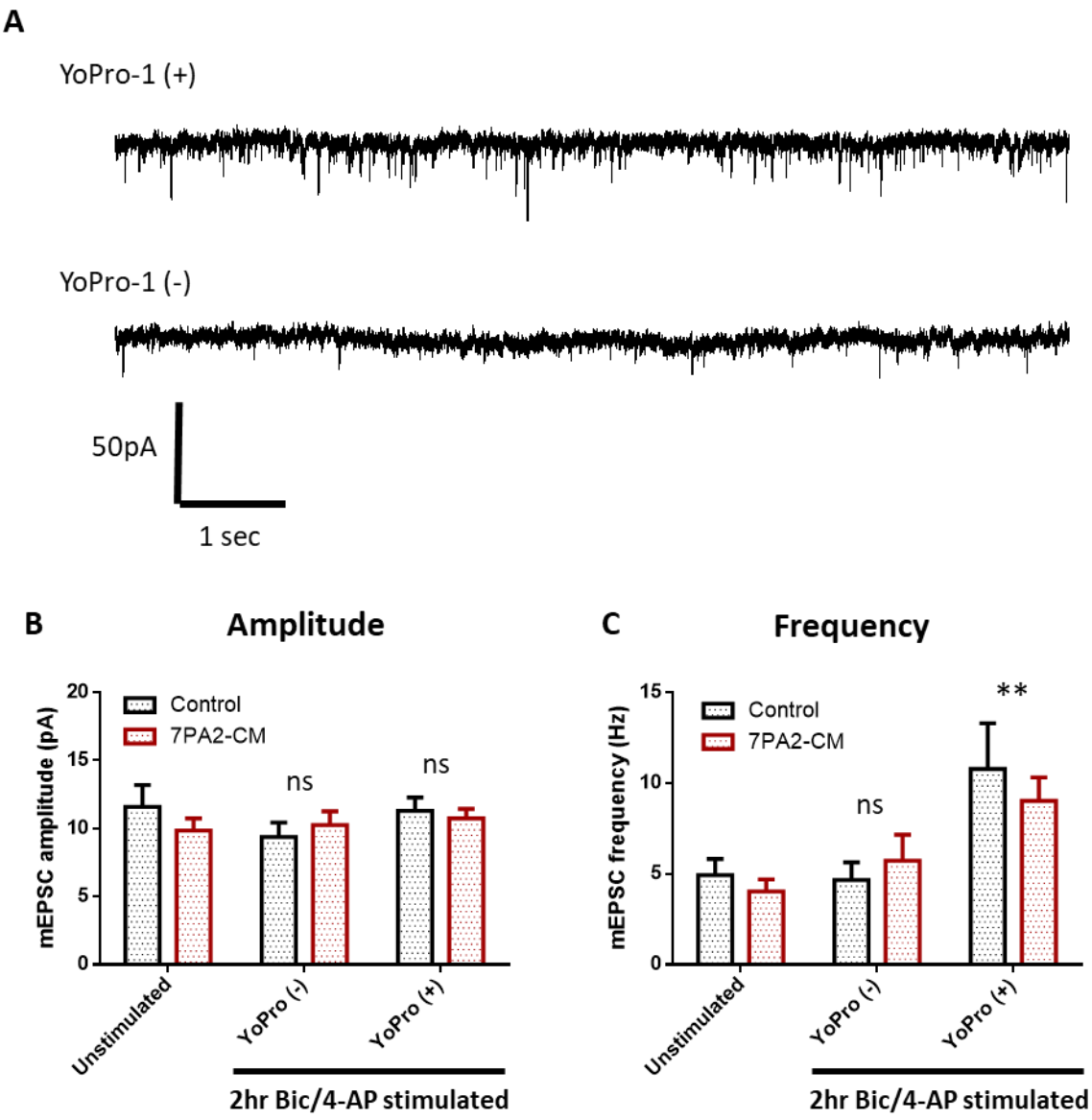

Figure 3.8: Bicuculline and 4-AP stimulated YoPro-1 positive neurons have a higher mEPSC frequency. (A) Representative mEPSC traces in bicuculline and 4-AP stimulated YoPro-1 negative and YoPro-1 positive neurons. Recordings were held at -60 mV in the presence of TTX. **(B)** Mean amplitude of mEPSCs were unchanged among treatment groups. **(C)** Frequency of mEPSCs were increased in stimulated YoPro-1 positive cells from control and 3 day 7PA2-CM treated cultures.

3.6 Effect of 7PA2-CM on synaptic protein expression in cultured neurons from Panx1 WT and KO mice

Given that the activity of Panx1 channels appear to be sensitized by AβOs following synaptic NMDA receptor stimulation, we hypothesized that Panx1 channels could contribute to AβO induced synaptotoxicity during extended 7PA2-CM treatment. Synapse numbers have been shown to be reduced with AβO toxicity before frank neuronal cell death; we therefore measured protein levels of synaptic markers by Western blot. Markers for both pre-synaptic and post-synaptic proteins are used to correlate changes in the number of pre-and post- synaptic terminals. PSD-95 and synaptophysin have been shown to be reduced in AD brains (De Wilde, Overk, Sijben, & Masliah, 2016), and reduction of these markers can be recapitulated in cell culture models of AD (J. Liu et al., 2010). PSD-95 is a scaffolding protein that is enriched at the post-synaptic density of excitatory synapses and is functionally important for anchoring glutamate receptors. Synaptophysin is a pre-synaptic protein which is part of the vesicular transmitter release machinery and regulates vesicular exocytosis and endocytosis.

To start, lysates from Panx1 WT and KO neurons were probed for Panx1 protein to confirm the absence of Panx1 in KO neurons. As expected, Panx1 WT samples expressed a band at approximately 48 kDa which was absent in Panx1 KO samples (Figure 3.9).

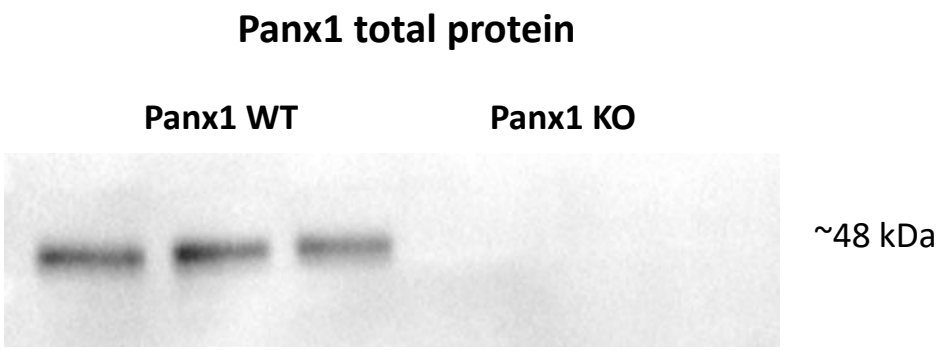

Figure 3.9: Panx1 protein is absent in Panx1 KO lysates from primary cultured hippocampal neurons. Western blots were performed on lysates from Panx1 WT and KO hippocampal neuronal cultures (DIV 18-23). Immunoblotting for Panx1 protein (predicted molecular weight between 48 kDa and 52 kDa) shows that Panx1 is present in lysates from Panx1 WT but not Panx1 KO neurons.

To look at the effect of AβOs on synaptic degeneration, cultured hippocampal neurons from Panx1 WT and Panx1 KO mice were treated with 7PA2-CM for 4 and 5 days. Treatment for 4 days was selected as a time point to asses synapse loss preceding overt degeneration seen at 5 days. Acute NMDA treatment was used as a positive control for excitotoxic synapse loss. Following cell lysis, immunoblotting was performed to quantify protein levels of PSD-95 and synaptophysin. Band intensities in each blot were first normalized to total protein added to each lane (detected by TCE protein staining). These values were then normalized to control before averaging across experiments.

3.6.1 PSD-95 expression is reduced in Panx1 WT and KO neurons following treatment with 7PA2-CM for 5 days

Immunoblotting for PSD-95 yields multiple bands at approximately 95 kDa corresponding to the 3 isoforms of the protein (Figure 3.10A). As shown in Figure 3.10B, 4 day treatment with 7PA2-CM did not significantly alter PSD-95 levels (Panx1 WT:. -0.0952, ns; Panx1 KO: -0.1909, ns). In contrast, 5 day treatment caused a 50% decrease in PSD-95 expression in both Panx1 WT (-0.4320, $p < 0.05$) and KO neurons (-0.6030, $p < 0.05$). This reduction was comparable to excitotoxic NMDA treatment (positive control) in Panx1 WT (-0.4476, $p < 0.05$) and Panx1 KO neurons (-0.4594, $p < 0.05$). There was no difference in PSD-95 protein levels between Panx1 WT and KO neurons across all treatment groups.

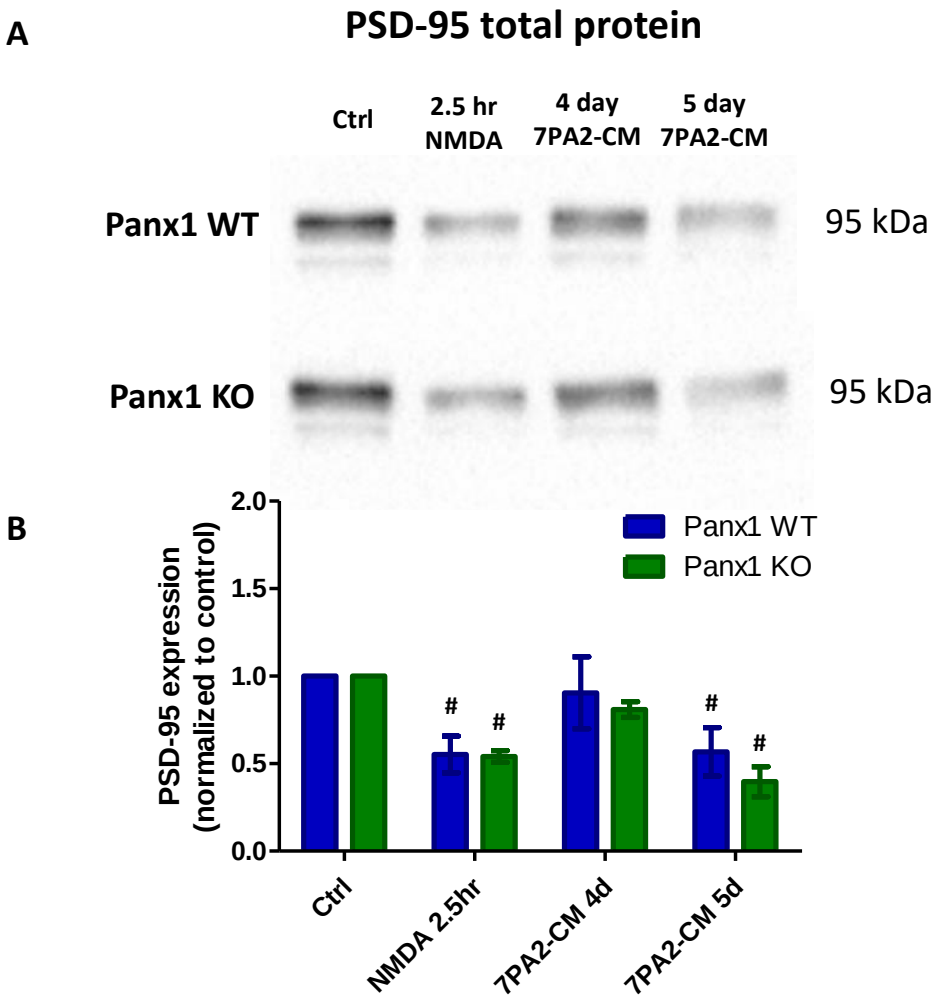

Figure 3.10: PSD-95 expression is reduced in Panx1 WT and KO hippocampal neurons following 5 day 7PA2-CM treatment. Western blots were performed on lysates from Panx1 WT and KO hippocampal neuronal cultures (DIV 18-23) treated for 4 and 5 days with 7PA2-CM, or for 2.5 hours with 30uM NMDA. **(A)** Representative blot probing PSD-95 (predicted molecular weight 95 kDa) for lysates from Panx1 WT and KO neurons treated with 7PA2-CM or NMDA. **(B)** Quantification of PSD-95 blots (N=3). Band intensity was first normalized to total lane protein as measured by TCE signal, then expressed as fold change from control. # $p < 0.05$, Ctrl vs treatment, two-way ANOVA with multiple comparisons.

3.6.2 Synaptophysin expression is reduced in Panx1 WT and KO neurons following treatment with 7PA2-CM for 5 days

We also wanted to assess changes in protein levels of the pre-synaptic marker synaptophysin (Figure 3.11). Like PSD-95, there was no change in synaptophysin levels following 4 days of treatment (WT: -0.3220, $p < 0.05$; KO: -0.3223, $p < 0.05$), while synaptophsyin expression was reduced by 5 days of treatment in both WT (-0.1755, $p > 0.05$) and KO (-0.0015, $p > 0$ .05) neurons (Figure 3.11B). Unexpectedly, NMDA caused an increase in synaptophysin levels in Panx1 WT neurons (0.3100, $p < 0.05$), with an even greater increase in Panx1 KO neurons (0.7101, $p < 0.001$). This increase may be due to an effect of NMDA treatment on total protein levels; in general, the amount of protein in NMDA treatment lanes were lower as measured by TCE luminescence despite similar confluency of cultures before treatment (appendix Figure A2). Therefore, normalizing to total protein could artificially inflate relative synaptophysin protein levels, especially if synaptophysin degradation is more limited. This may be the case, as synaptophysin is located at all pre-synaptic terminals including inhibitory synapses, while NMDA treatment leads to excitotoxic synapse loss of excitatory synaptic terminals. Together, this data suggests that there is not a major contribution of Panx1 channels to synaptic degeneration in neuronal cultures treated with 7PA2-CM for up to 5 days.

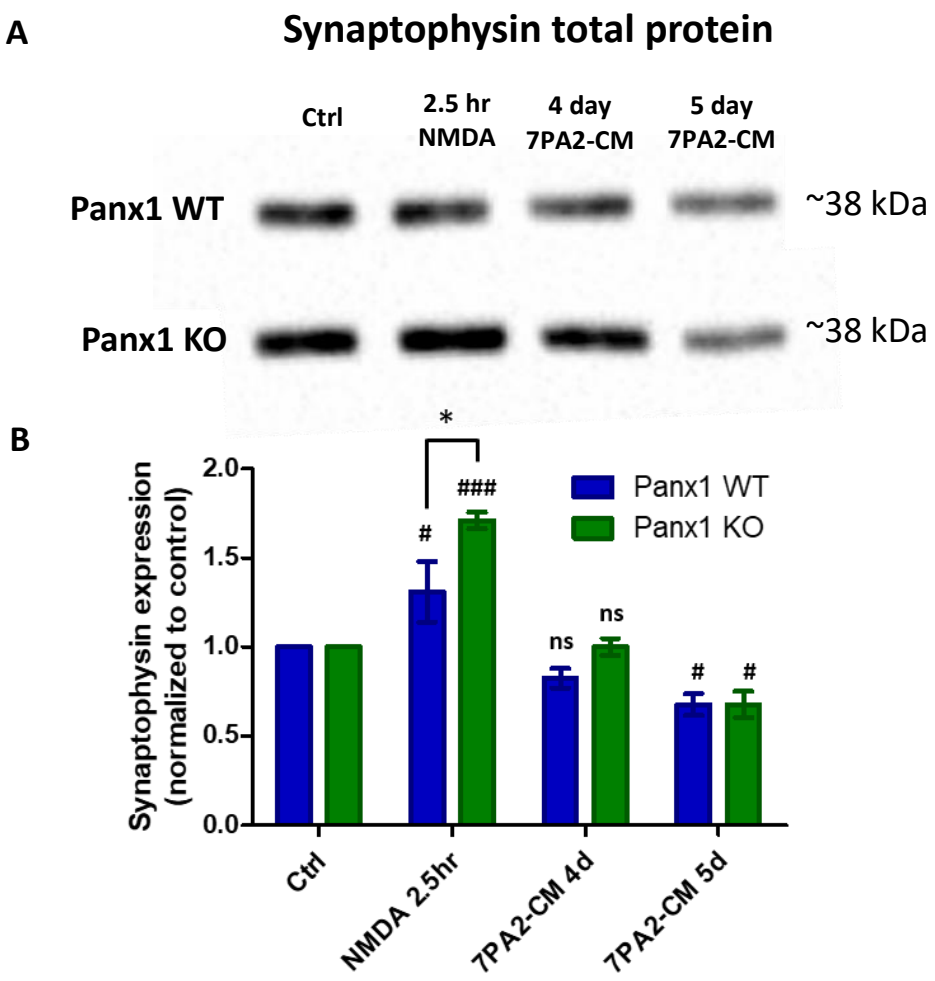

Figure 3.11: Synaptophysin expression is decreased in Panx1 WT and KO hippocampal neurons following 5 day 7PA2-CM treatment. Western blots were performed on lysates from Panx1 WT and KO hippocampal neuronal cultures (DIV 18-23) treated for 4 and 5 days with 7PA2-CM, or for 2.5 hours with 30uM NMDA. **(A)** Representative blot probing synaptophysin (predicted molecular weight ~38 kDa) for lysates from Panx1 WT and KO neurons treated with 7PA2-CM or NMDA. **(B)** Quantification of synaptophysin blots (N=3). Band intensity was first normalized to total lane protein as measured by TCE signal, then expressed as fold change from control. # $p < 0.05$, ### $p < 0.001$, Ctrl vs. treatment; * $p < 0.05$, Panx1 WT vs. KO, two-way ANOVA with multiple comparisons.

3.7 Synaptic plasticity deficits at the CA3-CA1 synapse induced by 7PA2-CM are similar in Panx1 WT and KO mice

Till now, experiments have looked at the effect of prolonged treatment (3-5 days) with AβOs in cultured Panx1 KO neurons, where we were unable to demonstrate protection from AβO induced synaptic degeneration. However, Panx1 channels could instead play a role in deficits in plasticity at the CA3-CA1 synapse of hippocampal slices induced with acute AβO treatment (hours). Given that the induction of LTP requires the strong activation of NMDA receptors during high-frequency stimulation, Panx1 channels could be recruited during this period and have a modulatory role on plasticity. We would expect that if Panx1 channels are involved, then LTP could be rescued with the knock-out of Panx1.

Field EPSP recordings at the CA3-CA1 synapse were performed on acute hippocampal slices prepared from 2-3 month old Panx1 WT and KO mice. Measures of excitability, short-term facillitation, and LTP from control slices were compared with slices pre-treated with 7PA2-CM for 2-3.5 hours.

3.7.1 Baseline excitability is unchanged with 7PA2-CM pre-treatment in Panx1 WT and KO hippocampal slices

To start, changes in baseline slice parameters were measured (Figure 3.12). Excitability was assessed by plotting the stimulation intensity (input) against fEPSP amplitude (output). The slope of the linear portion in each of these input-output curves was used to compare excitability between groups (Figure 3.12C). Pre-treatment with 7PA2-CM did not cause a change in input-output slope in Panx1 WT (0.1224 ± 0.0116 N=6 vs. 0.0920 ± 0.0156 N=4, p = 0.1486) or Panx1 KO slices (0.1292 ± 0.01292 N=7 vs. 0.1090 ± 0.01388 N=8, p = 0.3125).

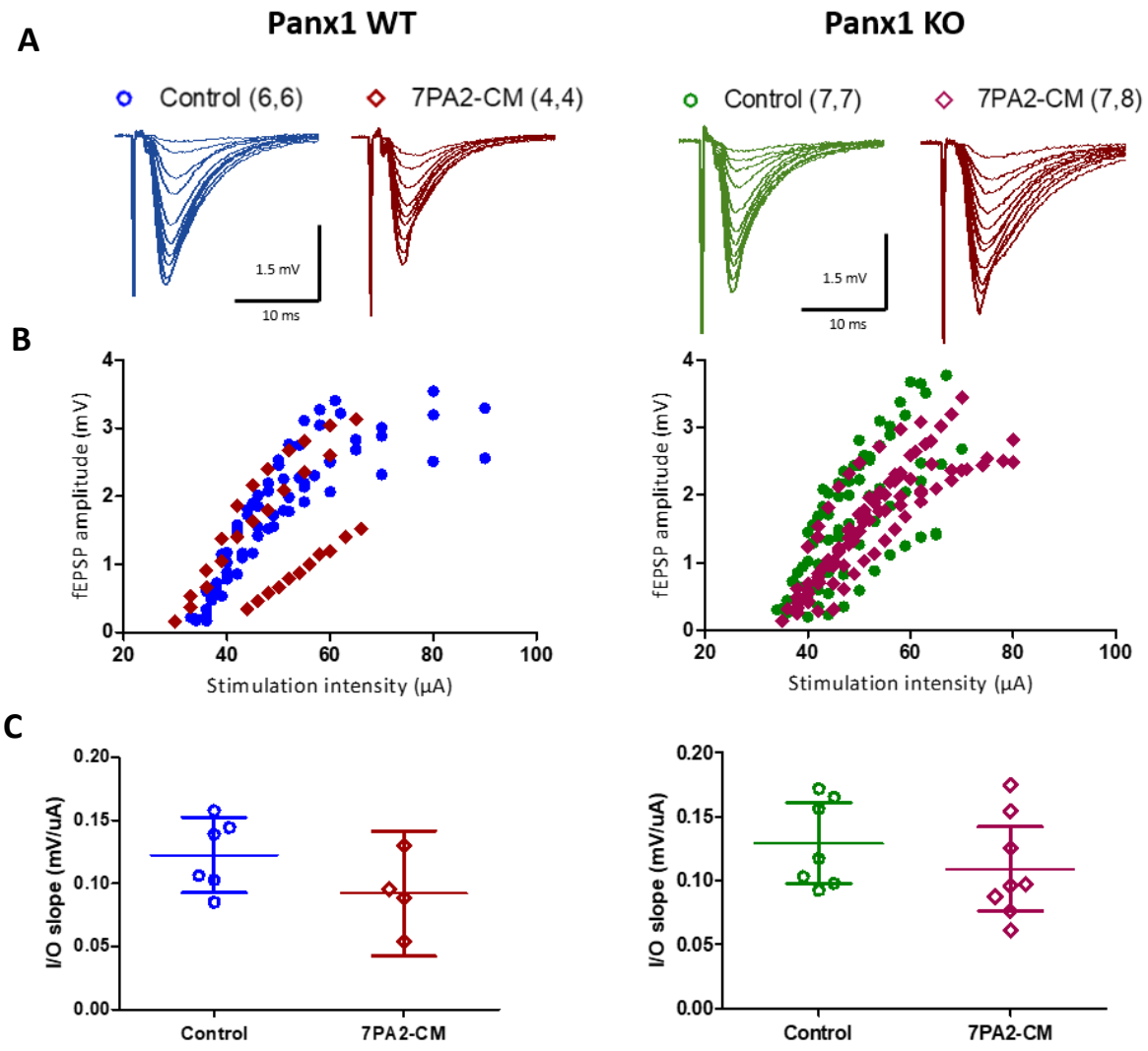

Figure 3.12: Excitability is unchanged with 7PA2-CM pre-treatment of Panx1 WT and KO hippocampal slices. (A) Representative traces of fEPSPs evoked with varying stimulation intensities in Panx1 WT and KO slices untreated (control) or pre-treated with 7PA2-CM. Numbers in brackets denote (# of animals, # of slices). **(B)** Stimulation intensity (input) plotted against evoked fEPSP amplitude (output). **(C)** Slopes from the linear portion of input/ouput curves represented as a scatter plot with mean and 95% confidence interval. There was no difference in input/output slope between control and 7PA2-CM treated slices (ns, students t-test).

3.7.2 Paired-pulse facilitation is unchanged with 7PA2-CM pre-treatment in Panx1 WT and KO hippocampal slices

Next, a form of short-term plasticity called paired-pulse facilitation (PPF) was assessed (Figure 3.13). Paired stimuli applied within short intervals (10-1000ms) leads to a temporary facilitation in the second fEPSP response. This is caused by the buildup of residual pre-synaptic calcium, leading to an increase in excitatory neurotransmitter release. PPF was not different between control and 7PA2-CM treated slices from Panx1 WT ($F=1.73$, $p = 0.2250$) or Panx1 KO mice ($F=1.21$, $p = 0.2937$) as analyzed by repeated measures two-way ANOVA (Figure 3.13B). The lack of an effect of acute 7PA2-CM treatment on slice excitability and paired-pulse facilitation is congruent with previous literature studying the acute treatment of hippocampal slices with 7PA2-CM (Townsend, Shankar, Mehta, Walsh, & Selkoe, 2006).

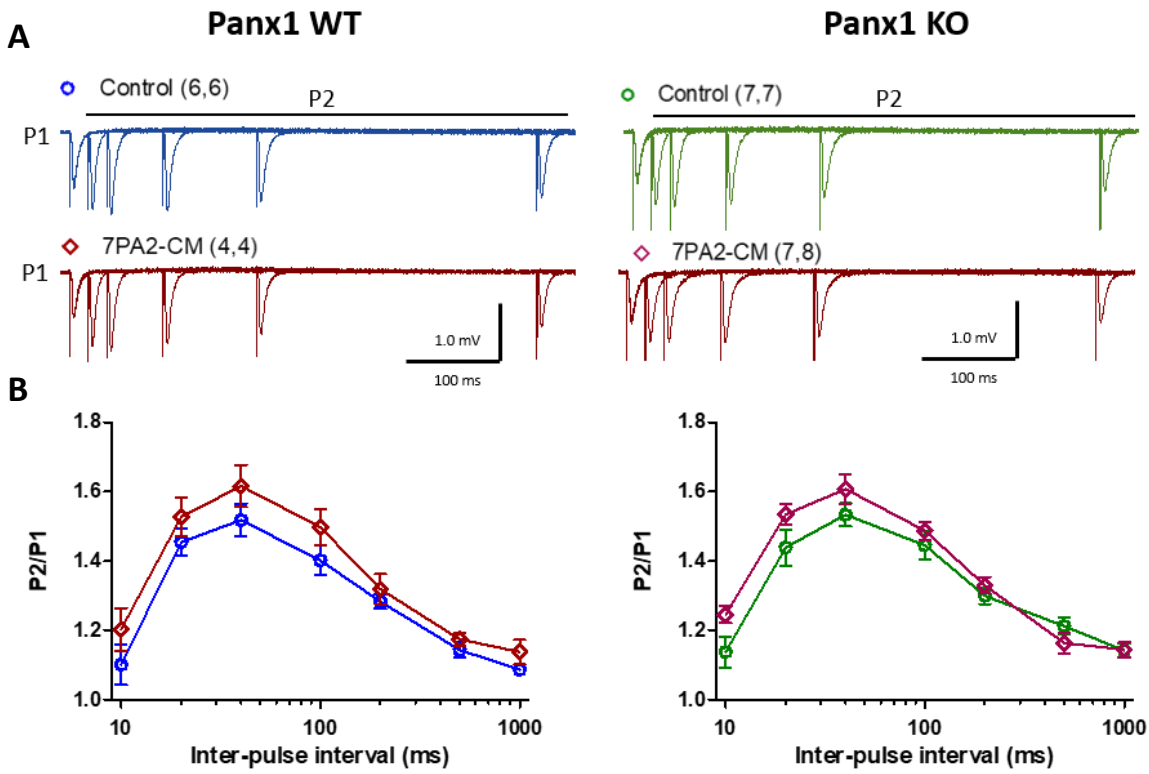

Figure 3.13: Paired-pulse facillitation is unaffected by 7PA2-CM pre-treatment in Panx1 WT and KO hippocampal slices. (A) Representative traces of paired fEPSPs evoked with multiple inter-stimulus intervals ranging from 10 ms to 1000 ms (only 20 ms – 500 ms shown in representative traces) in Panx1 WT and KO slices untreated (control) or pre-treated with 7PA2-CM. Compared to the first evoked fEPSP (P1), there is a facilitation of the second evoked fEPSP (P2) in each paired pulse dependent on the inter-stimulus interval. Numbers in brackets denote (# of animals, # of slices). **(B)** Paired-pulse facilitation represented as a ratio between the amplitude of the second fEPSP and the first fEPSP (P2/P1) across each inter-stimulus interval tested. No difference in paired-pulse ratio between control and 7PA2-CM treatment was detected in both Panx1 WT and KO slices (ns, two-way ANOVA).

3.7.3 Deficits in long-term potentiation with 7PA2-CM pre-treatment are present in both Panx1 WT and Panx1 KO hippocampal slices

Finally, we tested whether pre-treatment with 7PA2-CM causes deficits in long-term potentiation induced by high-frequency stimulation. Baseline fEPSPs were recorded for 20 min before induction of LTP by HFS (2 x 100Hz train lasting 1 sec, separated by 20 sec); fEPSPs were then recorded for an additional 60 min (Figure 3.14B). In control slices from Panx1 WT and KO mice, application of HFS caused the stable facilitation of fEPSP responses over 60 minutes; the average fEPSP slopes from the last 5 minutes of these recordings were roughly 150% of baseline (WT: 152.1 ± 6.729 N=6; KO: 145.2 ± 5.207 N=7). As expected, 7PA2-CM treatment of Panx1 WT slices caused a deficit in LTP; while there was an initial increase in fEPSP responses, this did not persist over 60 minutes of recording (116.8 ± 10.85 N=4 vs. 152.1 ± 6.729 N=6, $p < 0.05$). However, Panx1 KO slices treated with 7PA2-CM also showed deficits in LTP (109.0 ± 5.272 N=8 vs. 145.2 ± 5.207 N=7, $p < 0.001$). This data suggests that Panx1 channels are not contributing to AβO mediated inhibition of LTP expression in the CA1 region under these experimental conditions.

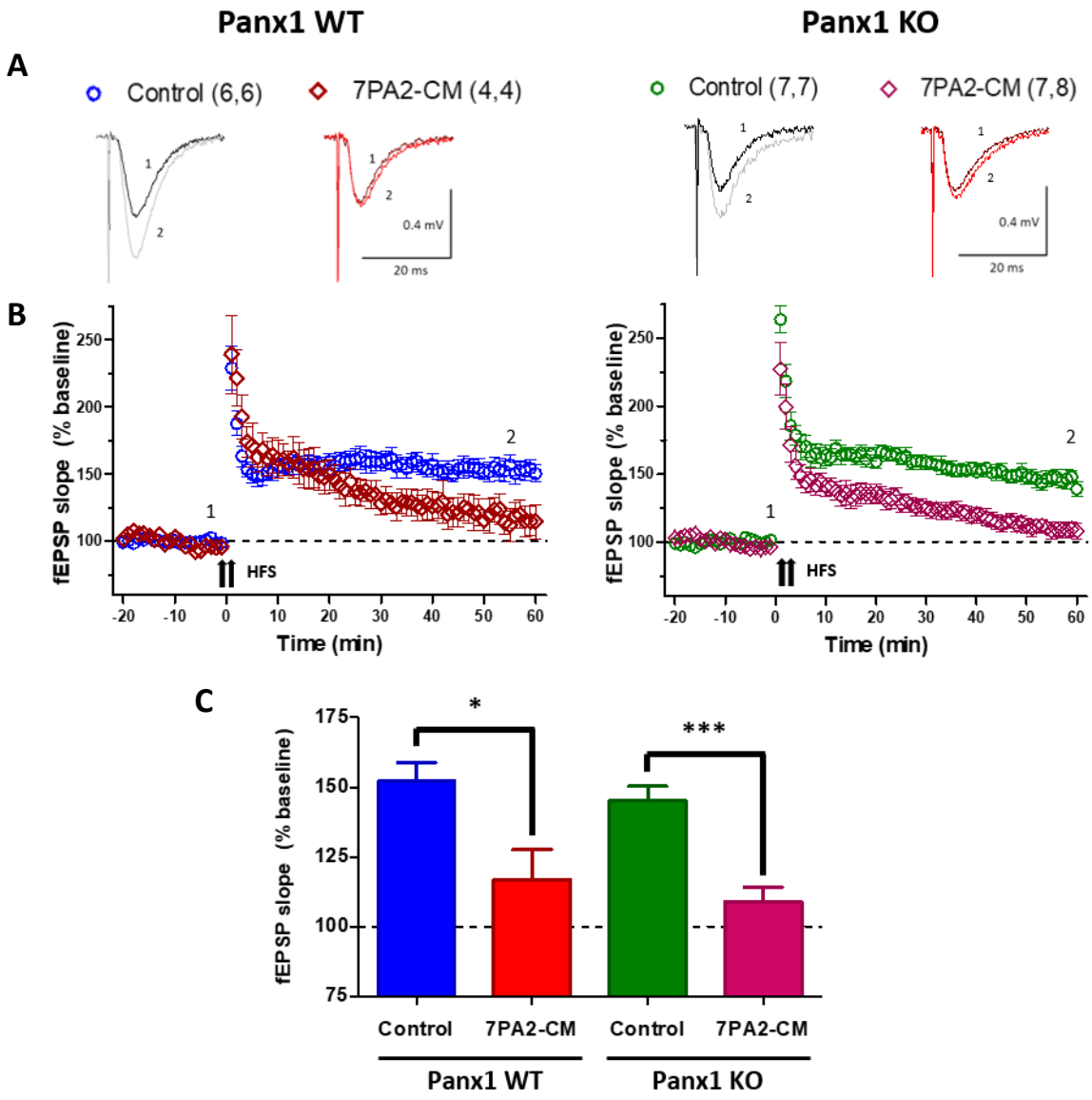

Figure 3.14: Deficits in LTP with 7PA2-CM pre-treatment are present in both Panx1 WT and Panx1 KO hippocampal slices. (A) Representative traces of fEPSP at baseline before tetanus (1) and 60 minutes post-tetanus (2) in untreated (control) or pre-treated with 7PA2-CM from Panx1 WT and KO mice. Numbers in brackets denote (# of animals, # of slices). **(B)** Plot of averaged fEPSP slopes as a percentage of baseline during each minute of recording. **(C)** Averaged fEPSP slopes from the last 5 minutes of each recording. There was a significant reduction in fEPSP slope in 7PA2-CM treated slices from both Panx1 WT and KO mice (* $p < 0.05$, *** $p < 0.001$, student t-test)

3.8 Synaptic plasticity at the MF-CA3 synapse in Panx1 WT and KO mice

Thus far, we have explored the contribution of Panx1 channels to the toxic effects of AβOs on synapse function. While Panx1 does not appear to be involved in mediating the inhibition of LTP at the CA3-CA1 synapses, it is possible that these channels play a role in AβO effects on other synapses or pathways, where Panx1 may have a more important function. However, there have been few studies characterizing the physiological functions of Panx1 in various regions of the adult brain, A secondary aim of the project was to study the modulatory role of Panx1 to plasticity mechanisms, and its contribution to learning and memory processes. As Panx1 channel modulation of synaptic plasticity has been previously described at the CA3-CA1 synapse, we wondered whether Panx1 channels may also modulate plasticity in other areas of the hippocampus.

There is evidence for Panx1 involvement in physiological and pathophysiological processes in the CA3 region of the hippocampus. It has been shown that mGluR5 induced seizures in hippocampal slices cause ATP release from Panx1 channels in the CA3 region, which further contributes bursting activity (Lopatář et al., 2015). On the other hand, glucose restriction in CA3 pyramidal neurons has been shown recruit to Panx1 channels, leading to a reduction in neuronal activity through adenosine signalling (M. Kawamura et al., 2010). We therefore decided to probe for changes in synaptic plasticity at the mossy fiber synapses of the CA3 region.

3.8.1 Short-term plasticity is unchanged at the MF-CA3 synapse

Field EPSPs were recorded from the CA3 stratum lucidum layer following stimulation of the mossy fiber pathway. Compared to the CA1, the CA3 region consists of multiple synapse

types (eg. MF and CA3 recurrent synapses) which are in close proximity to each other. MF synapses are known for their low release probability but exhibit a robust pre-synaptic potentiation (Nicoll & Schmitz, 2005). Testing short-term plasticity in these recordings therefore had the dual purpose of confirming that fEPSPs were predominantly contributed by MF-CA3 synapses in addition to probing for differences between Panx1 WT and KO slices. As expected, there was a large PPF which was expressed even at longer inter-pulse intervals; this was similar in Panx1 WT and KO slices ($F_{(6, 14)} = 0.6946$, ns) (Fig 3.15A). MF synapses are also known for frequency facillitation, where repeated stimuli given at certain frequencies (eg. 1 Hz) induces a 3-4 fold increase in response amplitudes. As seen in Figure 3.15B, a robust frequency facillitation was observed at 1 Hz stimulation in both Panx1 WT and KO slices (324.4 ± 42.68 N=3 vs. 334.0 ± 8.354 N=3, ns).

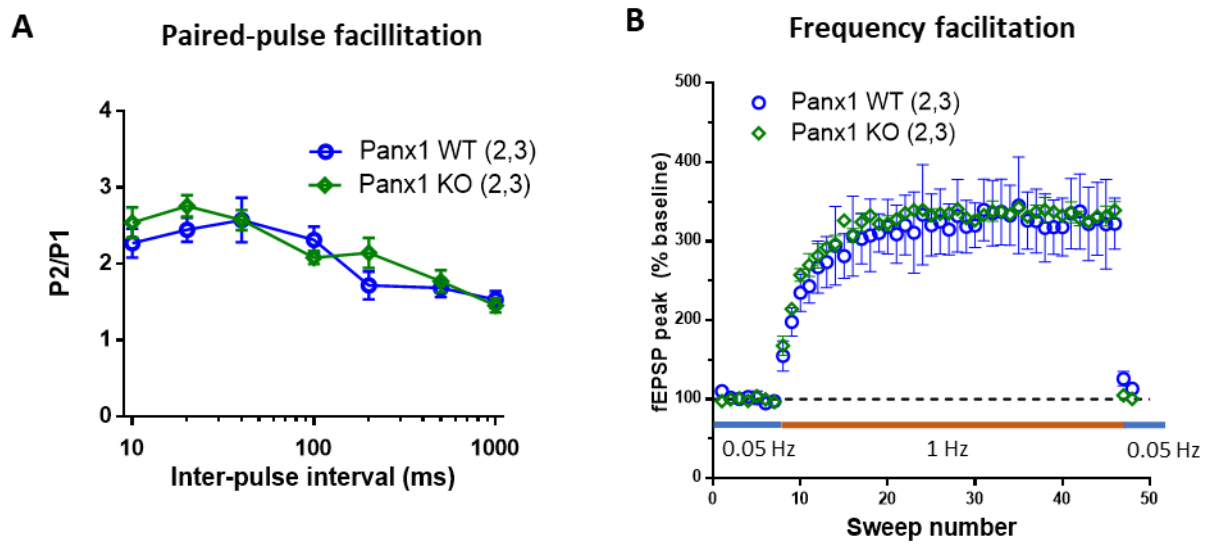

Figure 3.15: Short-term plasticity at the MF-CA3 synapse in Panx1 WT and KO acute hippocampal slices. Field EPSP recordings at the mossy fiber CA3 synapse in acute hippocampal slices from ~12 week old Panx1 WT and KO mice. Numbers in brackets denote (# of animals, # of slices). **(A)** Paired-pulse facilitation evoked with multiple inter-stimulus intervals ranging from 10 ms to 1000 ms. Larger facilitation is observed when compared to the CA3-CA1 synapses. **(B)** The mossy fiber synapse exhibits frequency facilitation, a characteristic short-term increase in fEPSP amplitude following modest increases in the frequency of stimulation (ie. 1Hz). (C) LTP induced by HFS (two 100Hz trains lasting 1 sec and separated by 20 seconds) is stable over 60 minutes. (D) Average of fEPSP slopes from the last 10 minutes of LTP.

3.8.2 LTP at the MF-CA3 synapse is reduced in Panx1 KO hippocampal slices

We then induced LTP by HFS (2 x 100 Hz) at the MF synapse to see if WT and KO slices exhibited any differences in plasticity. Post-stimulation, a large facilitation was observed which eventually plateaued and remained potentiated over 60 minutes of recording (Figure 3.15C). Panx1 WT slices showed a larger potentiation than Panx1 KO slices by the last 10

minutes of the recording (161.1 ± 4.088 N=3 vs. 137.1 ± 2.151 N=2, $p < 0.05$) (Figure 3.15D); however, more recordings need to be performed to reproduce this finding.

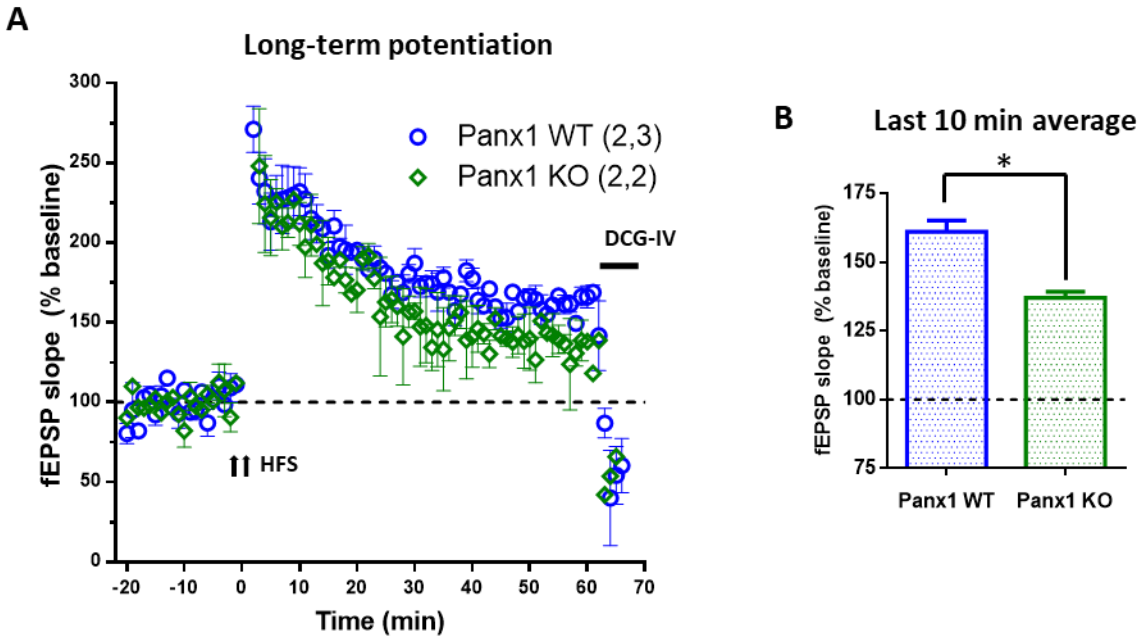

Figure 3.16: LTP at the MF-CA3 synapse in Panx1 WT and KO acute hippocampal slices. Field EPSP recordings at the mossy fiber CA3 synapse in acute hippocampal slices from ~12 week old Panx1 WT and KO mice. **(A)** LTP induced by HFS (two 100Hz trains lasting 1 sec and separated by 20 seconds) is stable over 60 minutes. **(B)** Average of fEPSP slopes from the last 10 minutes of LTP were significantly different between Panx1 WT and KO recordings. * $p < 0.05$, student t-test.

3.9 Behavioural characterization of Panx1 WT and KO mice

Synaptic plasticity at the tri-synaptic circuit of the hippocampus is known to be important for hippocampal dependent learning and memory tasks. However, other circuits within the hippocampus and in other areas of the brain can also contribute to memory expression. While our rationale for directly assessing plasticity at the CA3-CA1 and the MF-CA1 synapses was sound, we may be missing out on a functional contribution of Panx1 in other subsets of synapses. A top down approach looking at changes in the performance of behavioural tests can potentially point to deficits in different circuits. We conducted a battery of behavioural tests to probe for changes in anxiety-like behaviour, object recognition memory, and fear memory in a cohort of male Panx1 WT (n=8) and Panx1 KO (n=8) mice aged 6-11 months.

3.9.1 Anxiety levels tested by elevated plus maze are similar between Panx1 WT and KO mice

The elevated plus maze is widely used as a test for anxiety-like behaviours in genetic mouse models and drug screening. The maze is composed of an elevated platform in the shape of a plus sign; two arms of the maze have high walls (closed arms) while the other two arms do not (open arms). This test takes advantage of a mouse's natural aversion to open and elevated spaces, where mice will generally spend more time in the closed arms and less time in the open arms. Any difference in the time spent in the arms or the number of arm entries between test groups may indicate an effect on anxiety levels (Komada, Takao, & Miyakawa, 2008). Anxiety-like behaviours are centrally controlled by the amygdala and bed nucleus of the stria terminals (BNST), with higher circuit modulation by the medial prefrontal cortex (mPFC) and ventral hippocampus (Adhikari, 2014).

Panx1 WT and KO mice were subjected to the elevated plus maze. From Figure 3.16A, we see that there was no difference in the exploratory activity between Panx1 WT and KO mice; the total number of arm entries (as defined by movement from open to closed arm or vice versa) between groups were similar (6.25 ± 0.750 N=8 vs. 6.11 ± 0.484 N=9, ns). Also, an equal proportion of open arm and closed arm entries was observed in both the Panx1 WT and KO groups, meaning the mice were willing to explore both types of arms. When measuring the time spent in each arm, there was no difference between groups; Panx1 WT and KO mice spent the majority of their time in the closed arms (88.29 ± 3.950 N=7 vs. 81.78 ± 4.126 N=9, ns) (Figure 3.16B). Therefore, the Panx1 KO mice did not show a change in anxiety-like behaviour.

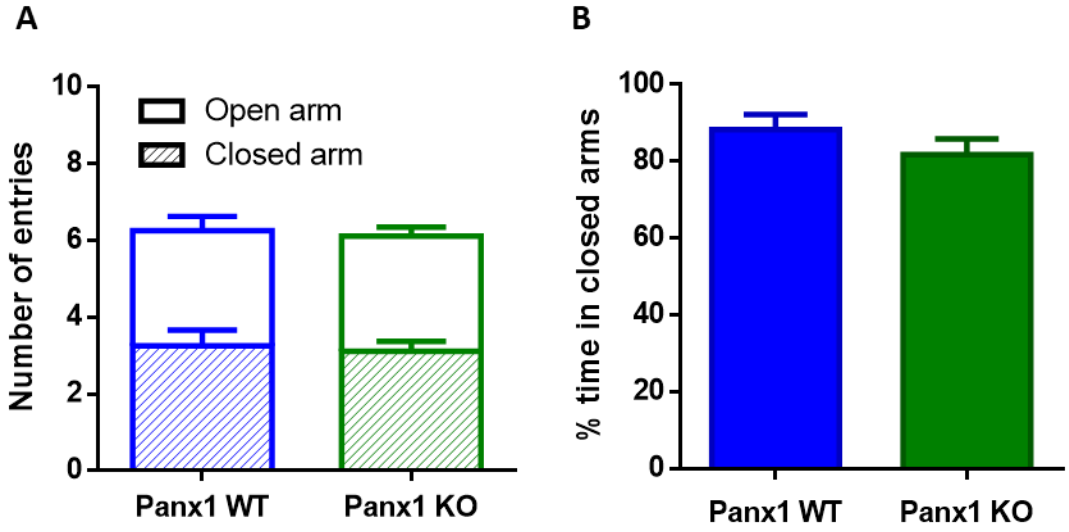

Figure 3.16: Panx1 WT and KO mice spend a similar amount of time in the closed arm of the elevated plus maze. Panx1 WT and KO mice were placed into the elevated plus maze for 5 minutes. **(A)** The number of entries into open and closed arms was not different between groups. **(B)** Panx1 WT and KO mice spent a similar amount of time in the closed arms of the maze.

3.9.2 Object recognition memory is not impaired in Panx1 KO mice

In the novel object recognition test, mice are familiarized with one kind of object in one session, and then presented with both a familiar object and a novel object in a subsequent session. This test relies on the mouse's innate drive to explore novel objects and therefore assesses their ability to recognize and distinguish a familiar object from a novel object. Object recognition memory has been shown to involve circuits of the hippocampus and the perirhinal cortex (Antunes & Biala, 2012). Mice with intact recognition memory spend a greater proportion of time exploring the novel object; those with impaired memory equally explore familiar and novel objects.

It has previously been reported that CNS specific conditional Panx1 KO mice exhibit a deficit in novel object recognition (Prochnow et al., 2012). Our aim was to see whether our Panx1 KO mice would also show these deficits. The novel object recognition test relies on animals being motivated to explore the objects. In our data set, 4 animals (2 WT and 2 KO) had to be excluded from analysis as they spent less than 8 seconds exploring the objects. Mean exploration times were 21.25 ± 4.327 sec for WT mice and 17.46 ± 4.128 sec for KO mice (Figure 3.17A). In Panx1 WT mice, there was no significant difference in the exploration of the novel object versus the familiar object due to the large variation between animals (mean difference 12.00 ± 51.98 %). However, Panx1 KO mice did spend more time exploring the novel object compared to the familiar object (mean difference 14.29 ± 13.39 %, $p < 0.05$, paired student t-test), suggesting that object recognition memory is not impaired in these mice (Figure 3.17B).

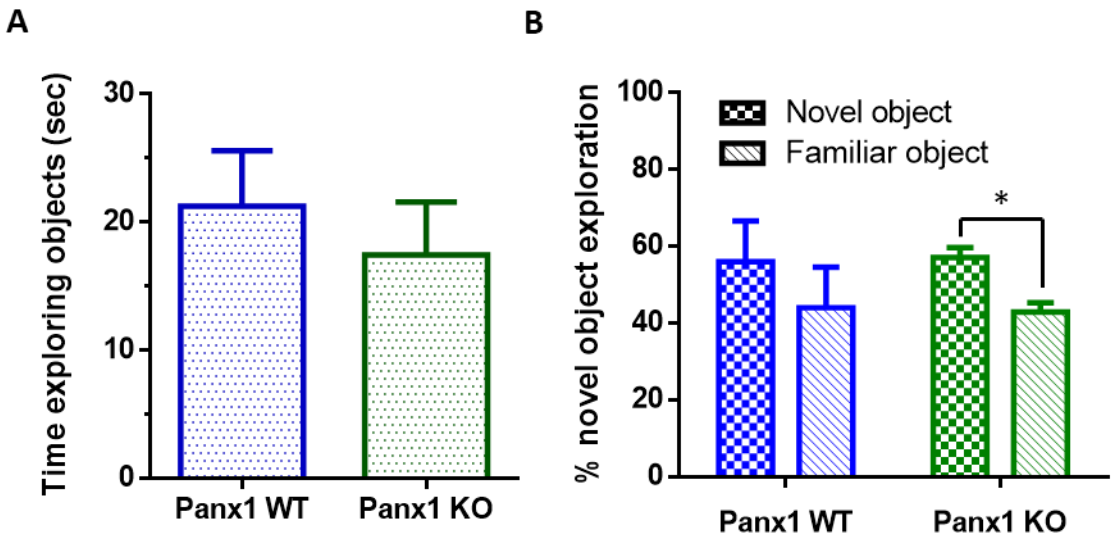

Figure 3.17: Panx1 KO mice prefer the exploration of the novel object. Panx1 WT and KO mice were allowed to explore a familiar and a novel object in an open field for 5 minutes. Four animals (2/8 WT and 2/8 KO) were excluded from analysis due to low exploratory drive (less than 8 seconds with each object). **(A)** Time spent exploring objects was highly variable among animals. **(B)** Panx1 KO mice favoured exploring the novel object. * $p < 0.05$, paired student t-test.

3.9.3 Contextual fear memory is similar between Panx1 WT and KO mice

Contextual fear conditioning is used to link a strongly aversive stimulus (eg. foot shock) with an environmental context (eg. the shocking chamber). Subsequent presentation of the context elicits a fear response which presents itself as freezing behaviour. This is defined as the complete immobilization of the animal except for respiration. Contextual fear learning requires the function of the amygdala, the structure of the brain important for emotional learning and memory. The hippocampus is also necessary as it involved in the memory of environmental context. Indeed, contextual fear memory has been shown to be associated with the LTP of

circuits within (and between) the hippocampus and the amygdala (Izquierdo, Furini, & Myskiw, 2016).

A contextual fear conditioning protocol was performed on Panx1 WT and KO mice. The environmental context consisted of the enclosed space of the shocking chamber, the texture of the flooring, and the smell of the cleaning solution. On the day of fear conditioning, mice were given three foot shocks separated by 30 seconds. A response to the shocks was elicited in all mice, which consisted of a sudden jump (and sometimes a vocalization) followed by a freezing response. The next day, mice were returned to the chamber and recorded for 5 minutes. Panx1 WT mice spent 59% of their time freezing while Panx1 KO mice spent 46% of their time freezing; however due to the high variability in freezing time between animals, this was not a significant difference (mean difference 13.58 ± 11.51 %, ns, student t-test) (Figure 3.18B).

When the fear context is presented in the absence of the aversive stimulus, this can result in a reduction in the conditioned fear response during subsequent presentations of the context. This process is called fear extinction, and it is thought to be primarily due to an inhibitory learning which suppresses the original contextual fear memory. We wanted to probe for any differences in fear extinction between Panx1 WT and KO mice in contrast to fear conditioning. Fear extinction protocols exist often consist of multiple or prolonged presentations of the context in the absence of the aversive stimulus. However, we decided to use a simple protocol wherein the testing day for fear memory performed 24 hours after fear conditioning also served as fear extinction training. Extinction of the fear memory can then be tested by returning the mice the context three days later and measuring changes in the fear response (Figure 3.18A). This protocol has been previously used to reliably induce and resolve differences in fear extinction learning (Zushida, Sakurai, Wada, & Sekiguchi, 2007). From Figure 3.18B, we see that when

Panx1 WT and KO mice were placed in the shock chamber 3 days after fear extinction training, they exhibited a reduction in freezing time (mean difference WT: 24.25 ± 4.441 %, $p < 0.001$; KO: 15.33 ± 4.188 %, $p < 0.01$, two-way ANOVA with multiple comparisons). However, there was no difference in freezing time between the two genotypes in the fear extinction test (mean difference 4.903 ± 11.64 %, ns, two-way ANOVA with multiple comparisons). Therefore, Panx1 KO mice did not exhibit a significant difference in either contextual fear memory or contextual fear extinction when compared to wildtype mice.

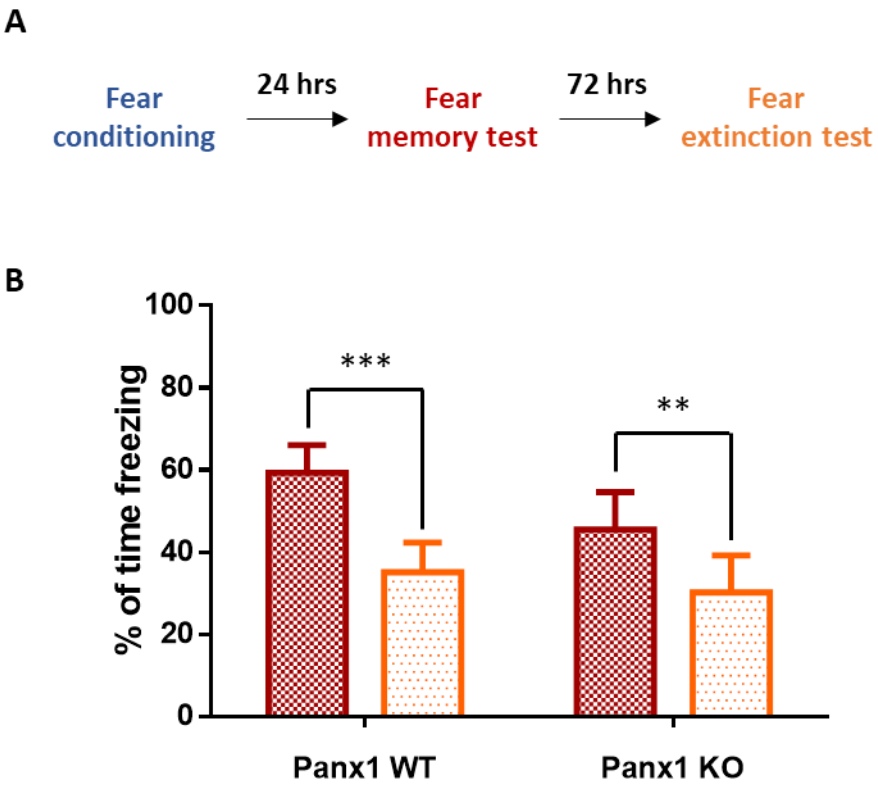

Figure 3.18: Contextual fear memory and extinction is unchanged in Panx1 KO mice. **(A)** Panx1 WT and KO mice were subjected to contextual fear conditioning consisting of 3 foot shocks applied within the shocking chamber. Fear memory was tested 24 hours later, where mice were place in the chamber and left undisturbed for 5 minutes. To test for fear extinction, mice were tested again after 72 hours. **(B)** Time spent freezing was reduced in both groups during the fear extinction test. However, time spent freezing was not significantly different between both groups during either the fear memory test or the fear extinction test.

CHAPTER 4: DISCUSSION

The primary aim of this thesis was to look at the role of the Panx1 channel in the pathogenesis of AD, with a specific focus on the AβO induced dysfunction of excitatory synapses on hippocampal neurons. We found that AβOs can facilitate the activity of Panx1 channels by sensitizing the upstream signalling of NMDA receptors. Yet we were unable to elucidate the pathological consequences of Panx1 activity on synaptic degeneration and synaptic plasticity at CA1 synapses. As a secondary aim, we also examined synaptic plasticity at MF synapses and probed for behavioural differences between Panx1 WT and KO mice to explore physiological roles of the channel in the CNS. The findings from these experiments, their limitations, and their relation to overall theories of AD and Panx1 channel function will be discussed in the pages to follow.

4.1 Amyloid-β oligomers increase the NMDAR dependent activation of Panx1 channels

YoPro-1 dye uptake can be used as a measure of large-pore Panx1 activity. In our dye flux experiments, the stimulation of neuronally enriched hippocampal cultures with Bic/4-AP induced YoPro-1 uptake in a population of neurons; the number of these cells was shown to increase in neuronal cultures which were treated for 3 days with 7PA2-CM. It was confirmed that the induction of dye uptake by neurons required the activity of NMDA receptors as block with APV during the 16-hour stimulation period completely reverted dye uptake to unstimulated levels. MK-801 also abolished dye uptake, which suggests that ion flux through the NMDA receptor (ie. ionotropic activity) is necessary for this effect. We further showed that the 7PA2-CM induced increase in YoPro-1 positive cells was abolished in Panx1 KO neurons. This

suggests that dye uptake is mediated by large-pore activated Panx1 channels. The results from these experiments therefore support our hypothesis that AβOs can sensitize the signalling between NMDA receptors and Panx1 channels, leading to the recruitment of large-pore Panx1 channels.

The prolonged Panx1 activity would presumably lead to calcium dysregulation, recruiting parallel mechanisms which contribute to an increase in membrane permeability. In this case, YoPro-1 dye uptake at the time of the assay would not be solely driven by Panx1 *per se*. This represents a limitation of the assay, where the timing of Panx1 activation cannot be resolved. A time course of dye uptake, where YoPro-1 would be loaded at the beginning of the experiment and monitored during synaptic NMDA receptor stimulation, may better resolve when Panx1 channels start to become active in 7PA2-CM treated cultures.

Another method in confirming the large-pore activation of Panx1 channels is to use whole-cell patch clamp to directly assess the membrane conductance and ion permeability of YoPro-1 positive neurons. In these experiments, cultures were stimulated for 2 hours before recording to study the early consequence of Panx1 activation. What we found was that of all the YoPro-1 positive neurons patched, half exhibited large holding currents at resting membrane potential. It was confirmed from their “ohmic” I-V relationship that these neurons exhibited a non-selective ion permeability characteristic of large-pore activated Panx1 channels. This gives us confidence that YoPro-1 uptake is mediated by Panx1 channels. However, it is also possible that non-selective conductances mediated by other channels could have been recruited. Application of a Panx1 blocker in future recordings of YoPro-1 positive neurons would confirm whether these are Panx1 specific conductances. Alternatively, these experiments could be repeated in Panx1 KO neurons.

Interestingly, the other half of YoPro-1 positive neurons exhibited a low (ie. normal) membrane conductance. This group more likely represents neurons which had transient Panx1 activity which led to dye uptake. We therefore wanted to assess whether the synaptic function of these neurons was altered by the activity of Panx1 channels. According to our hypothesis, increased Panx1 activity would lead to the degeneration of synapses and therefore a reduction in mEPSC frequency. To our surprise, we observed an increase in mEPSC frequency in these YoPro-1 positive neurons. Two explanations may account for this finding. These may be neurons which already had a greater number of synapses. Stimulation with bicuculline and 4-AP would then drive higher NMDA receptor activity, leading to more Panx1 mediated YoPro-1 uptake into the neuron. Alternatively, large-pore activation of Panx1 channels on these neurons could be facilitating the release of a signalling molecule which binds to pre-synaptic terminals and induces an increase in neurotransmitter release probability. Over time, it would be expected that this increased activity would promotes even greater Panx1 channel opening, leading to the degeneration of these neurons. In this way, low conductance YoPro-1 neurons and high conductance YoPro-1 neurons could represent the early and late consequences of Panx1 activity following synaptic NMDA receptor stimulation.

It is important to note that in these electrophysiological experiments, control and 7PA2-CM treated neurons behaved similarly across all treatment groups (including YoPro-1 positive neurons). This makes sense given that Panx1 activity can be promoted by NMDAR, irrespective of AβO treatment. Moreover, these findings suggest that once activated, Panx1 channels mediate similar endpoints with respect to membrane conductance and synaptic function. From all these results, we can conclude that 7PA2-CM sensitizes NMDA dependent Panx1 activation, leading to an increase in the population of neurons which exhibit Panx1 activity.

4.2 Possible mechanisms for Panx1 sensitization by amyloid-β oligomers

4.2.1 Src Family Kinases

What mechanisms may be responsible for AβO facilitation of Panx1 channels downstream of NMDA receptor stimulation? One possible mechanism is through phosphorylation by SFKs. Studies have shown a modulatory role of the SFK Src on Panx1 activity following excitotoxic NMDA receptor activation (Weilinger et al., 2016). This is through the action of Src on a tyrosine residue located at Y308 on the C-term tail of the channel, which was shown to facilitate large-pore Panx1 currents.

The synaptotoxic effects of AβOs are linked to the detrimental activation of the SFK Fyn. AβOs are thought to directly upregulate the activity of the SFK Fyn through its binding with the PrPc and mGluR5 complex (Larson et al., 2012). Downstream activation of Fyn in AD disease models cause NMDA receptor phosphorylation, leading to greater trafficking and activation of these channels at the membrane. This is followed by the homeostatic upregulation of STEP1 phosphatase which overcompensates for the effects of Fyn and results in a net increase in the internalization of NR2B containing receptors (J. W. Um et al., 2012). Interestingly, Fyn is also responsible for the phosphorylation of tau protein. The overactivation of Fyn has been proposed to be one of the pathogenic links between AβO toxicity and the hyperphophorylation of tau (Larson et al., 2012). While a specific interaction between Fyn and Panx1 has not yet been described, it is possible that Fyn has a similar role in modulating Panx1 channels and could provide a pathological mechanism of channel facilitation with AβO toxicity.

4.2.2 Caspase-3 mediated cleavage

Literature also supports a regulatory role of the apoptosis related protease caspase-3 in promoting increased Panx1 channel activity through cleavage of the C-term. The C-term tails of Panx1 interact with and obstruct the channel pore (e.g. ball-and-chain) and are thought to act as a modifiable gating mechanism. Cleavage of the C-term tails liberate this gating, causing an increase in the open probability of the channel. This has been linked to membrane permeabilization during apoptosis which cause apoptotic cells to release ATP (Chekeni et al., 2010). While the recruitment of Panx1 currents following 5 minute excitotoxic NMDA receptor activation was found to be independent of caspase activity (Weilinger et al., 2012), this does not exclude the role of caspases over longer time scales. Indeed, the influence of caspase-3 activity on Panx1 channels may be relevant in our experiments, where synaptic NMDA receptors were stimulated for 16 hours. If this is the case, co-treatment with caspase inhibitors during stimulation would reduce the number of YoPro-1 positive neurons.

The increased activity of caspase-3 has been observed in association with AD pathology. Caspase-3 is known as the executor of apoptosis due to its direct role in degrading cellular structures following its activation during apoptotic signalling pathways. However, caspase-3 does not exclusively mediate cellular apoptosis – it can also have restricted actions at the synaptic level. NMDA receptors and mGluR5 can mediate the synapse specific activation of caspase-3, and the activity of caspase-3 has been shown to be necessary for LTD (Z. Li et al., 2010). Caspase-3 is upregulated in the post-synaptic densities of AD brains (Louneva et al., 2008). Moreover, AβO induced inhibition of LTP, facilitation of LTD and degeneration of synapses, have all been shown to be mediated by increased caspase-3 activity (Chan, Griffin, & Mattson, 1999; X. Chen et al., 2013; Jo et al., 2011; J. Liu et al., 2010). Therefore, an AβO

induced increase in caspase-3 activity at the synapse may be one mechanism for the facilitation of Panx1 activity.

4.2.3 ER calcium signalling

The endoplasmic reticulum (ER) is a major store of calcium in neurons and is an important contributor to calcium signalling cascades. NMDA receptor-mediated calcium signals can be amplified through calcium-induced calcium release (CICR) from the ER. This is mediated by activity of the calcium dependent ryanodine receptors (RyR) and IP3 receptors (IP3R). The induction of NMDA receptor dependent plasticity mechanisms has been shown to require the activity of RyR and IP3R (Del Prete et al., 2014), underlining the importance of CICR to the downstream signalling of NMDA receptors.

CICR also leads to the depletion of ER calcium, triggering secondary influx of calcium across the plasma membrane through a process called store-operated calcium entry (SOCE). SOCE is facilitated by the ER resident calcium sensing proteins stromal interacting molecule 1 (STIM1) and stromal interacting molecule 2 (STIM2); upon depletion of ER calcium, STIM1 and STIM2 are recruited to the plasma membrane, where they primarily stimulate the influx of calcium through calcium selective Orai channels. While the primary function of SOCE is to refill ER calcium stores, it may also contribute to various calcium dependent processes such as the maintenance of mature synaptic spines (Dittmer, Wild, Dell'Acqua, & Sather, 2017). In addition, STIM1 and STIM2 have also been shown to regulate other membrane channels, including TRPV and VGCCs.

Unpublished work in our lab has uncovered an ER dependent pathway for the activation of Panx1 channels. Specifically, the depletion of ER calcium induces large-pore currents through

Panx1 channels. Evidence points to an interaction between Panx1 and STIM in this process. Our lab proposes that NMDA receptor dependent activation of the Panx1 channel is mediated through CICR and interactions with STIM. This is supported by substantial evidence suggesting the CICR is dysregulated in AD. Numerous studies report that ryanodine receptors are sensitized in AD models, leading to elevated intracellular calcium levels (Chakroborty, Goussakov, Miller, & Stutzmann, 2009; Chakroborty & Stutzmann, 2014; Ferreiro, Oliveira, & Pereira, 2004; Goussakov, Miller, & Stutzmann, 2010). In addition, the dysregulation of SOCE can contribute to either intracellular calcium overload or the chronic depletion of ER calcium in a variety of neurodegenerative diseases (Secondo, Bagetta, & Amantea, 2018). Therefore, a link between the dysregulation of ER calcium signalling in AD and the ER dependent recruitment of Panx1 is a major area of study in our lab and may represent a mechanism for the sensitization of Panx1 channel activity downstream of NMDA receptors stimulation.

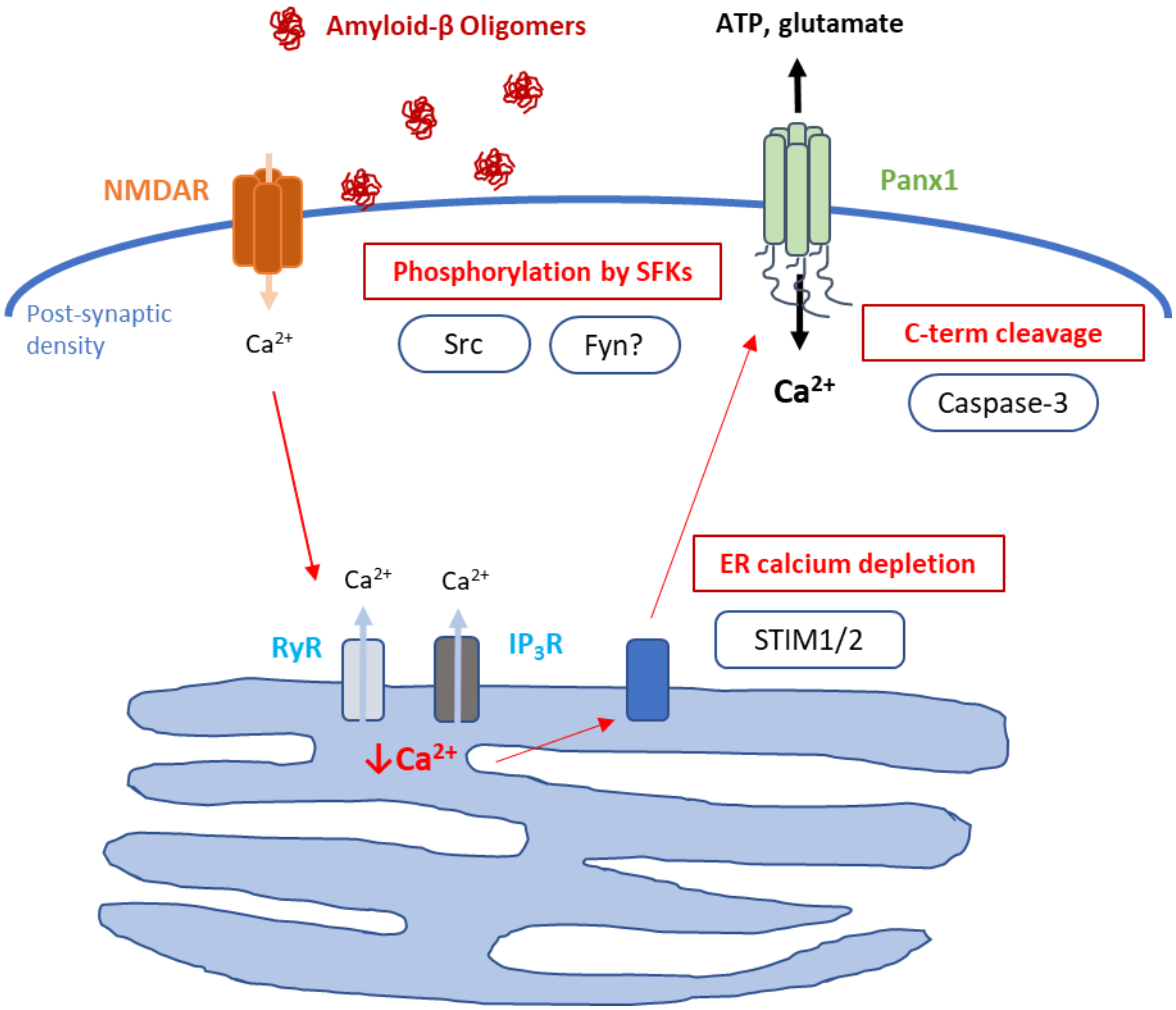

Figure 4.1. Hypothesized model the AβO induced sensitization of NMDA receptor dependent Panx1 activity.

4.3 Pathological consequences of Panx1 activity in AD

4.3.1 Panx1 in synaptic degeneration

Our dye flux experiments suggested that AβOs may facilitate the activation of Panx1 channels. The next questions were therefore aimed at elucidating the contribution of augmented Panx1 channel activity to AβO induced toxicity. We hypothesized that with prolonged AβO

treatment, Panx1 could contribute to AβO induced synaptic degeneration. Treatment of primary neuronal cultures from Panx1 WT mice with 7PA2-CM for 5 days led to a ~50% reduction in the protein expression of the post-synaptic protein PSD-95 and the pre-synaptic protein synaptophysin. This was correlated with overt neurodegeneration, which was observed at this time point. However, the reduction in synaptic markers following 5 day 7PA2-CM treatment was not prevented or delayed in neurons from Panx1 KO mice. These results suggest that 7PA2-CM induced degeneration in these cultures is independent of the activity of Panx1 channels.

Subtle changes in functional synapse numbers preceding overt neurodegeneration could be a more relevant period for studying the synaptotoxic effects of AβOs. We chose a 4 day treatment time to test this hypothesis. However, a significant reduction in PSD-95 and synaptophysin expression at this earlier time point was not detected with WB of whole-cell lysates. The quantification of synapse numbers by synaptic protein expression in whole-cell lysates is a crude measure of the total synaptic proteins of the culture. It does not tell us about the localization of these proteins, and their contribution to functional synapses As such, it may not be an appropriate method for detecting small changes in functional synapse numbers. Alternative methods such as immunocytochemistry could be a better approach. The co-localized puncta of pre-synaptic and post-synaptic markers represent functional synapses which can be quantified. Fluorescence filling of the neuron can also be used to directly visualize dendritic arborization and dendritic spines numbers and morphologies.

The experiments discussed so far were conducted in neuronally enriched primary hippocampal cultures. This allows us to isolate the effects of AβOs on the neuronal population and to study effects of neuronally expressed Panx1. However, the interaction of glial cells such

as astrocytes and microglia with neurons may also be an important aspect in synaptic degeneration in AD.

4.2.2 Panx1 in neuroinflammation

Thus far, we have ignored the consequences of ATP release from large-pore Panx1 channels. The extracellular signalling of ATP has an important role in promoting the inflammatory responses of microglia, the resident immune cell of the CNS. Neuroinflammation is increasingly implicated in the pathogenesis of AD; AβOs directly induce the activation of microglia, leading to increased expression and release of inflammatory cytokines (Parsons et al., 2007). This pro-inflammatory phenotype can have a negative impact on neuronal function. Some inflammatory cytokines, such as Il-1β, have been shown to directly impair LTP (Goshen et al., 2007; Lai, Swayze, El-Husseini, & Song, 2006). In addition, microglia are known to physically interact with synapses. This is best observed during the developmental process of synaptic pruning, where synapses are eliminated by microglia through phagocytosis (Schafer, Lehrman, & Stevens, 2013). It has been hypothesized that these pruning mechanisms can be reactivated in the context of CNS disease. In a highly influential study, Hong et al. demonstrated that early synapse loss and plasticity deficits in AD mouse models is mediated by microglia through an upregulation in complement protein signalling. They showed that reactive microglia in this context directly eliminate synapses by engulfing (ie. phagocytosing) the synaptic elements (Hong et al., 2016).

It has been previously suggested that ATP release from Panx1 channels can act as a “find me” signal for immune cells to phagocytose apoptotic cells (Chekeni et al., 2010). From our dye uptake experiments, we demonstrated that with AβO treatment, synaptic NMDA receptor

stimulation led to an increase in the large-pore activity of Panx1 channels. While ATP release was not measured directly, we can infer that these large-pore activated channels can mediate the flux of ATP. One could hypothesize that increased Panx1 activity and ATP release in pathological contexts such as AD may lead to aberrant microglial synapse interactions and contribute to synapse loss. Interestingly, ATP released by neuronal Panx1 has already been shown to facilitate the synaptic engagement of microglia in a physiological context. In vivo imaging studies of microglia in the optic tectum of larval zebrafish demonstrated that Panx1 mediated ATP release led to the steering of microglial processes towards active neurons. Contact of microglia with these neurons was shown to downregulate their activity (Y. Li, Du, Liu, Wen, & Du, 2012).

While neuronal Panx1 channels may play a role in attracting immune cells, the expression of Panx1 on glial cells may also contribute to the release of pro-inflammatory molecules. Panx1 in complex with the P2X7 receptor has been shown to facilitate ATP induced inflammasome formation, leading to the exocytotic release of the pro-inflammatory cytokine Il-1β. This was first described in macrophages (Pelegrin et al., 2006), but has also been demonstrated in neurons and astrocytes (Silverman et al., 2009). Thus, Panx1 can mediate pro-inflammatory signalling between glial cells and neurons through the release of ATP and the secretion of Il-1β.

In one of the only reports studying the role of Panx1 in AD, Orellana et al. showed that microglial Panx1 channels are activated with toxic concentrations of $A\beta_{25-35}$ and contribute to the release of ATP and glutamate. The excitotoxic levels of extracellular ATP and glutamate then led to neuronal cell death in this experimental model (Orellana, Shoji, et al., 2011). However, this study did not look at the role of AβOs in early synaptic dysfunction, which is a more

relevant model for AD pathogenesis. While microglial contributions to synaptic dysfunction in AD were not a focus of this thesis, I performed experiments as part of a separate project to probe for changes in synaptic plasticity in the 3xTg AD mouse model crossed with the microglia specific KO of the pro-inflammatory master regulator poly-ADP ribose polymerase (PARP) (Appendix Figure A3). Future experiments studying the synaptotoxic effects of AβOs in co-cultures of microglia and neurons may reveal a pathological role of Panx1 channels in inflammatory crosstalk. Alternatively, the establishment of hippocampal slice cultures would allow for the study of the synaptotoxic effects of prolonged AβO treatment over several days, with the advantage of preserved cytoarchitecture and the influence of glial cells on pyramidal cell function and morphology.

4.3.3. Panx1 in hippocampal plasticity deficits

The expression of LTP and LTD at the CA3-CA1 synapse is largely dependent on NMDA receptor activity. However, these plasticity mechanisms are also modulated through the action of other synaptic receptors. Literature suggests that Panx1 could play such a modulatory role; field recordings in hippocampal slices from Panx1 KO mice showed that the threshold for LTP induction is shifted, where LTP is induced at much lower frequencies of stimulation (Ardiles et al., 2014). In other words, Panx1 appears to play a role in limiting LTP induction and favouring LTD induction, similar to the effect of AβOs on plasticity at hippocampal synapses. Given that our dye flux experiments suggest an NMDA receptor dependent increase in Panx1 activity following 7PA2-CM treatment, we reasoned that a similar increase in Panx1 activity during the induction of LTP could partially drive AβO induced plasticity deficits. Our hippocampal field recording experiments were aimed at elucidating whether Panx1 channels

contribute to AβO induced deficits in LTP by comparing Panx1 WT and KO slices following 7PA2-CM pre-treatment. The pre-treatment of Panx1 WT slices with 7PA2-CM containing nM concentrations of AβOs lead to a decrease in the expression of LTP without changes to excitability and paired-pulse facilitation. However, parallel experiments in Panx1 KO slices demonstrate that the reduction of LTP magnitude with 7PA2-CM pre-treatment remained, suggesting that Panx1 channels are not necessary for the AβO induced deficit in LTP.

4.4 Panx1 in plasticity and memory

4.4.1 Synaptic plasticity in Panx1 KO mice

A secondary aim of this thesis was to explore the physiological roles of Panx1 channels in plasticity and memory systems of the adult brain. Our field recordings at the CA3-CA1 synapse showed no difference in the magnitude of LTP expression between control hippocampal slices from Panx1 WT and Panx1 KO mice (Appendix Figure A4). This is counter to results reported by Prochnow et al and Ardiles et al, where Panx1 KO slices expressed a larger magnitude of LTP (Ardiles et al., 2014; Prochnow et al., 2012). Several factors may account for this discrepancy:

i) A difference in the preparation of slices may also affect the phenotypes seen with Panx1 KO mice. Cutting solutions are often used to improve slice health with the intent of better preserving the physiological properties of the circuits. In these solutions, sodium is often replaced with sucrose or NMDG, and the ratio of magnesium to calcium is increased to limit excitotoxicity. Differences in slice preparation have been shown to differentially effect the expression of plasticity

mechanisms (Kuenzi, Fitzjohn, Morton, Collingridge, & Seabrook, 2000). In our hands, the use of standard aCSF for slice preparation is sufficient for recording stable fEPSPs and inducing a robust LTP, but this differs from the Ardiles et al, who used a sucrose cutting solution to prepare slices.

ii) Recording conditions and parameters may also account for differences in LTP expression. The ratio of magnesium and calcium and the concentration of potassium in the recording aCSF can all affect the expression of LTP or LTD. In addition, different stimulation protocols used to induce LTP can recruit alternative plasticity mechanisms. For example, 200 Hz stimulation and theta-burst stimulation (TBS) can induce a pre-synaptic L-VGCC dependent component of LTP in parallel with the post-synaptic component (Bayazitov et al., 2007). Ardiles et al. showed that the Panx1 KO plasticity phenotype was present with both a TBS protocol and continuous HFS trains. The recording conditions and the HFS protocol were similar to the ones used in our experiments.

iii) Ardiles et al. reported that the Panx1 KO plasticity phenotype was absent in young mice (1 month of age), only manifesting in adult mice (6 months of age). This hints at an age-dependent contribution of Panx1 to synaptic plasticity and may explain the lack of plasticity phenotype in our experiments, where animals ranged from 6 – 10 weeks of age. Recordings in slightly older animals (12-14 weeks) also did not yield a difference in LTP magnitude (appendix figure A4); replicating these experiments in animals 6 months of age or older may definitively answer whether age is a factor in the reported plasticity phenotype. We currently have an aged cohort (7-12 months of age) which will allow us to probe for an age dependent change in plasticity in Panx1

KO mice. In addition, this gives us the opportunity to look at changes in memory behaviours.

Given that we were unable to see a difference in LTP at the CA3-CA1 synapse, we decided to probe for Panx1 involvement in the MF-CA3 synapse of the hippocampus to further explore the role of this channel in synaptic plasticity and memory systems. This was based on evidence suggesting that Panx1 plays a prominent role in promoting release of ATP in the CA3 rather than CA1 region (M. Kawamura et al., 2010; Lopatář et al., 2015). In preliminary recordings of these synapses, we observed a slight but significant reduction in the LTP of Panx1 KO slices compared to Panx1 WT slices. More recordings should be performed to increase the sample size in order to better support this data. A modulatory role of Panx1 channels in MF plasticity would be intriguing as these terminals predominantly express a pre-synaptic form of LTP which is independent of post-synaptic NMDA receptor activity. The transient release of metabolites such as purines from Panx1 channels could potentially have an effect at the pre-synaptic terminal. As discussed in Section 4.1, such a mechanism could explain the increase in mEPSC frequency seen in some YoPro-1 positive neurons following synaptic NMDA receptor stimulation.

4.4.2 Memory and learning behaviours in Panx1 KO mice

Previous studies have shown that Panx1 KO mice exhibit changes in cognitive and memory function. Specifically Panx1 KO were shown to have impairments in novel object recognition and spatial memory (Prochnow et al., 2012), as well as deficits in learning flexibility tested by Morris Water Maze and delayed non-match to place T-maze tasks (Gajardo et al.,

2018). An increase in anxiety levels was also reported in Panx1 KO, which was supported by the blunting of pre-pulse inhibition in an acoustic startle response test.

Behavioural tests were therefore undertaken on a cohort of Panx1 WT and KO mice from our colony in order to build on this literature and to probe for deficits in different memory circuits. Unlike Prochnow et al., we were unable to see a deficit in object recognition memory in Panx1 KO; however the validity of this test is in question as the performance of mice in this task was highly variable. An increase in anxiety-like behaviour was also not found between Panx1 WT and KO mice when tested with the elevated plus maze.

We chose to test contextual fear memory as the influence of Panx1 in this type of memory has not been previously reported. A large body of literature describes the mechanisms behind contextual fear memory, which involves the plasticity of circuits in the hippocampus and the amygdala. We were unable to detect a significant difference in contextual fear memory between Panx1 WT and KO mice. We also assessed fear extinction by introducing the mouse to the fear context a second time. It is thought that fear extinction is contributed by two independent mechanisms. As fear memory is induced by the synaptic potentiation in the lateral amygdala, the depotentiation of these synapses is thought to cause extinction of the fear memory. At the same time, fear extinction has been shown to behave as a type of inhibitory learning mediated by plasticity in the basal lateral amygdala (BLA) and the mPFC. While fear extinction was observed in Panx1 WT and KO mice, there was no significant difference in the fear response between these two genotypes.

Future behavioural studies may focus on further exploring the learning flexibility deficits which have been described in Panx1 KO mice. We are currently using an 8-arm radial maze protocol which tests both working memory and spatial reference memory. Four arms of the maze

are baited with food, and mice are trained to learn the position of the baited arms over time. Once the mice are trained and demonstrate sufficient reference memory, the location of the food is switched into previously empty arms. We would expect Panx1 KO mice to learn slower following this switch if they indeed exhibit deficits in reversal learning.

4.5 Study Limitations

There were a few overarching limitations in our study. Our cell culture experiments were performed on neuronally enriched hippocampal cultures. This allowed us to answer questions surrounding the primary aim of our study, which was to look at the direct impact of AβOs on Panx1 activity and the synaptic function of neurons. However, this restriction in study design ignores the role of Panx1 channels on glial cells, which could have an important impact on the function of neurons. This is supported by evidence that AβOs can induce microglial Panx1 activity which contributes to neuronal cell death (Orellana, Shoji, et al., 2011). Also, while cell culture models of AD can be useful in looking at specific interactions and mechanisms in the disease, the results should be interpreted with caution as the pathogenesis of AD in the whole organism system is much more complex.

Acute hippocampal slice preparations have been extensively used as a model for the study of the effects of AβOs on synaptic plasticity. Our studies limited to assessing the contribution of the Panx1 channel to AβO induced deficits in LTP, specifically at the CA1 synapse. However, AβOs are also known to cause a facilitation of LTD, and it is possible that the Panx1 channels are differentially involved in these two processes. Another limitation of these experiments is that acute hippocampal slices prepared and maintained in these experiments are only viable for up to 10 hours. The establishment of hippocampal slice cultures would allow for

treatments with AβOs over several days, letting us assess the effect of Panx1 channels on synaptic degeneration with the advantage of intact tissue cytoarchitecture.

Lastly, the primary method for assessing the function of Panx1 channels in these studies was through the use of Panx1 KO mice. While genetic KO models are pervasive in biomedical research, a major concern in the use of these models is the presence of genetic compensation. This is the upregulation genes which may make up for the function of the knocked-out gene. Panx1 KO mice do not exhibit any gross abnormalities, despite their expression and function in all organ systems as well as their high expression during neurodevelopment. This contrasts with the first report of a human Panx1 point mutation, where the patient exhibited multi-organ abnormalities and intellectual disability (Shao et al., 2016). Indeed, while gene compensation and redundancy has been associated with the deficiency of various connexins, compensation is more limited with point mutations which alter the function of the channel but not necessarily their expression (Bedner, Steinhäuser, & Theis, 2012). Therefore, it is important to keep in mind that some of the functions of Panx1 channels in plasticity and memory may be masked by genetic compensation when performing these studies in Panx1 KO mice.

4.6 Therapeutic potential of Panx1 in CNS disease

The potential for the pharmacological targeting of Panx1 in CNS disease has been best demonstrated through in vivo disease models. Santiago et al. first showed that block of Panx1 by mefloquine was able to prevent kainate induced status epilepticus (Santiago et al., 2011). Pharmacological block of Panx1 is also effective in models of stroke. Probenecid and mefloquine attenuated ischemic cell death following transient middle cerebral artery occlusion (MCAO) (Cisneros-Mejorado et al., 2015), while experiments using a permanent MCAO model

demonstrated a reduction in infarct volume in female but not male mice treated with probenecid (Freitas-Andrade et al., 2017). A study looking at morphine withdrawal in rodents demonstrated that probenecid and mefloquine effectively reduce the severity of withdrawal symptoms by blocking Panx1 mediated ATP release from spinal microglia (Burma et al., 2017). Given the non-specific nature of these drugs, the beneficial effects of blocking Panx1 channels was simultaneously confirmed with Panx1 KO mice in each of these studies.

Probenecid and mefloquine are both FDA approved drugs and are already widely prescribed for the primary treatment of gout and malaria respectively. As dosing and safety profiles have already been established, they are attractive drug candidates for the targeting Panx1 channels in the clinical setting. Nevertheless, a better understanding of the regulatory mechanisms of Panx1 can reveal more specific targeting strategies. Weilinger et al. developed the TAT conjugated interfering peptide blocker $Panx_{308}$, which prevents the SFK dependent upregulation of channel function downstream of NMDA receptor stimulation. $Panx_{308}$ was able to reduce lesion size and improve functional outcomes in a transient MCAO model of stroke. Such context specific inhibition of Panx1 could more effectively reduce the pathological activity of the channel while limiting side effects.

Given the pathological role of Panx1 in CNS disease and the availability of clinically approved drugs which effectively block channel function, Panx1 inhibition could become an accepted therapeutic strategy sooner rather than later. Therefore, determining the extent of Panx1 involvement in AD pathology has major relevance in defining new treatment options.

CHAPTER 5: CONCLUSION

There is a pressing need for the development of new therapeutics in AD. The population of patients living with AD is projected to double within the next 15 years with the aging population. The last drug to be approved for the treatment of AD was memantine, providing some benefit to those with moderate to severe AD. Yet 15 years has already passed since the approval of this drug. Amyloid-β plays a central role in the pathogenesis of AD and has been a major target for new therapies. However, the development of amyloid-targeted therapies aimed at reducing the levels of the protein in the brain have largely been unsuccessful. While there is still some hope for this therapeutic approach, successful AD management will likely involve the targeting of multiple mechanisms of disease and will need to adapt to different stages of the disease as it progresses. The work of this thesis has explored a possible role of the Panx1 channel in AD with respects to the AβO mediated synaptic dysfunction in the hippocampus.

5.1 Significance of findings

Since the discovery of the Panx1 channel at the turn of the millennium, studies have begun to describe its role in neurological diseases. However, work exploring the role of Panx1 in AD has been more limited. The results of this thesis have shown that AβOs can increase the activity of Panx1 channels in neurons by sensitizing signalling downstream of NMDA receptors. This links Panx1 activity to the glutamate excitotoxicity model of AD. From our electrophysiology experiments, we showed that large-pore activity of Panx1channels increase the permeability of neurons to sodium and calcium, which would eventually lead to excitotoxic degeneration. Given that the targeting of glutamate excitotoxicity with the NMDA receptor pore

blocker memantine has demonstrated clinical benefit to AD patients, it is worth studying Panx1 channels as an additional therapeutic target which may further improve outcomes.

5.2 Future directions

The future directions of this project would focus on elucidating the pathways underlying the AβO induced sensitization of NMDAR-Panx1 signalling. Work in our lab is studying whether AβOs increase Panx1 activity by modulating an ER calcium and STIM dependent pathway. In addition, the pathological significance of the Panx1 channel in AD needs to be explored. One of the unique properties of the Panx1 channel is its ability to release ATP, contributing to purine signalling in a variety of physiological and pathophysiological contexts in the body. In AD, ATP release may be a mediator of neuroinflammation, which may be a contributing mechanism to excitotoxicity and the dysfunction of excitatory synapses. As glial cells also express Panx1, the crosstalk between microglia, astrocytes and neurons through ATP (and glutamate) release from Panx1 channels is worth pursuing. In a simple experiment, the co-culture of Panx1 WT or KO microglia with Panx1 WT or KO neurons could be treated with AβOs and monitored for synapse loss and neurodegeneration.

Alternatives for studying Panx1 function in AD should be employed. In the mice used in our studies, the global KO of Panx1 during development has the risk of the gene compensation which can indirectly impact the phenotype. Focus on the adult function of Panx1 should be studied through the conditional KO of Panx1 in the adult, or the viral targeted KD of Panx1 in brain regions of interest such as the hippocampus. Lastly, genetic crossing of the Panx1 KO animals with AD animals would provide a top down approach for looking at Panx1 within the context of the disease in the whole animal. This would allow for the study of Panx1 impacts on

behavioural, histological, and electrophysiological endpoints in AD. Conditonal KO of neuronal versus microglial Panx1 could also be used as a way to tease out the distinct pathological contribution of the channel in these cellular populations.

REFERENCES

Adhikari, A. (2014). Distributed circuits underlying anxiety. *Frontiers in Behavioral Neuroscience, 8*, 112. https://doi.org/10.3389/fnbeh.2014.00112

Agostini, M., & Fasolato, C. (2016). When, where and how? Focus on neuronal calcium dysfunctions in Alzheimer's Disease. *Cell Calcium*. https://doi.org/10.1016/j.ceca.2016.06.008

Alberini, C. M. (2009). Transcription Factors in Long-Term Memory and Synaptic Plasticity. *Physiological Reviews*, *89*(1), 121–145. https://doi.org/10.1152/physrev.00017.2008

Alzheimer Society of Canada. (2016). Prevalence and monetary costs of dementia in Canada (2016): a report by the Alzheimer Society of Canada. *Health Promot Chronic Dis Prev Can*, *36*(10), 231–232. https://doi.org/10.1017/CBO9781107415324.004

Antunes, M., & Biala, G. (2012, May). The novel object recognition memory: Neurobiology, test procedure, and its modifications. *Cognitive Processing*. Springer. https://doi.org/10.1007/s10339-011-0430-z

Arbel-Ornath, M., Hudry, E., Boivin, J. R., Hashimoto, T., Takeda, S., Kuchibhotla, K. V, … Bacskai, B. J. (2017). Soluble oligomeric amyloid-β induces calcium dyshomeostasis that precedes synapse loss in the living mouse brain. *Molecular Neurodegeneration*, *12*(1), 27. https://doi.org/10.1186/s13024-017-0169-9

Ardiles, A. O., Flores-Muñoz, C., Toro-Ayala, G., Cárdenas, A. M., Palacios, A. G., Muñoz, P., … Martínez, A. D. (2014). Pannexin 1 regulates bidirectional hippocampal synaptic plasticity in adult mice. *Frontiers in Cellular Neuroscience*, *8*(October), 326. https://doi.org/10.3389/fncel.2014.00326

Bao, L., Locovei, S., & Dahl, G. (2004). Pannexin membrane channels are mechanosensitive

conduits for ATP. *FEBS Letters*, *572*(1–3), 65–68. https://doi.org/10.1016/j.febslet.2004.07.009

Baranello, R. J., Bharani, K. L., Padmaraju, V., Chopra, N., Lahiri, D. K., Greig, N. H., … Sambamurti, K. (2015). Amyloid-Beta Protein Clearance and Degradation (ABCD) Pathways and their Role in Alzheimer's Disease. *Current Alzheimer Research*, *12*(1), 32–46. https://doi.org/http://dx.doi.org/10.2174/1567205012666141218140953

Bateman, R. J., Benzinger, T. L., Berry, S., Clifford, D. B., Duggan, C., Fagan, A. M., … Xiong, C. (2017). The DIAN-TU Next Generation Alzheimer's prevention trial: Adaptive design and disease progression model. *Alzheimer's and Dementia*, *13*(1), 8–19. https://doi.org/10.1016/j.jalz.2016.07.005

Bayazitov, I. T., Richardson, R. J., Fricke, R. G., & Zakharenko, S. S. (2007). Slow Presynaptic and Fast Postsynaptic Components of Compound Long-Term Potentiation. *Journal of Neuroscience*, *27*(43), 11510–11521. https://doi.org/10.1523/JNEUROSCI.3077-07.2007

Bedner, P., Steinhäuser, C., & Theis, M. (2012, August 1). Functional redundancy and compensation among members of gap junction protein families? *Biochimica et Biophysica Acta - Biomembranes*. Elsevier. https://doi.org/10.1016/j.bbamem.2011.10.016

Billaud, M., Lohman, A. W., Straub, A. C., Looft-Wilson, R., Johnstone, S. R., Araj, C. A., … Isakson, B. E. (2011). Pannexin1 Regulates 1-Adrenergic Receptor- Mediated Vasoconstriction. *Circulation Research*, *109*(1), 80–85. https://doi.org/10.1161/CIRCRESAHA.110.237594

Birnbaum, J. H., Bali, J., Rajendran, L., Nitsch, R. M., & Tackenberg, C. (2015). Calcium flux-independent NMDA receptor activity is required for Aβ oligomer-induced synaptic loss. *Cell Death and Disease*, *6*(6), e1791. https://doi.org/10.1038/cddis.2015.160

Black, S. A. G., Stys, P. K., Zamponi, G. W., & Tsutsui, S. (2014). Cellular prion protein and NMDA receptor modulation: protecting against excitotoxicity. *Frontiers in Cell and Developmental Biology*, *2*, 45. https://doi.org/10.3389/fcell.2014.00045

Bloom, G. S. (2014). Amyloid-β and tau: The trigger and bullet in Alzheimer disease pathogenesis. *JAMA Neurology*, *71*(4), 505–508. https://doi.org/10.1001/jamaneurol.2013.5847

Boassa, D., Ambrosi, C., Qiu, F., Dahl, G., Gaietta, G., & Sosinsky, G. (2007). Pannexin1 channels contain a glycosylation site that targets the hexamer to the plasma membrane. *The Journal of Biological Chemistry*, *282*(43), 31733–31743. https://doi.org/10.1074/jbc.M702422200

Bosch, M., Castro, J., Saneyoshi, T., Matsuno, H., Sur, M., & Hayashi, Y. (2014). Structural and molecular remodeling of dendritic spine substructures during long-term potentiation. *Neuron*, *82*(2), 444–459. https://doi.org/10.1016/j.neuron.2014.03.021

Bosch, M., & Hayashi, Y. (2012). Structural plasticity of dendritic spines. *Current Opinion in Neurobiology*. https://doi.org/10.1016/j.conb.2011.09.002

Bravo, D., Ibarra, P., Retamal, J., Pelissier, T., Laurido, C., Hernandez, A., & Constandil, L. (2014). Pannexin 1: a novel participant in neuropathic pain signaling in the rat spinal cord. *Pain*, *155*(10), 2108–2115. https://doi.org/10.1016/j.pain.2014.07.024

Burma, N. E., Bonin, R. P., Leduc-Pessah, H., Baimel, C., Cairncross, Z. F., Mousseau, M., … Trang, T. (2017). Blocking microglial pannexin-1 channels alleviates morphine withdrawal in rodents. *Nature Medicine*, *23*(3), 355–360. https://doi.org/10.1038/nm.4281

Calabrese, B., Shaked, G. M., Tabarean, I. V, Braga, J., Koo, E. H., & Halpain, S. (2007). Rapid, concurrent alterations in pre-and postsynaptic structure induced by naturally-secreted

amyloid-β protein. https://doi.org/10.1016/j.mcn.2007.02.006

Castellani, G. C., Quinlan, E. M., Bersani, F., Cooper, L. N., & Shouval, H. Z. (2005). A model of bidirectional synaptic plasticity: from signaling network to channel conductance. *Learning & Memory (Cold Spring Harbor, N.Y.)*, *12*(4), 423–432. https://doi.org/10.1101/lm.80705

Chakroborty, S., Goussakov, I., Miller, M. B., & Stutzmann, G. E. (2009). Deviant Ryanodine Receptor-Mediated Calcium Release Resets Synaptic Homeostasis in Presymptomatic 3xTg-AD Mice. *Journal of Neuroscience*, *29*(30), 9458–9470. https://doi.org/10.1523/JNEUROSCI.2047-09.2009

Chakroborty, S., Kim, J., Schneider, C., Jacobson, C., Molgo, J., & Stutzmann, G. E. (2012). Early Presynaptic and Postsynaptic Calcium Signaling Abnormalities Mask Underlying Synaptic Depression in Presymptomatic Alzheimer's Disease Mice. *Journal of Neuroscience*, *32*(24), 8341–8353. https://doi.org/10.1523/JNEUROSCI.0936-12.2012

Chakroborty, S., & Stutzmann, G. E. (2014). Calcium channelopathies and Alzheimer's disease: Insight into therapeutic success and failures. *European Journal of Pharmacology*, *739*, 83–95. https://doi.org/10.1016/j.ejphar.2013.11.012

Chan, S. L., Griffin, W. S. T., & Mattson, M. P. (1999). Evidence for Caspase-Mediated Cleavage of AMPA Receptor Subunits in Neuronal Apoptosis and Alzheimer ' s Disease. *Journal of Neuroscience Research*, *57*(April), 315–323.

Chekeni, F. B., Elliott, M. R., Sandilos, J. K., Walk, S. F., Kinchen, J. M., Lazarowski, E. R., … Ravichandran, K. S. (2010). Pannexin 1 channels mediate "find-me" signal release and membrane permeability during apoptosis. *Nature*, *467*(7317), 863–867. https://doi.org/10.1038/nature09413

Chen, S.-P., Qin, T., Seidel, J. L., Zheng, Y., Eikermann, M., Ferrari, M. D., … Eikermann-Haerter, K. (2017). Inhibition of the P2X7-PANX1 complex suppresses spreading depolarization and neuroinflammation. *Brain : A Journal of Neurology*. https://doi.org/10.1093/brain/awx085

Chen, X., Lin, R., Chang, L., Xu, S., Wei, X., Zhang, J., … Wang, Q. (2013). Enhancement of long-term depression by soluble amyloid β protein in rat hippocampus is mediated by metabotropic glutamate receptor and involves activation of p38MAPK, STEP and caspase-3. *Neuroscience*, *253*, 435–443. https://doi.org/10.1016/j.neuroscience.2013.08.054

Chiu, Y.-H., Jin, X., Medina, C. B., Leonhardt, S. A., Kiessling, V., Bennett, B. C., … Bayliss, D. A. (2017). A quantized mechanism for activation of pannexin channels. *Nature Communications*, *8*, 14324. https://doi.org/10.1038/ncomms14324

Cisneros-Mejorado, A., Gottlieb, M., Cavaliere, F., Magnus, T., Koch-Nolte, F., Scemes, E., … Matute, C. (2015). Blockade of P2X7 receptors or pannexin-1 channels similarly attenuates postischemic damage. *Journal of Cerebral Blood Flow and Metabolism : Official Journal of the International Society of Cerebral Blood Flow and Metabolism*, *35*(5), 843–850. https://doi.org/10.1038/jcbfm.2014.262

Collingridge, G. L., Kehl, S. J., & McLennan, H. (1983). Excitatory amino acids in synaptic transmission in the Schaffer collateral-commissural pathway of the rat hippocampus. *The Journal of Physiology*, *334*, 33–46. Retrieved from http://www.ncbi.nlm.nih.gov/pubmed/6306230

Contreras, J. E., Saez, J. C., Bukauskas, F. F., & Bennett, M. V. (2003). Gating and regulation of connexin 43 (Cx43) hemichannels. *Proc Natl Acad Sci U S A*, *100*(20), 11388–11393. https://doi.org/10.1073/pnas.1434298100

Cummings, J. L., Schneider, E., Tariot, P. N., & Graham, S. M. (2006). Behavioral effects of memantine in Alzheimer disease patients receiving donepezil treatment. *Neurology*, *67*(1), 57–63. https://doi.org/10.1212/01.wnl.0000223333.42368.f1

Dahl, G., Qiu, F., & Wang, J. (2013). The bizarre pharmacology of the ATP release channel pannexin1. *Neuropharmacology*, *75*, 583–593. https://doi.org/10.1016/j.neuropharm.2013.02.019

Davis, S., Butcher, S. P., & Morris, R. G. (1992). The NMDA receptor antagonist D-2-amino-5-phosphonopentanoate (D-AP5) impairs spatial learning and LTP in vivo at intracerebral concentrations comparable to those that block LTP in vitro. *The Journal of Neuroscience : The Official Journal of the Society for Neuroscience*, *12*(1), 21–34. https://doi.org/1345945

De Wilde, M. C., Overk, C. R., Sijben, J. W., & Masliah, E. (2016). Meta-analysis of synaptic pathology in Alzheimer's disease reveals selective molecular vesicular machinery vulnerability. *Alzheimer's and Dementia*, *12*(6), 633–644. https://doi.org/10.1016/j.jalz.2015.12.005

Del Prete, D., Checler, F., Chami, M., Lindeboom, J., Weinstein, H., Checler, F., … Bullock, R. (2014). Ryanodine receptors: physiological function and deregulation in Alzheimer disease. *Molecular Neurodegeneration*, *9*(1), 21. https://doi.org/10.1186/1750-1326-9-21

Delekate, A., Füchtemeier, M., Schumacher, T., Ulbrich, C., Foddis, M., & Petzold, G. C. (2014). Metabotropic P2Y1 receptor signalling mediates astrocytic hyperactivity in vivo in an Alzheimer's disease mouse model. *Nature Communications*, *5*, 5422. https://doi.org/10.1038/ncomms6422

Dittmer, P. J., Wild, A. R., Dell'Acqua, M. L., & Sather, W. A. (2017). STIM1 Ca2+Sensor Control of L-type Ca2+-Channel-Dependent Dendritic Spine Structural Plasticity and

Nuclear Signaling. *Cell Reports*, *19*(2), 321–334. https://doi.org/10.1016/j.celrep.2017.03.056

Doody, R. S., Raman, R., Farlow, M., Iwatsubo, T., Vellas, B., Joffe, S., … Mohs, R. (2013). A Phase 3 Trial of Semagacestat for Treatment of Alzheimer's Disease. *New England Journal of Medicine*, *369*(4), 341–350. https://doi.org/10.1056/NEJMoa1210951

Doody, R. S., Thomas, R. G., Farlow, M., Iwatsubo, T., Vellas, B., Joffe, S., … Mohs, R. (2014). Phase 3 Trials of Solanezumab for Mild-to-Moderate Alzheimer's Disease. *New England Journal of Medicine*, *370*(4), 311–321. https://doi.org/10.1056/NEJMoa1312889

Doody, R., Wirth, Y., Schmitt, F., & Möbius, H. J. (2004). Specific functional effects of memantine treatment in patients with moderate to severe Alzheimer's disease. *Dementia and Geriatric Cognitive Disorders*, *18*(2), 227–232. https://doi.org/10.1159/000079833

Dore, K., Aow, J., & Malinow, R. (2016). The emergence of NMDA receptor metabotropic function: Insights from imaging. *Frontiers in Synaptic Neuroscience*, *8*, 20. https://doi.org/10.3389/fnsyn.2016.00020

Dourado, M., Wong, E., Hackos, D. H., Wang, Y., & Goldin, A. (2014). Pannexin-1 Is Blocked by Its C-Terminus through a Delocalized Non-Specific Interaction Surface. *PLoS ONE*, *9*(6), e99596. https://doi.org/10.1371/journal.pone.0099596

Dvoriantchikova, G., Ivanov, D., Barakat, D., Grinberg, A., Wen, R., Slepak, V. Z., … Weinberg, J. (2012). Genetic Ablation of Pannexin1 Protects Retinal Neurons from Ischemic Injury. *PLoS ONE*, *7*(2), e31991. https://doi.org/10.1371/journal.pone.0031991

Dvoriantchikova, G., Pronin, A., Kurtenbach, S., Toychiev, A., Chou, T. H., Yee, C. W., … Shestopalov, V. I. (2018). Pannexin 1 sustains the electrophysiological responsiveness of retinal ganglion cells. *Scientific Reports*, *8*(1). https://doi.org/10.1038/s41598-018-23894-2

Esparza, T. J., Zhao, H., Cirrito, J. R., Cairns, N. J., Bateman, R. J., Holtzman, D. M., & Brody, D. L. (2013). Amyloid-beta oligomerization in Alzheimer dementia versus high-pathology controls. *Annals of Neurology*, *73*(1), 104–119. https://doi.org/10.1002/ana.23748

Ferreiro, E., Oliveira, C. R., & Pereira, C. M. F. (2004). Involvement of endoplasmic reticulum Ca2+ release through ryanodine and inositol 1,4,5-triphosphate receptors in the neurotoxic effects induced by the amyloid-β peptide. *Journal of Neuroscience Research*, *76*(6), 872–880. https://doi.org/10.1002/jnr.20135

Freitas-Andrade, M., Bechberger, J. F., MacVicar, B. A., Viau, V., Naus, C. C., Freitas-Andrade, M., … Naus, C. C. (2017). Pannexin1 knockout and blockade reduces ischemic stroke injury in female, but not in male mice. *Oncotarget*, *8*(23), 36973–36983. https://doi.org/10.18632/oncotarget.16937

Gajardo, I., Salazar, C. S., Lopez-Espíndola, D., Estay, C., Flores-Muñoz, C., Elgueta, C., … Ardiles, Á. O. (2018). Lack of pannexin 1 alters synaptic glun2 subunit composition and spatial reversal learning in mice. *Frontiers in Molecular Neuroscience*, *11*(April), 114. https://doi.org/10.3389/fnmol.2018.00114

Gauthier, S., Wirth, Y., & Möbius, H. J. (2005). Effects of memantine on behavioural symptoms in Alzheimer's disease patients: An analysis of the Neuropsychiatric Inventory (NPI) data of two randomised, controlled studies. *International Journal of Geriatric Psychiatry*, *20*(5), 459–464. https://doi.org/10.1002/gps.1341

Gaynullina, D., Shestopalov, V. I., Panchin, Y., & Tarasova, O. S. (2015). Pannexin 1 facilitates arterial relaxation via an endothelium-derived hyperpolarization mechanism. *FEBS Letters*, *589*(10), 1164–1170. https://doi.org/10.1016/j.febslet.2015.03.018

Glass, A. M., Elizabeth Snyder, B. G., & Steven Taffet, B. M. (1966). Connexins and pannexins

in the immune system and lymphatic organs. https://doi.org/10.1007/s00018-015-1966-3

Good, M. E., Begandt, D., DeLalio, L. J., Keller, A. S., Billaud, M., & Isakson, B. E. (2015a). Emerging concepts regarding pannexin 1 in the vasculature. *Biochemical Society Transactions*, *43*(3), 495–501. https://doi.org/10.1042/BST20150045

Good, M. E., Begandt, D., DeLalio, L. J., Keller, A. S., Billaud, M., & Isakson, B. E. (2015b). Emerging concepts regarding pannexin 1 in the vasculature. *Biochemical Society Transactions*, *43*(3), 495–501. https://doi.org/10.1042/BST20150045

Goshen, I., Kreisel, T., Ounallah-Saad, H., Renbaum, P., Zalzstein, Y., Ben-Hur, T., … Yirmiya, R. (2007). A dual role for interleukin-1 in hippocampal-dependent memory processes. *Psychoneuroendocrinology*, *32*, 1106–1115. https://doi.org/10.1016/j.psyneuen.2007.09.004

Goussakov, I., Miller, M. B., & Stutzmann, G. E. (2010). NMDA-Mediated Ca2+ Influx Drives Aberrant Ryanodine Receptor Activation in Dendrites of Young Alzheimer ' s Disease Mice. *J Neurosci*, *30*(36), 12128–12137. https://doi.org/10.1523/JNEUROSCI.2474-10.2010

Hardingham, G. E., & Bading, H. (2010). Synaptic versus extrasynaptic NMDA receptor signalling: implications for neurodegenerative disorders. *Nature Publishing Group*, *11*. https://doi.org/10.1038/nrn2911

Hardingham, G. E., Fukunaga, Y., & Bading, H. (2002). Extrasynaptic NMDARs oppose synaptic NMDARs by triggering CREB shut-off and cell death pathways. *Nature Neuroscience*. https://doi.org/10.1038/nn835

Hardt, O., Migues, P. V., Hastings, M., Wong, J., & Nader, K. (2009). PKMζ maintains 1-day- and 6-day-old long-term object location but not object identity memory in dorsal hippocampus. *Hippocampus*, *20*(6), NA-NA. https://doi.org/10.1002/hipo.20708

Hayashi, Y., Shi, S. H., Esteban, J. A., Piccini, A., Poncer, J. C., & Malinow, R. (2000). Driving AMPA receptors into synapses by LTP and CaMKII: requirement for GluR1 and PDZ domain interaction. *Science (New York, N.Y.), 287*(5461), 2262–2267. Retrieved from http://www.ncbi.nlm.nih.gov/pubmed/10731148

Heinrich, A., Andõ, R. D., Túri, G., Rõzsa, B., & Sperlágh, B. (2012). K+ depolarization evokes ATP, adenosine and glutamate release from glia in rat hippocampus: A microelectrode biosensor study. *British Journal of Pharmacology*, *167*(5), 1003–1020. https://doi.org/10.1111/j.1476-5381.2012.01932.x

Henriques, A. G., Oliveira, J. M., Carvalho, L. P., & da Cruz e Silva, O. A. B. (2015). Aβ Influences Cytoskeletal Signaling Cascades with Consequences to Alzheimer's Disease. *Molecular Neurobiology*. https://doi.org/10.1007/s12035-014-8913-4

Hong, S., Beja-Glasser, V. F., Nfonoyim, B. M., Frouin, A., Li, S., Ramakrishnan, S., … Stevens, B. (2016). Complement and microglia mediate early synapse loss in Alzheimer mouse models. *Science*, *352*(6286), 712–716. https://doi.org/10.1126/science.aad8373

Hu, N.-W., Klyubin, I., Anwyl, R., & Rowan, M. J. (2009). GluN2B subunit-containing NMDA receptor antagonists prevent A -mediated synaptic plasticity disruption in vivo. *Proceedings of the National Academy of Sciences*, *106*(48), 20504–20509. https://doi.org/10.1073/pnas.0908083106

Hu, N.-W., Nicoll, A. J., Zhang, D., Mably, A. J., O'Malley, T., Purro, S. A., … Rowan, M. J. (2014). mGlu5 receptors and cellular prion protein mediate amyloid-β-facilitated synaptic long-term depression in vivo. *Nature Communications*, *5*, 3374. https://doi.org/10.1038/ncomms4374

Huang, Y., Grinspan, J. B., Abrams, C. K., & Scherer, S. S. (2007). Pannexin1 is expressed by

neurons and glia but does not form functional gap junctions. *GLIA*, *55*(1), 46–56. https://doi.org/10.1002/glia.20435

Iacobucci, G. J., & Popescu, G. K. (2017, April 1). NMDA receptors: Linking physiological output to biophysical operation. *Nature Reviews Neuroscience*. Nature Publishing Group. https://doi.org/10.1038/nrn.2017.24

Iglesias, R., Locovei, S., Roque, A., Alberto, A. P., Dahl, G., Spray, D. C., & Scemes, E. (2008). P2X7 receptor-Pannexin1 complex: pharmacology and signaling. *American Journal of Physiology. Cell Physiology*, *295*(3), C752-60. https://doi.org/10.1152/ajpcell.00228.2008

Iglesias, R., Spray, D. C., & Scemes, E. (2010). Mefloquine Blockade of Pannexin1 Currents: Resolution of a Conflict. *Cell Communication & Adhesion*, *16*(5–6), 131–137. https://doi.org/10.3109/15419061003642618

Iqbal, K., Liu, F., Gong, C.-X., & Grundke-Iqbal, I. (2010). Tau in Alzheimer Disease and Related Tauopathies. *Current Alzheimer Research*. https://doi.org/10.2174/156720510793611592

Ittner, L. M., Ke, Y. D., Delerue, F., Bi, M., Gladbach, A., van Eersel, J., … Götz, J. (2010). Dendritic Function of Tau Mediates Amyloid-β Toxicity in Alzheimer's Disease Mouse Models. *Cell*, *142*(3), 387–397. https://doi.org/10.1016/j.cell.2010.06.036

Izquierdo, I., Furini, C. R. G., & Myskiw, J. C. (2016). Fear Memory. *Physiological Reviews*, *96*(2), 695–750. https://doi.org/10.1152/physrev.00018.2015

Jack, C. R., Knopman, D. S., Jagust, W. J., Petersen, R. C., Weiner, M. W., Aisen, P. S., … Trojanowski, J. Q. (2013, February). Tracking pathophysiological processes in Alzheimer's disease: An updated hypothetical model of dynamic biomarkers. *The Lancet Neurology*. NIH Public Access. https://doi.org/10.1016/S1474-4422(12)70291-0

Jang, S.-S., & Chung, H. J. (2016). Emerging Link between Alzheimer's Disease and Homeostatic Synaptic Plasticity. *Neural Plasticity*, *2016*, 1–19. https://doi.org/10.1155/2016/7969272

Jo, J., Whitcomb, D. J., Olsen, K. M., Kerrigan, T. L., Lo, S.-C., Bru-Mercier, G., … Cho, K. (2011). Aβ(1-42) inhibition of LTP is mediated by a signaling pathway involving caspase-3, Akt1 and GSK-3β. *Nature Neuroscience*, *14*(5), 545–547. https://doi.org/10.1038/nn.2785

Josselyn, S. A., Köhler, S., & Frankland, P. W. (2015, August 20). Finding the engram. *Nature Reviews Neuroscience*. Nature Publishing Group. https://doi.org/10.1038/nrn4000

Karatas, H., Erdener, S. E., Gursoy-Ozdemir, Y., Lule, S., Eren-Koçak, E., Sen, Z. D., & Dalkara, T. (2013). Spreading Depression Triggers Headache by Activating Neuronal Panx1 Channels. *Science*, *339*(6123).

Karpova, A., Mikhaylova, M., Bera, S., Bär, J., Reddy, P. P., Behnisch, T., … Kreutz, M. R. (2013). Encoding and transducing the synaptic or extrasynaptic origin of NMDA receptor signals to the nucleus. *Cell*, *152*(5), 1119–1133. https://doi.org/10.1016/j.cell.2013.02.002

Kauer, J. A., Malenka, R. C., & Nicoll, R. A. (1988). A persistent postsynaptic modification mediates long-term potentiation in the hippocampus. *Neuron*, *1*(10), 911–917. Retrieved from http://www.ncbi.nlm.nih.gov/pubmed/2908443

Kawamura, M., Ruskin, D. N., & Masino, S. A. (2010). Metabolic Autocrine Regulation of Neurons Involves Cooperation among Pannexin Hemichannels, Adenosine Receptors, and KATP Channels. *Journal of Neuroscience*, *30*(11), 3886–3895. https://doi.org/10.1523/JNEUROSCI.0055-10.2010

Kawamura, Y., Manita, S., Nakamura, T., Inoue, M., Kudo, Y., & Miyakawa, H. (2004). Glutamate release increases during mossy-CA3 LTP but not during Schaffer-CA1 LTP.

European Journal of Neuroscience, *19*(6), 1591–1600. https://doi.org/10.1111/j.1460-9568.2004.03258.x

Kayed, R., & Lasagna-Reeves, C. A. (2013). Molecular Mechanisms of Amyloid Oligomers Toxicity. *Journal of Alzheimer's Disease*, *33*, 67–78. https://doi.org/10.3233/JAD-2012-129001

Kessels, H. W., Nabavi, S., & Malinow, R. (2013). Metabotropic NMDA receptor function is required for β-amyloid-induced synaptic depression. *Proceedings of the National Academy of Sciences*, *110*(10), 4033–4038. https://doi.org/10.1073/pnas.1219605110

Kobayashi, K., Manabe, T., & Takahashi, T. (1996). Presynaptic long-term depression at the hippocampal mossy fiber-CA3 synapse. *Science (New York, N.Y.)*, *273*(5275), 648–650. Retrieved from http://www.ncbi.nlm.nih.gov/pubmed/8662556

Komada, M., Takao, K., & Miyakawa, T. (2008). Elevated Plus Maze for Mice. *Journal of Visualized Experiments*, (22), 1–4. https://doi.org/10.3791/1088

Kornhauser, J. M., Cowan, C. W., Shaywitz, A. J., Dolmetsch, R. E., Griffith, E. C., Hu, L. S., … Greenberg, M. E. (2002). CREB transcriptional activity in neurons is regulated by multiple, calcium-specific phosphorylation events. *Neuron*, *34*(2), 221–233. https://doi.org/10.1016/S0896-6273(02)00655-4

Kuchibhotla, K. V, Goldman, S. T., Lattarulo, C. R., Wu, H. Y., Hyman, B. T., & Bacskai, B. J. (2008). Aβ Plaques Lead to Aberrant Regulation of Calcium Homeostasis In Vivo Resulting in Structural and Functional Disruption of Neuronal Networks. *Neuron*, *59*(2), 214–225. https://doi.org/10.1016/j.neuron.2008.06.008

Kuenzi, F. M., Fitzjohn, S. M., Morton, R. A., Collingridge, G. L., & Seabrook, G. R. (2000). Reduced long-term potentiation in hippocampal slices prepared using sucrose-based

artificial cerebrospinal fluid. *Journal of Neuroscience Methods*, *100*(1–2), 117–122. https://doi.org/10.1016/S0165-0270(00)00239-9

Kummer, M. P., & Heneka, M. T. (2014). Truncated and modified amyloid-beta species. *Alzheimer's Research & Therapy*, *6*(3), 28. https://doi.org/10.1186/alzrt258

Lacor, P. N. (2004). Synaptic Targeting by Alzheimer's-Related Amyloid Oligomers. *Journal of Neuroscience*, *24*(45), 10191–10200. https://doi.org/10.1523/JNEUROSCI.3432-04.2004

Lacor, P. N., Buniel, M. C., Furlow, P. W., Sanz Clemente, A., Velasco, P. T., Wood, M., … Klein, W. L. (2007). A Oligomer-Induced Aberrations in Synapse Composition, Shape, and Density Provide a Molecular Basis for Loss of Connectivity in Alzheimer's Disease. *Journal of Neuroscience*, *27*(4), 796–807. https://doi.org/10.1523/JNEUROSCI.3501-06.2007

Lai, A. Y., & McLaurin, J. (2012, March 1). Clearance of amyloid-β peptides by microglia and macrophages: The issue of what, when and where. *Future Neurology*. PMC Canada manuscript submission. https://doi.org/10.2217/fnl.12.6

Lai, A. Y., Swayze, R. D., El-Husseini, A., & Song, C. (2006). Interleukin-1 beta modulates AMPA receptor expression and phosphorylation in hippocampal neurons. *Journal of Neuroimmunology*, *175*(1–2), 97–106. https://doi.org/10.1016/J.JNEUROIM.2006.03.001

Larson, M., Sherman, M. A., Amar, F., Nuvolone, M., Schneider, J. A., Bennett, D. A., … Lesne, S. E. (2012). The Complex PrPc-Fyn Couples Human Oligomeric A with Pathological Tau Changes in Alzheimer's Disease. *Journal of Neuroscience*, *32*(47), 16857–16871. https://doi.org/10.1523/JNEUROSCI.1858-12.2012

Lesne, S. E. (2014). Toxic oligomer species of amyloid-β in Alzheimer's disease, a timing issue. *Swiss Medical Weekly*, *144*(November), w14021. https://doi.org/10.4414/smw.2014.14021

Leutgeb, J. K., Leutgeb, S., Moser, M.-B., & Moser, E. I. (2007). Pattern Separation in the Dentate Gyrus and CA3 of the Hippocampus. *Science*, *315*(5814), 961–966. https://doi.org/10.1126/science.1135801

Li, S., Hong, S., Shepardson, N. E., Walsh, D. M., Shankar, G. M., & Selkoe, D. (2009). Soluble Oligomers of Amyloid β Protein Facilitate Hippocampal Long-Term Depression by Disrupting Neuronal Glutamate Uptake. *Neuron*, *62*(6), 788–801. https://doi.org/10.1016/j.neuron.2009.05.012

Li, S., Jin, M., Koeglsperger, T., Shepardson, N. E., Shankar, G. M., & Selkoe, D. J. (2011). Soluble Aβ oligomers inhibit long-term potentiation through a mechanism involving excessive activation of extrasynaptic NR2B-containing NMDA receptors. *The Journal of Neuroscience : The Official Journal of the Society for Neuroscience*, *31*(18), 6627–6638. https://doi.org/10.1523/JNEUROSCI.0203-11.2011

Li, Y., Du, X. F., Liu, C. S., Wen, Z. L., & Du, J. L. (2012). Reciprocal Regulation between Resting Microglial Dynamics and Neuronal Activity In Vivo. *Developmental Cell*, *23*(6), 1189–1202. https://doi.org/10.1016/j.devcel.2012.10.027

Li, Z., Jo, J., Jia, J. M., Lo, S. C., Whitcomb, D. J., Jiao, S., … Sheng, M. (2010). Caspase-3 activation via mitochondria is required for long-term depression and AMPA receptor internalization. *Cell*, *141*(5), 859–871. https://doi.org/10.1016/j.cell.2010.03.053

Liu, J., Chang, L., Roselli, F., Almeida, O. F. X., Gao, X., Wang, X., … Wu, Y. (2010). Amyloid-β induces caspase-dependent loss of PSD-95 and synaptophysin through NMDA receptors. *Journal of Alzheimer's Disease*, *22*(2), 541–556. https://doi.org/10.3233/JAD-2010-100948

Liu, L. D., Wong, T. P., Pozza, M. F., Lingenhoehl, K., Wang, Y. S., Sheng, M., … Wang, Y. T.

(2004). Role of NMDA receptor subtypes in governing the direction of hippocampal synaptic plasticity. *Science*, *304*(5673), 1021–1024. https://doi.org/10.1126/science.1096615

Locovei, S., Bao, L., & Dahl, G. (2006). Pannexin 1 in erythrocytes: Function without a gap. *Proceedings of the National Academy of Sciences*, *103*(20), 7655–7659. https://doi.org/10.1073/pnas.0601037103

Locovei, S., Bao, L., & Dahl, G. (2006). Pannexin 1 in erythrocytes: Function without a gap. *Proceedings of the National Academy of Sciences*, *103*(20), 7655–7659. https://doi.org/10.1073/pnas.0601037103

Locovei, S., Wang, J., & Dahl, G. (2006). Activation of pannexin 1 channels by ATP through P2Y receptors and by cytoplasmic calcium. *FEBS Letters*, *580*(1), 239–244. https://doi.org/10.1016/j.febslet.2005.12.004

Lopatář, J., Dale, N., & Frenguelli, B. G. (2015). Pannexin-1-mediated ATP release from area CA3 drives mGlu5-dependent neuronal oscillations. *Neuropharmacology*, *93*, 219–228. https://doi.org/10.1016/j.neuropharm.2015.01.014

Louneva, N., Cohen, J. W., Han, L.-Y., Talbot, K., Wilson, R. S., Bennett, D. A., … Arnold, S. E. (2008). Caspase-3 Is Enriched in Postsynaptic Densities and Increased in Alzheimer's Disease. *The American Journal of Pathology*, *173*, 1488–1495. https://doi.org/10.2353/ajpath.2008.080434

Luscher, C., & Malenka, R. C. (2012). NMDA Receptor-Dependent Long-Term Potentiation and Long-Term Depression (LTP/LTD). *Cold Spring Harbor Perspectives in Biology*, *4*(6), a005710–a005710. https://doi.org/10.1101/cshperspect.a005710

Maeda, S., Nakagawa, S., Suga, M., Yamashita, E., Oshima, A., Fujiyoshi, Y., & Tsukihara, T.

(2009). Structure of the connexin 26 gap junction channel at 3.5 Å resolution. *Nature*, *458*(7238), 597–602. https://doi.org/10.1038/nature07869

Magi, S., Castaldo, P., Macrì, M. L., Maiolino, M., Matteucci, A., Bastioli, G., … Lariccia, V. (2016). Intracellular Calcium Dysregulation: Implications for Alzheimer's Disease. *BioMed Research International*, *2016*, 1–14. https://doi.org/10.1155/2016/6701324

Man, H. Y. (2011, April). GluA2-lacking, calcium-permeable AMPA receptors - inducers of plasticity? *Current Opinion in Neurobiology*. https://doi.org/10.1016/j.conb.2011.01.001

Mannelli, L., Marcoli, M., Micheli, L., Zanardelli, M., Maura, G., Ghelardini, C., & Cervetto, C. (2015). Oxaliplatin evokes P2X7-dependent glutamate release in the cerebral cortex: A pain mechanism mediated by Pannexin 1. *Neuropharmacology*, *97*, 133–141. https://doi.org/10.1016/j.neuropharm.2015.05.037

Maslieieva, V., & Thompson, R. J. (2014). A critical role for pannexin-1 in activation of innate immune cells of the choroid plexus. *Channels*, *8*(2), 131–141. https://doi.org/10.4161/chan.27653

Matos, M., Augusto, E., MacHado, N. J., Dos Santos-Rodrigues, A., Cunha, R. A., & Agostinho, P. (2012). Astrocytic adenosine A 2A receptors control the amyloid-β peptide-induced decrease of glutamate uptake. *Journal of Alzheimer's Disease*, *31*(3), 555–567. https://doi.org/10.3233/JAD-2012-120469

Matsuo, N., Reijmers, L., & Mayford, M. (2008). Spine-Type-Specific Recruitment of Newly Synthesized AMPA Receptors with Learning. *Science*, *319*(5866), 1104–1107. https://doi.org/10.1126/science.1149967

Matus, S., Glimcher, L. H., & Hetz, C. (2011). Protein folding stress in neurodegenerative diseases: a glimpse into the ER. *Current Opinion in Cell Biology*, *23*(2), 239–252.

https://doi.org/10.1016/j.ceb.2011.01.003

McHugh, T. J., Jones, M. W., Quinn, J. J., Balthasar, N., Coppari, R., Elmquist, J. K., … Tonegawa, S. (2007). Dentate Gyrus NMDA Receptors Mediate Rapid Pattern Separation in the Hippocampal Network. *Science*, *317*(5834), 94–99. https://doi.org/10.1126/science.1140263

Mehta, D., Jackson, R., Paul, G., Shi, J., & Sabbagh, M. (2017). Why do trials for Alzheimer's disease drugs keep failing? A discontinued drug perspective for 2010-2015. *Expert Opinion on Investigational Drugs*, *26*(6), 735–739. https://doi.org/10.1080/13543784.2017.1323868

Michalski, K., & Kawate, T. (2016). Carbenoxolone inhibits Pannexin1 channels through interactions in the first extracellular loop. *The Journal of General Physiology*, *147*(2), 165–174. https://doi.org/10.1085/jgp.201511505

Morris, R. G. M., Anderson, E., Lynch, G. S., & Baudry, M. (1986). Selective impairment of learning and blockade of long-term potentiation by an N-methyl-D-aspartate receptor antagonist, AP5. *Nature*, *319*(6056), 774–776. https://doi.org/10.1038/319774a0

Mucke, L., & Selkoe, D. J. (2012). Neurotoxicity of amyloid β-protein: Synaptic and network dysfunction. *Cold Spring Harbor Perspectives in Medicine*, *2*(7), a006338. https://doi.org/10.1101/cshperspect.a006338

Nabavi, S., Kessels, H. W., Alfonso, S., Aow, J., Fox, R., & Malinow, R. (2013). Metabotropic NMDA receptor function is required for NMDA receptor-dependent long-term depression. *Proceedings of the National Academy of Sciences*, *110*(10), 4027–4032. https://doi.org/10.1073/pnas.1219454110

Naito, Y., Tanabe, Y., Lee, A. K., Hamel, E., & Takahashi, H. (2017). Amyloid-β Oligomers Interact with Neurexin and Diminish Neurexin-mediated Excitatory Presynaptic

Organization. *Scientific Reports*, *7*, 42548. https://doi.org/10.1038/srep42548

Nakazawa, K., Sun, L. D., Quirk, M. C., Rondi-Reig, L., Wilson, M. A., & Tonegawa, S. (2002). Requirement for Hippocampal CA3 NMDA Receptors in Associative Memory Recall. *Science*, *297*(5579), 211–218. https://doi.org/10.1126/science.1071795

Nakazawa, K., Sun, L. D., Quirk, M. C., Rondi-Reig, L., Wilson, M. A., & Tonegawa, S. (2003). Hippocampal CA3 NMDA receptors are crucial for memory acquisition of one-time experience. *Neuron*, *38*(2), 305–315. https://doi.org/10.1016/S0896-6273(03)00165-X

Neves, G., Cooke, S. F., & Bliss, T. V. P. (2008). Synaptic plasticity, memory and the hippocampus - a neural network aproach to causality. *Nature Reviews Neuroscience*, *9*(January 2008), 65–75. https://doi.org/nrn2303 [pii] 10.1038/nrn2303

Nicoll, R. A. (2017). Review A Brief History of Long-Term Potentiation. *Neuron*, *93*(2), 281–290. https://doi.org/10.1016/j.neuron.2016.12.015

Nicoll, R. A., & Schmitz, D. (2005). Synaptic plasticity at hippocampal mossy fibre synapses. *Nature Reviews Neuroscience*, *6*(11), 863–876. https://doi.org/10.1038/nrn1786

Nomura, T., Taruno, A., Shiraishi, M., Nakahari, T., Inui, T., Sokabe, M., … Marunaka, Y. (2017). Current-direction/amplitude-dependent single channel gating kinetics of mouse pannexin 1 channel: A new concept for gating kinetics. *Scientific Reports*, *7*(1). https://doi.org/10.1038/s41598-017-10921-x

Olivier, E., Dutot, M., Regazzetti, A., Leguillier, T., Dargère, D., Auzeil, N., … Rat, P. (2016). P2X7-pannexin-1 and amyloid β-induced oxysterol input in human retinal cell: Role in age-related macular degeneration? *Biochimie*, *127*, 70–78. https://doi.org/10.1016/j.biochi.2016.04.014

Orellana, J. A., Froger, N., Ezan, P., Jiang, J. X., Bennett, M. V. L., Naus, C. C., … Sáez, J. C.

(2011). ATP and glutamate released via astroglial connexin 43 hemichannels mediate neuronal death through activation of pannexin 1 hemichannels. *Journal of Neurochemistry, 118*(5), 826–840. https://doi.org/10.1111/j.1471-4159.2011.07210.x

Orellana, J. A., Shoji, K. F., Ezan, P., Amigou, E., Sáez, P. J., Jiang, J. X., … Giaume, C. (2011). Amyloid B-Induced death in neurons involves glial and neuronal hemichannels. *The Journal of Neuroscience, 31*(13), 4962–4977. https://doi.org/10.1523/JNEUROSCI.6417-10.2011

Oshima, A., Tani, K., & Fujiyoshi, Y. (2016). Atomic structure of the innexin-6 gap junction channel determined by cryo-EM. *Nature Communications, 7*, 13681. https://doi.org/10.1038/ncomms13681

Ostapchenko, V. G., Chen, M., Guzman, M. S., Xie, Y.-F., Lavine, N., Fan, J., … Jackson, M. F. (2015). The Transient Receptor Potential Melastatin 2 (TRPM2) Channel Contributes to β-Amyloid Oligomer-Related Neurotoxicity and Memory Impairment. *Journal of Neuroscience, 35*(45), 15157–15169. https://doi.org/10.1523/JNEUROSCI.4081-14.2015

Panchina, Y., Kelmanson, I., Matz, M., Lukyanov, K., Usman, N., & Lukyanov, S. (2000, June 29). A ubiquitous family of putative gap junction molecules. *Current Biology*. Elsevier. https://doi.org/10.1016/S0960-9822(00)00576-5

Parsons, C. G., Stöffler, A., & Danysz, W. (2007). Memantine: a NMDA receptor antagonist that improves memory by restoration of homeostasis in the glutamatergic system - too little activation is bad, too much is even worse. *Neuropharmacology*. https://doi.org/10.1016/j.neuropharm.2007.07.013

Pastalkova, E., Serrano, P., Pinkhasova, D., Wallace, E., Fenton, A. A., & Sacktor, T. C. (2006). Storage of Spatial Information by the Maintenance Mechanism of LTP. *Science, 313*(5790),

1141–1144. https://doi.org/10.1126/science.1128657

Pelegrin, P., Surprenant, A., Bao, L., Locovei, S., Dahl, G., Barbe, M., … MacVicar, B. (2006). Pannexin-1 mediates large pore formation and interleukin-1β release by the ATP-gated P2X7 receptor. *The EMBO Journal*, *25*(21), 5071–5082. https://doi.org/10.1038/sj.emboj.7601378

Penuela, S., Bhalla, R., Gong, X.-Q., Cowan, K. N., Celetti, S. J., Cowan, B. J., … Laird, D. W. (2007). Pannexin 1 and pannexin 3 are glycoproteins that exhibit many distinct characteristics from the connexin family of gap junction proteins. *Journal of Cell Science*, *120*(Pt 21), 3772–3783. https://doi.org/10.1242/jcs.009514

Penuela, S., & Laird, D. W. (2012). The cellular life of pannexins. *Wiley Interdisciplinary Reviews: Membrane Transport and Signaling*, *1*(5), 621–632. https://doi.org/10.1002/wmts.63

Poon, I. K. H., Chiu, Y.-H., Armstrong, A. J., Kinchen, J. M., Juncadella, I. J., Bayliss, D. A., & Ravichandran, K. S. (2014). Unexpected link between an antibiotic, pannexin channels and apoptosis. *Nature*, *507*(7492), 329–334. https://doi.org/10.1038/nature13147

Prince, M., Bryce, R., Albanese, E., Wimo, A., Ribeiro, W., & Ferri, C. P. (2013). The global prevalence of dementia: A systematic review and metaanalysis. *Alzheimer's & Dementia*, *9*, 63–75.e2. https://doi.org/10.1016/j.jalz.2012.11.007

Prochnow, N., Abdulazim, A., Kurtenbach, S., Wildförster, V., Dvoriantchikova, G., Hanske, J., … Zoidl, G. (2012). Pannexin1 Stabilizes Synaptic Plasticity and Is Needed for Learning. *PLoS ONE*, *7*(12), e51767. https://doi.org/10.1371/journal.pone.0051767

Rammes, G., Hasenjäger, A., Sroka-Saidi, K., Deussing, J. M., & Parsons, C. G. (2011). Therapeutic significance of NR2B-containing NMDA receptors and mGluR5 metabotropic

glutamate receptors in mediating the synaptotoxic effects of ??-amyloid oligomers on long-term potentiation (LTP) in murine hippocampal slices. *Neuropharmacology*, *60*(6), 982–990. https://doi.org/10.1016/j.neuropharm.2011.01.051

Ransford, G. A., Fregien, N., Qiu, F., Dahl, G., Conner, G. E., & Salathe, M. (2009). Pannexin 1 Contributes to ATP Release in Airway Epithelia. *American Journal of Respiratory Cell and Molecular Biology*, *41*(5), 525–534. https://doi.org/10.1165/rcmb.2008-0367OC

Rebola, N., Carta, M., & Mulle, C. (2017). Operation and plasticity of hippocampal CA3 circuits: implications for memory encoding. *Nature Reviews Neuroscience*, *18*(4), 208–220. https://doi.org/10.1038/nrn.2017.10

Renner, M., Lacor, P. N., Velasco, P. T., Xu, J., Contractor, A., Klein, W. L., & Triller, A. (2010). Deleterious Effects of Amyloid β Oligomers Acting as an Extracellular Scaffold for mGluR5. *Neuron*, *66*(5), 739–754. https://doi.org/10.1016/j.neuron.2010.04.029

Rochefort, N. L., & Konnerth, A. (2012). Dendritic spines: from structure to in vivo function. *Nature Publishing Group*, *13*(10). https://doi.org/10.1038/embor.2012.102

Rönicke, R., Mikhaylova, M., Rönicke, S., Meinhardt, J., Schröder, U. H., Fändrich, M., … Reymann, K. G. (2011). Early neuronal dysfunction by amyloid β oligomers depends on activation of NR2B-containing NMDA receptors. *Neurobiology of Aging*, *32*(12), 2219–2228. https://doi.org/10.1016/j.neurobiolaging.2010.01.011

Russell, C. L., Semerdjieva, S., Empson, R. M., Austen, B. M., Beesley, P. W., & Alifragis, P. (2012). Amyloid-β Acts as a Regulator of Neurotransmitter Release Disrupting the Interaction between Synaptophysin and VAMP2. *PLoS ONE*, *7*(8), e43201. https://doi.org/10.1371/journal.pone.0043201

Ryan, N. S., & Rossor, M. N. (2010, February). Correlating familial Alzheimers disease gene

mutations with clinical phenotype. *Biomarkers in Medicine*. NIH Public Access. https://doi.org/10.2217/bmm.09.92

Ryan, T. J., Roy, D. S., Pignatelli, M., Arons, A., & Tonegawa, S. (2015). Engram cells retain memory under retrograde amnesia. *Science*, *348*(6238), 1007–1013. https://doi.org/10.1126/science.aaa5542

Sala, C., & Segal, M. (2014). Dendritic Spines: The Locus of Structural and Functional Plasticity. *Physiological Reviews*, *94*(1), 141–188. https://doi.org/10.1152/physrev.00012.2013

Salloway, S., Sperling, R., Fox, N. C., Blennow, K., Klunk, W., Raskind, M., … Brashear, H. R. (2014). Two Phase 3 Trials of Bapineuzumab in Mild-to-Moderate Alzheimer's Disease. *New England Journal of Medicine*, *370*(4), 322–333. https://doi.org/10.1056/NEJMoa1304839

Sandilos, J. K., Bayliss, D. A., & Sandilos, J. K. (2012). Physiological mechanisms for the modulation of pannexin 1 channel activity. *J Physiol*, *59024*, 6257–6266. https://doi.org/10.1113/jphysiol.2012.240911

Sandilos, J. K., Chiu, Y.-H., Chekeni, F. B., Armstrong, A. J., Walk, S. F., Ravichandran, K. S., & Bayliss, D. A. (2012). Pannexin 1, an ATP release channel, is activated by caspase cleavage of its pore-associated C-terminal autoinhibitory region. *The Journal of Biological Chemistry*, *287*(14), 11303–11311. https://doi.org/10.1074/jbc.M111.323378

Santiago, M. F., Veliskova, J., Patel, N. K., Lutz, S. E., Caille, D., Charollais, A., … Scemes, E. (2011). Targeting Pannexin1 Improves Seizure Outcome. *PLoS ONE*, *6*(9), e25178. https://doi.org/10.1371/journal.pone.0025178

Sarantis, K., Tsiamaki, E., Kouvaros, S., Papatheodoropoulos, C., & Angelatou, F. (2015).

Adenosine A2A receptors permit mGluR5-evoked tyrosine phosphorylation of NR2B (Tyr1472) in rat hippocampus: A possible key mechanism in NMDA receptor modulation. *Journal of Neurochemistry*, *135*(4), 714–726. https://doi.org/10.1111/jnc.13291

Schafer, D. P., Lehrman, E. K., & Stevens, B. (2013). The "quad-partite" synapse: Microglia-synapse interactions in the developing and mature CNS. *Glia*, *61*(1), 24–36. https://doi.org/10.1002/glia.22389

Schneider, L. S. (2011). Lack of Evidence for the Efficacy of Memantine in Mild Alzheimer Disease. *Archives of Neurology*, *68*(8), 991. https://doi.org/10.1001/archneurol.2011.69

Secondo, A., Bagetta, G., & Amantea, D. (2018). On the Role of Store-Operated Calcium Entry in Acute and Chronic Neurodegenerative Diseases. *Frontiers in Molecular Neuroscience*, *11*(March), 1–14. https://doi.org/10.3389/fnmol.2018.00087

Selkoe, D. J. (2008). Soluble oligomers of the amyloid β-protein impair synaptic plasticity and behavior. *Behavioural Brain Research*. https://doi.org/10.1016/j.bbr.2008.02.016

Selkoe, D. J., & Hardy, J. (2016). The amyloid hypothesis of Alzheimer's disease at 25 years. *EMBO Mol Med*, *8*, 595–608. https://doi.org/10.15252/emmm

Sevigny, J., Chiao, P., Bussière, T., Weinreb, P. H., Williams, L., Maier, M., … Sandrock, A. (2016). The antibody aducanumab reduces Aβ plaques in Alzheimer's disease. *Nature*, *537*(7618), 50–56. https://doi.org/10.1038/nature19323

Shankar, G. M., Bloodgood, B. L., Townsend, M., Walsh, D. M., Selkoe, D. J., & Sabatini, B. L. (2007). Natural Oligomers of the Alzheimer Amyloid-β Protein Induce Reversible Synapse Loss by Modulating an NMDA-Type Glutamate Receptor-Dependent Signaling Pathway. *J Neurosci*, *27*(11), 2866–2875. https://doi.org/10.1523/JNEUROSCI.4970-06.2007

Shankar, G. M., Li, S., Mehta, T. H., Garcia-Munoz, A., Shepardson, N. E., Smith, I., … Selkoe,

D. J. (2008). Amyloid-beta protein dimers isolated directly from Alzheimer's brains impair synaptic plasticity and memory. *Nature Medicine*, *14*(8), 837–842. https://doi.org/10.1038/nm1782

Shankar, G. M., & Walsh, D. M. (2009). Alzheimer's disease: synaptic dysfunction and Aβ. *Molecular Neurodegeneration*, *4*(1), 48. https://doi.org/10.1186/1750-1326-4-48

Shankar, G. M., Welzel, A. T., McDonald, J. M., Selkoe, D. J., & Walsh, D. M. (2011). Isolation of low-n amyloid β-Protein oligomers from cultured cells, CSF, and brain. *Methods in Molecular Biology*, *670*, 33–44. https://doi.org/10.1007/978-1-60761-744-0_3

Shao, Q., Lindstrom, K., Shi, R., Kelly, J., Schroeder, A., Juusola, J., … Laird, D. W. (2016). A germline variant in the PANX1 gene has reduced channel function and is associated with multisystem dysfunction. *Journal of Biological Chemistry*, *291*(24), 12432–12443. https://doi.org/10.1074/jbc.M116.717934

Silverman, W. R., de Rivero Vaccari, J. P., Locovei, S., Qiu, F., Carlsson, S. K., Scemes, E., … Dahl, G. (2009). The pannexin 1 channel activates the inflammasome in neurons and astrocytes. *The Journal of Biological Chemistry*, *284*(27), 18143–18151. https://doi.org/10.1074/jbc.M109.004804

Sinnen, B. L., Bowen, A. B., Gibson, E. S., & Kennedy, M. J. (2016). Local and Use-Dependent Effects of β-Amyloid Oligomers on NMDA Receptor Function Revealed by Optical Quantal Analysis. *The Journal of Neuroscience*, *36*(45), 11532–11543. https://doi.org/10.1523/JNEUROSCI.1603-16.2016

Spires-Jones, T. L., & Hyman, B. T. (2014). The Intersection of Amyloid Beta and Tau at Synapses in Alzheimer's Disease. *Neuron*, *82*(4), 756–771. https://doi.org/10.1016/j.neuron.2014.05.004

Suadicani, S. O., Iglesias, R., Spray, D. C., & Scemes, E. (2009). Point mutation in the mouse P2X7 receptor affects intercellular calcium waves in astrocytes. *ASN Neuro*, *1*(1), e00005. https://doi.org/10.1042/AN20090001

Supnet, C., & Bezprozvanny, I. (2010). The dysregulation of intracellular calcium in Alzheimer disease. *Cell Calcium*, *47*, 183–189. https://doi.org/10.1016/j.ceca.2009.12.014

Swayne, L. A., & Bennett, S. A. L. (2016). Connexins and pannexins in neuronal development and adult neurogenesis. *BMC Cell Biology*, *17*(S1), S10. https://doi.org/10.1186/s12860-016-0089-5

Takeuchi, T., Duszkiewicz, A. J., & Morris, R. G. M. (2013). The synaptic plasticity and memory hypothesis: encoding, storage and persistence. *Philosophical Transactions of the Royal Society B: Biological Sciences*, *369*(1633), 20130288–20130288. https://doi.org/10.1098/rstb.2013.0288

Tamburri, A., Dudilot, A., Licea, S., Bourgeois, C., & Boehm, J. (2013). NMDA-Receptor Activation but Not Ion Flux Is Required for Amyloid-Beta Induced Synaptic Depression. *PLoS ONE*, *8*(6), e65350. https://doi.org/10.1371/journal.pone.0065350

Tauskela, J. S., Fang, H., Hewitt, M., Brunette, E., Ahuja, T., Thivierge, J.-P., … Mealing, G. A. R. (2008). Elevated synaptic activity preconditions neurons against an in vitro model of ischemia. *The Journal of Biological Chemistry*, *283*(50), 34667–34676. https://doi.org/10.1074/jbc.M805624200

Thompson, R. J., Jackson, M. F., Olah, M. E., Rungta, R. L., Hines, D. J., Beazely, M. A., … MacVicar, B. A. (2008). Activation of pannexin-1 hemichannels augments aberrant bursting in the hippocampus. *Science (New York, N.Y.)*, *322*(5907), 1555–1559. https://doi.org/10.1126/science.1165209

Thompson, R. J., Zhou, N., & MacVicar, B. A. (2006). Ischemia Opens Neuronal Gap Junction Hemichannels. *Science*, *312*(5775), 924–927. https://doi.org/10.1126/science.1126241

Townsend, M., Shankar, G. M., Mehta, T., Walsh, D. M., & Selkoe, D. J. (2006). Effects of secreted oligomers of amyloid beta-protein on hippocampal synaptic plasticity: a potent role for trimers. *The Journal of Physiology*, *572*(Pt 2), 477–492. https://doi.org/10.1113/jphysiol.2005.103754

Trinchese, F., Fa', M., Liu, S., Zhang, H., Hidalgo, A., Schmidt, S. D., … Arancio, O. (2008). Inhibition of calpains improves memory and synaptic transmission in a mouse model of Alzheimer disease. *Journal of Clinical Investigation*, *118*(8), 2796–2807. https://doi.org/10.1172/JCI34254

Tzounopoulos, T., Janz, R., Südhof, T. C., Nicoll, R. A., & Malenka, R. C. (1998). A role for cAMP in long-term depression at hippocampal mossy fiber synapses. *Neuron*, *21*(4), 837–845. Retrieved from http://www.ncbi.nlm.nih.gov/pubmed/9808469

Um, J., Kaufman, A., Kostylev, M., Heiss, J., Stagi, M., Takahashi, H., … Strittmatter, S. (2013). Metabotropic Glutamate Receptor 5 Is a Coreceptor for Alzheimer Aβ Oligomer Bound to Cellular Prion Protein. *Neuron, 79*(5), 887–902. https://doi.org/10.1016/j.neuron.2013.06.036

Um, J. W., Nygaard, H. B., Heiss, J. K., Kostylev, M. A., Stagi, M., Vortmeyer, A., … Strittmatter, S. M. (2012). Alzheimer amyloid-beta oligomer bound to postsynaptic prion protein activates Fyn to impair neurons. *Nat Neurosci*, *15*(9), 1227–1235. https://doi.org/10.1038/nn.3178

Velasquez, S., Malik, S., Lutz, S. E., Scemes, E., & Eugenin, E. A. (2016). Pannexin1 Channels Are Required for Chemokine-Mediated Migration of CD4+ T Lymphocytes: Role in

Inflammation and Experimental Autoimmune Encephalomyelitis. *Journal of Immunology (Baltimore, Md. : 1950)*, *196*(10), 4338–4347. https://doi.org/10.4049/jimmunol.1502440

Verghese, P. B., Castellano, J. M., Garai, K., Wang, Y., Jiang, H., Shah, A., … Holtzman, D. M. (2013). ApoE influences amyloid- (A) clearance despite minimal apoE/A association in physiological conditions. *Proceedings of the National Academy of Sciences*, *110*(19), E1807–E1816. https://doi.org/10.1073/pnas.1220484110

Virginia Migues, P., Hardt, O., Chuan Wu, D., Gamache, K., Charlton Sacktor, T., Tian Wang, Y., & Nader, K. (2010). PKMζ maintains memories by regulating GluR2-dependent AMPA receptor trafficking. *Nature Publishing Group*, *13*. https://doi.org/10.1038/nn.2531

Vogt, A., Hormuzdi, S. G., & Monyer, H. (2005). Pannexin1 and Pannexin2 expression in the developing and mature rat brain. *Molecular Brain Research*, *141*(1), 113–120. https://doi.org/10.1016/j.molbrainres.2005.08.002

Wang, J., Ambrosi, C., Qiu, F., Jackson, D. G., Sosinsky, G., & Dahl, G. (2014). The membrane protein Pannexin1 forms two open-channel conformations depending on the mode of activation. *Science Signaling*, *7*(335), ra69-ra69. https://doi.org/10.1126/scisignal.2005431

Wang, J., & Dahl, G. (2010). SCAM analysis of Panx1 suggests a peculiar pore structure. *The Journal of General Physiology*, *136*(5), 515–527. https://doi.org/10.1085/jgp.201010440

Wang, J., & Dahl, G. (2018). Pannexin1: a multi-function and multi-conductance/-permeability membrane channel. *American Journal of Physiology-Cell Physiology*, ajpcell.00302.2017. https://doi.org/10.1152/ajpcell.00302.2017

Wang, J., Ma, M., Locovei, S., Keane, R. W., & Dahl, G. (2007). Modulation of membrane channel currents by gap junction protein mimetic peptides: size matters. *Am J Physiol Cell Physiol*, *293*(3), C1112-9. https://doi.org/10.1152/ajpcell.00097.2007

Wei, L., Caseley, E., Li, D., & Jiang, L. H. (2016). ATP-induced P2X receptor-dependent large pore formation: How much do we know? *Frontiers in Pharmacology*, *7*(JAN), 5–8. https://doi.org/10.3389/fphar.2016.00005

Weilinger, N. L., Lohman, A. W., Rakai, B. D., Ma, E. M. M., Bialecki, J., Maslieieva, V., … Thompson, R. J. (2016). Metabotropic NMDA receptor signaling couples Src family kinases to pannexin-1 during excitotoxicity. *Nature Neuroscience*, *19*(3), 432–442. https://doi.org/10.1038/nn.4236

Weilinger, N. L., Tang, P. L., & Thompson, R. J. (2012). Anoxia-Induced NMDA Receptor Activation Opens Pannexin Channels via Src Family Kinases. *Journal of Neuroscience*, *32*(36), 12579–12588. https://doi.org/10.1523/JNEUROSCI.1267-12.2012

World Health Organization. (2012). Dementia: a public health priority. *Dementia*, 112. https://doi.org/978 92 4 156445 8

Wulf, M.-A., Senatore, A., & Aguzzi, A. (2017). The biological function of the cellular prion protein: an update. *BMC Biology*, *15*(1), 34. https://doi.org/10.1186/s12915-017-0375-5

You, H., Tsutsui, S., Hameed, S., Kannanayakal, T. J., Chen, L., Xia, P., … Zamponi, G. W. (2012). A neurotoxicity depends on interactions between copper ions, prion protein, and N-methyl-D-aspartate receptors. *Proceedings of the National Academy of Sciences*, *109*(5), 1737–1742. https://doi.org/10.1073/pnas.1110789109

Yu, J.-T., Chang, R. C.-C., & Tan, L. (2009). Calcium dysregulation in Alzheimer's disease: From mechanisms to therapeutic opportunities. *Progress in Neurobiology*, *89*(3), 240–255. https://doi.org/10.1016/j.pneurobio.2009.07.009

Zhang, W., Lohman, A. W., Zhuravlova, Y., Lu, X., Wiens, M. D., Hoi, H., … Campbell, R. E. (2017). Optogenetic control with a photocleavable protein, PhoCl. *Nature Methods*, *14*(4),

391–394. https://doi.org/10.1038/nmeth.4222

Zoidl, G., Petrasch-Parwez, E., Ray, A., Meier, C., Bunse, S., Habbes, H. W., … Dermietzel, R. (2007). Localization of the pannexin1 protein at postsynaptic sites in the cerebral cortex and hippocampus. *Neuroscience*, *146*(1), 9–16. https://doi.org/10.1016/j.neuroscience.2007.01.061

Zushida, K., Sakurai, M., Wada, K., & Sekiguchi, M. (2007). Facilitation of Extinction Learning for Contextual Fear Memory by PEPA: A Potentiator of AMPA Receptors. *Journal of Neuroscience*, *27*(1), 158–166. https://doi.org/10.1523/JNEUROSCI.3842-06.2007

APPENDIX

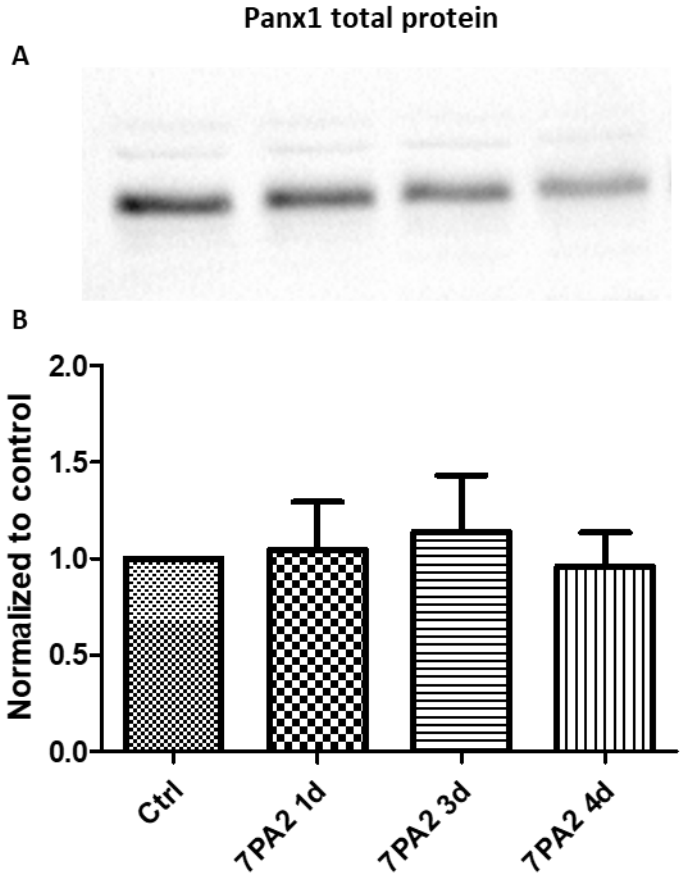

Figure A1: Total Panx1 protein levels in cultured hippocampal neurons are unchanged over 4 days of 7PA2-CM treatment. Western blots were performed on lysates from CD1 hippocampal neuronal cultures (DIV 18-23). **(A)** Representative blot probing for Panx1 protein (predicted molecular weight between 48 kDa and 52 kDa). **(B)** Quantification of Panx1 blots. Band intensity was first normalized to total lane protein as measured by TCE signal, then expressed as fold change from control.

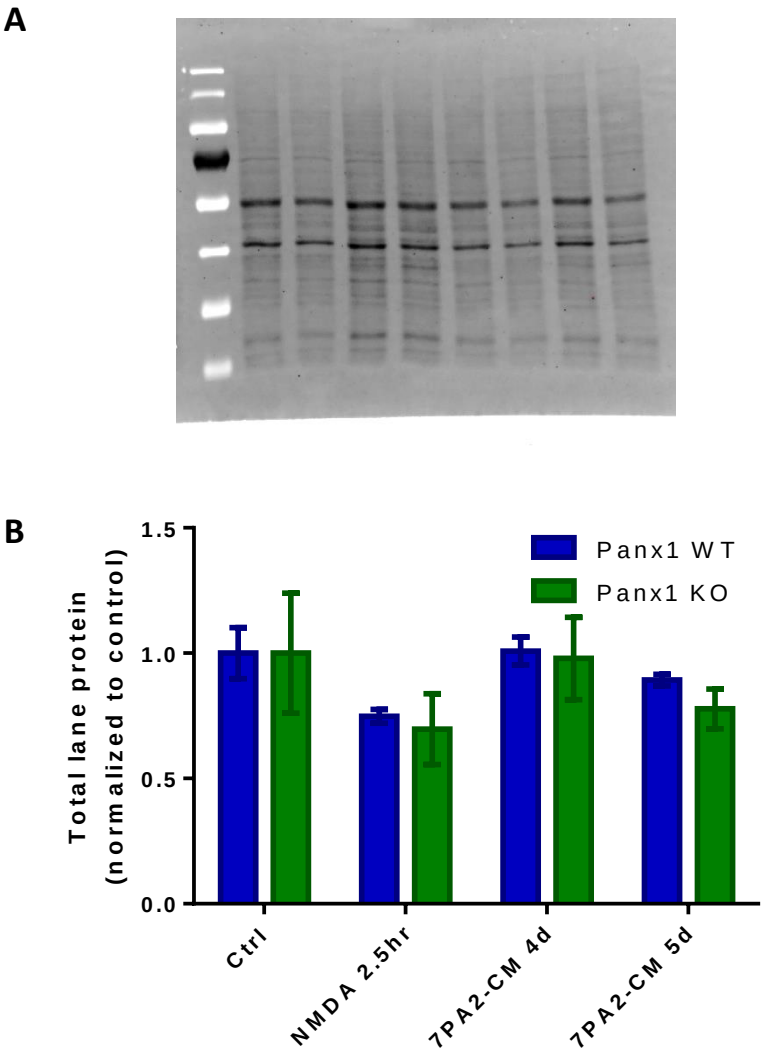

Figure A2: Total lane protein levels visualized by TCE luminescence from treated Panx1 WT and KO cultured hippocampal neuron lysates. Western blots were performed on lysates (N=3) from Panx1 WT and KO hippocampal neuronal cultures (DIV 18-23). **(A)** Representative image of total blot protein visualized by TCE luminescence. **(B)** Quantification of total lane protein. Total lane intensities were averaged and normalized to control. There was a reduction in total protein in the NMDA treatment groups despite equal density of neuronal cultures before treatment and lysis.

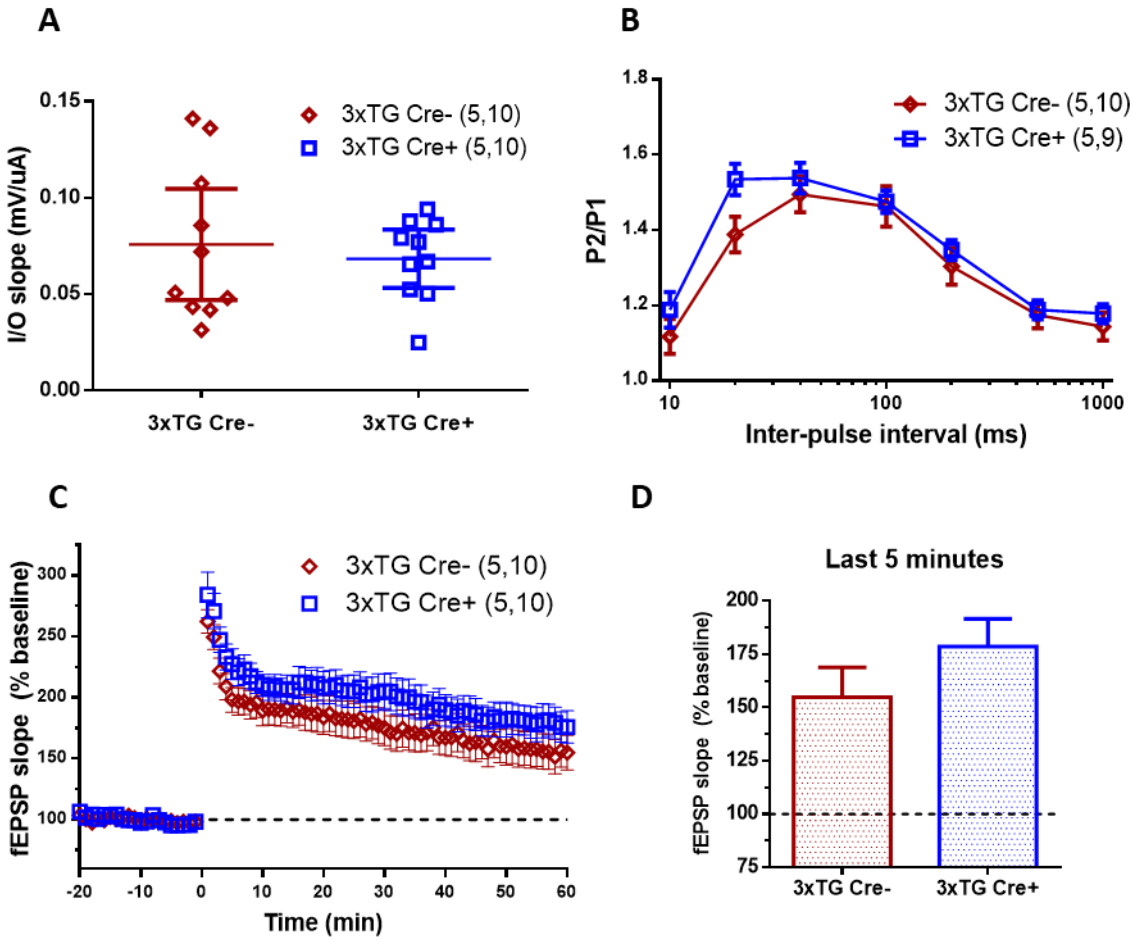

Figure A3: LTP in hippocampal slices from 6 month old 3xTg AD mice crossed with a Cre driven microglial specific Parp KO. Field EPSP recordings at the CA3-CA1 synapse in acute hippocampal slices from ~5-6 month old 3xTg mice with (Cre +) and without (Cre -) microglial specific Parp KO. **(A)** Excitability measured by slopes of input-output curves. **(B)** Paired-pulse facilliatation tested at 7 different inter-pulse intervals between 10 ms and 1000 ms. **(C)** LTP induced by HFS (2x 100 Hz) and recorded over 60 minutes. **(D)** Averaged fEPSP slopes from last 5 minutes of LTP recordings. There was no significant difference between groups. p = 0.23, student t-test.

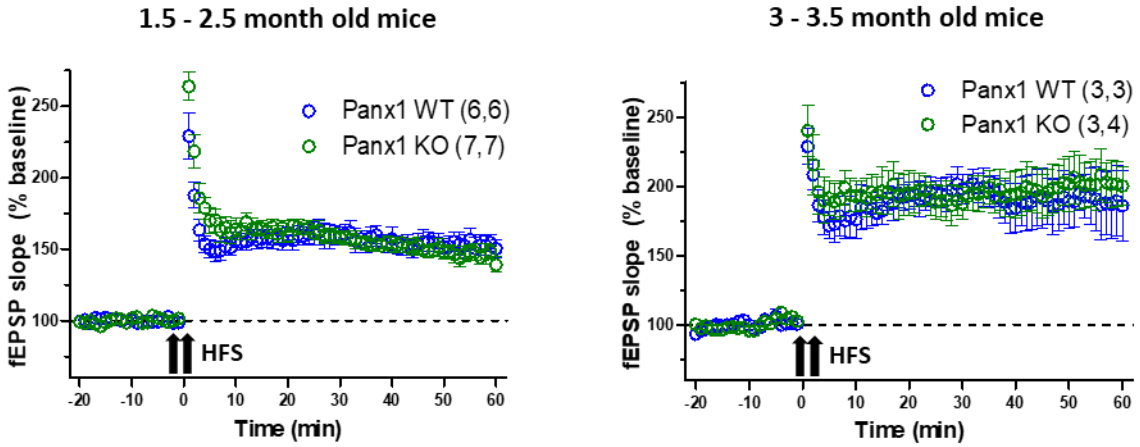

Figure A4: LTP in younger and older Panx1 WT and KO mice. Field EPSP recordings at the CA3-CA1 synapse in acute hippocampal slices from 1.5-2.5 month old and 3-3.5 old Panx1 WT and KO mice. Averaged fEPSP slopes as a percentage of baseline during each minute of recording plotted. LTP remained stable in control slices from Panx1 WT and KO mice and did not differ from each other.